Using stable isotopes to understand relative contributions of evaporation and evapotranspiration on groundwater recharge in the Verlorenvlei catchment, west coast, South Africa.

Siyabulela Ben Mafilika

This thesis is submitted in fulfilment of the requirements for the degree Master of Science in Geology/Isotopic Hydrology Stellenbosch University

Supervisor: Prof Jodie Miller

Faculty of Science

Department of Earth Sciences, Stellenbosch University

December 2021

DECLARATION

I declare that “The use of stable isotopes to understand relative contributions of evaporation and evapotranspiration on groundwater recharge” in the Verlorenvlei catchment is my own work, that it has not been submitted for any degree or examination in any other university, and that all the sources I have used or quoted have been indicated and acknowledge by complete references.

Full name: Siyabulela Ben Mafilika

Date: December 2021

DEDICATION

I would like to dedicate this thesis to my late mother, who has been my source of inspiration and my pillar of strength when I thought of giving up. Thank you for your spiritual and emotional support, you were my driving force that always kept me going, and I wouldn't be where I am today if it wasn't for your constant support. This one is for you, and I hope that you are proud of your son has achieved. Thank you!

ACKNOWLEDGEMENTS

Firstly, I would like to thank my God for guiding and providing me with the strength to complete my thesis.

I would also like to express my sincere gratitude to my supervisor Prof Jodie Miller for arranging a research topic that I was eager to, for the continuous support, her invaluable guidance, motivation. My supervisor introduced to Isotopic Hydrology, and I have benefited greatly from her expertise and knowledge. Your constructive comments and suggestions are greatly appreciated. Thank you so much Prof, you were like a mother to me.

My sincere thanks also goes to all the farmers who supported my project, by collecting the rainwater and groundwater samples, you made this project possible. To Dr Andrew Watson and Dr Jared van Rooyen, for their willingness to help in any way needed, and for providing useful information that benefited this project. I would also like to thank Prof Torsten Venneman who contributed to the data analysis, and NRF for providing funding for this project.

Last but not least, I would like to thank my family, friends, and my girlfriend for their encouragement and support.

This project has been severely impacted by the Covid 19 pandemic, and other factors that have been outlined in the project.

ABSTRACT

In Southern Africa, especially in arid and semi-arid regions, there has been an increase in dependency on groundwater resources for both domestic and agricultural supplies. This has been caused by variations in regional precipitation patterns, climate change, increased abstraction rates, and increased population. These impacts have imposed significant pressure on available water resources and have also impacted recharge rates; therefore, it is very vital that proper management strategies are implemented to protect our groundwater resources. This has driven a variety of methods to be applied in hydrological investigations and assessments in support of sustainable development and management of groundwater resources. The stable isotope technique has been an area of significant scientific advancement, and has been applied successfully in semi-arid regions of South Africa, and where there is poor physical data coverage. This method is well-established, straightforward, and has been widely used in support of water resource management. The Verlorenvlei is a semi-arid region located in the west coast of South Africa, and has been faced with challenges of implementing water resource management due to its lack of information on temporal and spatial distribution of groundwater recharge across the catchment. This project aims to outline how the stable isotope technique can be used to provide an in-depth understanding of the hydrological system, how the processes of evaporation and evapotranspiration influence rainfall and groundwater recharge. To do this, groundwater samples, river water, springwater, and rainfall samples were collected across 10 locations (farms) within the catchment for a period of a year, and these samples were taken for stable isotope analysis. Based on the observed trends from the analysis of d-excess, $\delta^{18}O$, $\delta^{2}H$, and ^{17}O-excess values, the rainfall across the catchment, rainfall was affected by the “seasonal effect” and “elevation differences”, resulting in spatial and temporal variation in $\delta^{18}O$ and $\delta^{2}H$ values. Furthermore, the rainfall was not heavily influenced by evaporation prior to its formation, but its source may have resulted from evapotranspiration of the surrounding natural vegetation, and this has been supported by high ^{17}O-excess values. The groundwater isotopic composition had similar composition to that of the springwater and rainfall, suggesting that the rainfall could be their source. Groundwater has been recharged by local precipitation, with minimal evaporation prior to infiltration. There was no evidence of evapotranspiration influences on the isotopic composition of fraction of groundwater that has been recharged. Furthermore, this study has not been able to explain the evapotranspiration process the way it hoped it would, and this project has suggested that the method used should be used in conjunction with other methods to understand complex process like evapotranspiration.

Key words: Recharge, Evaporation, Evapotranspiration, Semi-arid, Stable isotope.

ABBREVIATIONS AND SYMBOLS

δ – Delta

‰ – Per Mil

$\delta^{17}O/\delta^{18}O$ – Oxygen Isotope Values (‰)

$\delta^{2}H$ – Hydrogen Isotope Value (‰)

CTMWL – Cape Town Meteoric Water Line

d – Deuterium Excess

E- Evaporation

ET – Evapotranspiration

GMWL – Global Meteoric Water Line

km - Kilometre

LMWL – Local Meteoric Water Line

m – Metre

mm – Millimetre

TABLE OF CONTENTS

LIST OF FIGURES

LIST OF TABLES

1. INTRODUCTION

1.1 General Introduction

Globally, water resource management is important for the development of nations (Adelana & Olasehinde, 2005), protecting food security, adequate supply for human health and consumption, and to preserve the integrity of ecosystems (Pietersen & Beekman, 2016). However, these water resources around the world are subjected to change due to increased population resulting in increased water demand (Kattan, 2001; Oiro et al., 2018) and depletion of aquifers, anthropogenic activities such as land use changes, and climate change (Sharma et al., 2015). Together, these impacts have imposed significant pressure on available water resources globally (Kattan, 2001; Adelana & Olasehinde, 2005; Sharma et al., 2015). Along with climate change induced droughts and increased abstraction rates to mitigate drought and the decline in groundwater levels (Weyhenmeyer et al., 2002), these process have resulted in a reduction in both quality and quantity of groundwater resources (Sharma et al., 2015; van Rooyen et al., 2020). To mitigate these impacts, proper management and study of water resources is needed (Weyhenmeyer et al., 2002; Wirmvem et al., 2017).

In Southern Africa, there has been an increasing dependency on groundwater resources for both domestic and agricultural supplies (Braune & Xu, 2009; Pietersen et al., 2011), especially in arid and semi-arid regions (Kumar, 2013). This situation has been caused by variations in regional precipitation patterns (Biran et al., 2009), and the effects of population and economic growth (Pietersen et al., 2011; Nemaxwi et al., 2019). These changes have caused problems for implementing effective management of the water resources (Braune & Xu, 2009). Given the importance of groundwater resources across Southern Africa, and in light of the growing impacts of climate change, it is important that methods that increase water use efficiency are established, and sustainable groundwater management is implemented (Oiro et al., 2018). However, poor data coverage on hydrological systems in some parts of the region has been a major challenge in managing water resources (Houghton-Carr & Matt, 2006), and this has caused major challenges for managing and protecting different water catchments (Adelana et al., 2015). One of the most important elements of managing water resources sustainably is the establishment of qualitative and quantitative estimates of recharge patterns and volumes (Yeh et al., 2014).

Groundwater recharge has been defined as the deep percolation of water from land surfaces through the vadose zone, causing a rise in groundwater levels (Rukundo & Doğan, 2019). Increased temperatures which limit the ability of precipitation to percolate through the vadose zone, together with variable rainfall patterns have caused fluctuations in groundwater

levels in aquifers, making it difficult to provide reliable recharge estimates in some regions (Kumar, 2010; Obiefuna & Orazulike, 2011; Nemaxwi et al., 2019). This has driven a variety of tools and methods for determining recharge to be applied in hydrological investigations and assessments in support of sustainable development and management of groundwater resources (Sharma et al., 2015). Quantitative assessments of groundwater recharge have played a central role in the management and development of groundwater resources (Scanlon et al., 2002), but understanding the timing and magnitude of recharge at regional scales is also crucial to maintain sustainable groundwater management (Wu et al., 2019). However, choosing the most appropriate technique in estimating recharge can be difficult, as various factors such as the variation in topography, vegetation, and soil type need to be considered when choosing the correct technique to calculate recharge rates (Scanlon et al., 2002). The use of stable isotopes in recharge estimation has been an area of significant scientific advancement in recent decades, and has been used successfully in investigating and mapping water flow paths, storage dynamics along with groundwater recharge rates (Adomako et al., 2010; Oiro et al., 2018; Good, 2019).

The most frequently used environmental isotopes, are the stable isotopes of hydrogen (expressed as δ^2H) and oxygen (expressed as $\delta^{18}O$) (Mook, 2001). They have been extensively used to provide information on past precipitation, temperature and atmospheric circulation (Mook, 2001; Fleitmann & Leuenberger, 2015). Another isotope tracer which has been used in recent years, and has been very successful in providing better understanding of atmospheric conditions, and mechanisms of multiple hydrological and meteorological processes, is the ^{17}O-excess (Luz & Barkan, 2010; Tian et al., 2018). ^{17}O-excess is an indicator of climatic conditions at the oceanic source (Uemura et al., 2010), and can provide comprehensive information on past climatic environments, local temperatures, and moisture origins when combined with other tracers, such as deuterium excess and $\delta^{18}O$ (Risi et al., 2013). The ^{17}O tracer has also been used as an indicator of evaporation and evapotranspiration conditions at the moisture source (Luz & Barkan, 2010; Uemura et al., 2010), with its variation reflecting the different controls on precipitation in different regions. However, it has been and continues to be very hard to measure accurately and precisely because the magnitude of the ^{17}O-excess is very small and has to be multiplied by 10^6, and is generally restricted in the number of situations where it can be used effectively. The ^{17}O-excess value is usually obtained from high precision measurements of $\delta^{17}O$, and $\delta^{18}O$ (Tian et al., 2019).

The application of these stable isotopes is based on the concept of “tracing” (Elliot, 2014). This concept relies on the fact that water retains its distinct isotopic signature, unless there has been dilution or mixing with waters of different composition, or from fractionation during phase change (Kumar, 2013; Barbieri, 2019). The conservation of these water stable isotope compositions facilitates the identification of different distinct hydrological processes, identification of groundwater recharge areas and determination of groundwater flow directions through their natural distribution within a hydrological system on a temporal and spatial scale (Elliot, 2014). The approach has been used particularly successfully in many semi-arid to arid regions where evaporation is an important process modifying the stable isotope composition of precipitation and groundwater (Kattan, 2001).

The Verlorenvlei catchment is a semi-arid region, with a variable rainfall. This variable rainfall pattern across the catchment places significant limits on both natural recharge to aquifers and the availability of water for agricultural development in the catchment (Miller et al., 2018), resulting in competition for water resources by industrial and domestic users (Watson et al., 2018). The catchment is located on the west coast of South Africa, and is known as both an important agricultural region, and a region with significant natural biodiversity. However, groundwater is variably saline in the catchment (Sigidi et al., 2017; Watson et al., 2020), which can cause damage to sensitive ecological systems, and is often not suitable for either agricultural and domestic use (Miller et al., 2018). The catchment has also faced challenges with water resource management in the face of climate change (Fleischer et al., 2016). This challenge has, in part, been caused by a lack of information on the scale, temporal, and spatial distribution of groundwater recharge across much of the catchment, with variable availability of long term data records (Watson et al., 2018). These challenges cause problems in implementing groundwater resource protection and management, and have implications on how water movement can be understood in this water stressed and data poor catchment (Watson et al., 2019). Therefore, a better understanding of recharge processes and aquifer responses to a changing climate is necessary for a better management of the water resource (Fleischer et al., 2016).

This project uses the stable isotopes of hydrogen (expressed as δ^2H) and oxygen (expressed as $\delta^{18}O$), together with ^{17}O-excess to understand the influences of evaporation and evapotranspiration conditions to groundwater recharge. This project also outlined the factors that influence the variations of the isotopic composition of these isotopes in precipitation in the Verlorenvlei sub-catchment, in order to promote better management of water resources generally within the catchment. Groundwater and rainfall samples were collected over a period of a year and analysed for the stable isotopes of oxygen and hydrogen. The stable isotopic trends/signatures were used to provide an insight on the groundwater recharge processes. The study also took into account the natural vegetation present in the study area, as this affects the evaporation and evapotranspiration rates, and the amount of precipitation that is recharged to groundwater. The lessons learned in this study may form a starting point to analyse other poor data catchments facing similar challenges along the West Coast as well as other parts of the world, to better improve the understanding of world's hydrology and how to mitigate the effects of climate change.

1.2 Aims and Objectives

The key aim of this study is to use the stable isotopes of hydrogen (expressed as δ^2H) and oxygen (expressed as $\delta^{18}O$) to provide an understanding on the relative contributions of evaporation and evapotranspiration processes to groundwater recharge, and how these processes may affect the stable isotopic composition of groundwater and precipitation in the Verlorenvlei catchment. The following key objectives have been defined to achieve this aim.

Key objective 1: To isotopically characterize precipitation in the Verlorenvlei catchment.

1. What is the range of stable isotopic values and their spatial distribution in precipitation?
2. How does the stable isotopic composition in precipitation vary with increasing distance from the ocean/coast?
3. Based on the stable isotopic values and their distribution, is rainfall formation a result of evaporation or evapotranspiration processes?

Key objective 2: To isotopically characterize the groundwater in the Verlorenvlei catchment.

1. What is the range of isotopic values and their spatial distribution in groundwater?
2. How do the stable isotopic values of groundwater relate to those in precipitation?
3. Does the fraction of precipitation that becomes groundwater recharge show evaporation or evapotranspiration signals based on their isotopic values and distribution?

Key objective 3: To evaluate the relationship between precipitation and groundwater in the Verlorenvlei catchment.

1. Are precipitation evaporation signals, if present, transferred to the groundwater system?
2. Can these signals be differentiated from evapotranspiration signals?
3. How can the information obtained in this study be used to understand the hydrology of the catchment, and facilitate improved management of its water resources?

2. THE HYDROLOGICAL CYCLE

The hydrological cycle describes the continuous distribution and movement of water from the earth to the atmosphere, and it involves the continual circulation of water between the oceans, atmosphere, vegetation, and land (Ball, 2000). The hydrological cycle is made up of many varied and interrelated processes namely condensation, precipitation, evaporation, and evapotranspiration (Fig. 1). Surface water collected from oceans, dams, ponds, swamps, lakes, land surfaces and plants evaporates and transpires, and becomes water vapour. This water vapour is distributed across the planet through atmospheric circulation (Balasubramanian & Nagaraju, 1994), and it condenses and returned to the land and oceans via precipitation. Vegetation cover intercepts precipitation before it reaches the land, contributing to overland flow, with processes like infiltration and percolation moving the water down to the groundwater systems (Sharda et al., 2006). Solar energy (the excess of incoming radiation over the outgoing radiation), is the main driver of this immense movement of water, and this makes the sun the prime mover of water moisture through the hydrological cycle (Engman et al., 1991).

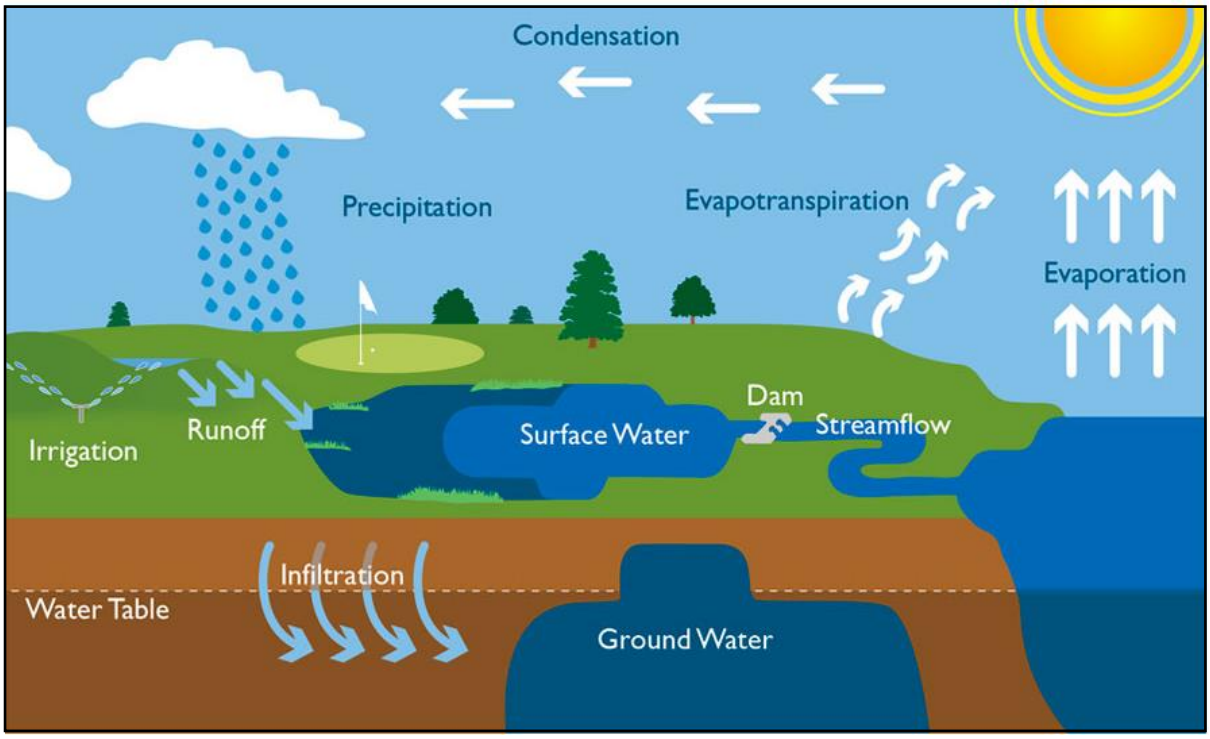

Figure 1: Schematic diagram of the hydrological cycle (Sharda et al., 2006).

2.1 Components of the hydrological cycle

2.1.1 Evaporation

Evaporation (E) is the process by which water or liquid is converted to water vapour (Yagbasan, 2016). This water may be evaporated from surfaces such as lakes, rivers, soils and wet vegetation (Alazard et al., 2015), representing the effective water loss from the water system which impacts reservoir storage efficiency, (Majidi et al., 2015). Evaporation forms one of the components of the water budget for reservoirs under different climate regimes, and is sensitive to climate change and rising temperatures which threaten to decrease the availability of water (Althoff et al., 2019).

Physical drivers of evaporation might be seen as simple, but the process in reservoirs relies on hidden drivers, such as time-scale dependent feedbacks and heterogeneous conditions controlling the evaporation rate (Alazard et al., 2015). In arid and semi-arid regions potential evaporation is driven by energy, and in these regions evaporation implies loss of water resource at a basin scale (Saadi et al., 2018). Generally, increasing temperatures results in an increase in evaporation rates, largely because of an increase in the holding capacity of air. In humid regions, however, atmospheric moisture is the major limitation to evaporation and has a significant effect on evaporation rate (Alazard et al., 2015). The rate of evaporation can also be controlled by water availability, and reduced soil water, that could lead to a reduction in evaporation rate of a catchment (Gao et al., 2017).

Open water evaporation studies and accurate estimates of evaporation losses are very useful for water resource managers who are interested in estimating the impact of this process on water budgets, and to develop effective policies and water resource management strategies (Najmaddin et al., 2017; Althoff et al., 2019; Meng et al., 2020). Furthermore, monitoring of the evaporation phenomena can result in recommendations for irrigation practises being formulated to enhance irrigation program planning and to enable accurate estimations of agricultural production and irrigation needs under variable conditions (Fisher et al., 2017). However, obtaining representative quantification of evaporation is a major challenge, since the variability of air temperature and vapour pressure considerably differ even across small areas and depends on microclimate variability (Najmaddin et al., 2017).

The rate of evaporation from the land surface is driven by meteorological controls, characteristics of vegetation and soils, and constrained by the availability of water. Additionally, the relative importance of these meteorological controls on evaporation may vary geographically (Althoff et al., 2019). The type of vegetation cover, and vegetation properties play an important role in evaporation, as they produce different amount of turbulence above the canopy that impacts evaporation rates and therefore catchment water balance (Yagbasan, 2016). Evaporation studies have used different models to understand the evaporation process and the effect of climate change to evaluate the effect of changes in meteorological controls on evaporation (Majidi et al., 2015). These changes can affect the hydrological cycle and are expected to alter the amount of water available for groundwater

recharge to aquifers and stored in surface water reservoirs, (Saadi et al., 2018; Beamer et al., 2013).

2.1.1.1 Methods of estimating evaporation

Most evaporation estimation methods, especially in semi-arid regions suffer from lack of available data or biased field measurements. It is thus, very important that hydrologists assess the relative importance of various available methods used to estimate this water loss, as well as their uncertainties (Majidi et al., 2015; Meng et al., 2020; Kumar & Arakeri, 2021). Currently used methods to estimate evaporation rely on meteorological data from open water reservoirs (Althoff et al., 2019). Based on the simplicity and accuracy of the application of these methods, they each have advantages and disadvantages, and it is essential that logical scenarios are evaluated for estimating evaporation under conditions with poor coverage of measured data (Majidi et al., 2015; Meng et al., 2020). Furthermore, it is very important that satisfactory estimation methods of evaporation are established for a better management of water resources and ecosystems, and to contribute to research (Gorjizade et al., 2014). Xu and Singh (2000) have generally categorized the methods for quantifying evaporation into: mass-transfer, isotopic mass-balance method, pan coefficient, energy budget, and combination methods.

(a) Energy budget method

The energy budget method is used to estimate evaporation rate from the surfaces such as, lakes, and is based on the simple principle of energy conservation (Finch & Hall, 2001). It has been widely evaluated and is found to be very accurate in semi-arid areas, with its accuracy dependent upon the age and size of the water body. This method requires large amounts of data which can be very difficult to measure, and that is often problematic (Gorjizade et al., 2014). To improve its accuracy, the temperatures of the surface and water surface profile are required as representative points (Alazard et al., 2015). The energy budget method can expressed as (Gorjizade et al., 2014):

$$\lambda E = R_{net} + H_{sea} + A_{net} - H - S \qquad [1]$$

Where λE is the latent heat used by evaporation of lake water with λ the latent heat of vaporization and E the vaporization within a given period, R_{net} is the net radiation, H_{sea} is the heat released by the sediment and is negligible in most cases, A_{net} is the heat advected into the lake from precipitation, inflows and outflows, and is also negligible in most cases, H is the sensible heat transfer from the lake surface to atmosphere and can be expressed as $H = B \times \lambda E$, where *B* is the mean Bowen ratio for a particular period, and S is the change of the heat stored in the lake during a certain period. Once the negligible terms have been removed, equation [1] can be rewritten as:

$$E = \frac{R_{net} - S}{\lambda(1 + B)} \qquad [1.1]$$

S in equation (1 and 1.1) can be obtained from using vertical lake zones and lake profile temperatures.

(b) Mass transfer method

In this method evaporation is assumed to be a function of wind speed, and the difference between water vapour pressure of the water surface and the atmosphere (Oswald and Rouse, 2004; Liou & Kar, 2014; Wang et al., 2019). The method relies on an the empirical mass transfer coefficient that can be used to explain the relationship between the different parameters through the wind function (speed at which air flows over the water surface) (Alazard et al., 2015). Once the value of the empirical coefficient is known, the method is relatively straightforward to use and reasonably accurate. Using this method, evaporation can be calculated as (Finch & Hall, 2001):

$$E = C_u(e_s - e_a) \quad [2]$$

Where E is the evaporation rate, C is the mass transfer coefficient and reflects transfer characteristics of a water body based on their geometry, plant cover, topography, land use and climate of the surrounding land, u is the wind speed, e_s is the pressure of saturated water vapour at the temperature of the surface, and e_a is the water vapour above the evaporating surface as a function of relative humidity and air temperature. Calculation of *C* differs for uniform surfaces and in conditions where conditions of surface uniformity are not met. For uniform surfaces, *C* can be calculated from theory, and in for most inland water bodies where ununiform surfaces exist it is necessary to make more restrictive assumptions to find a more theoretical solution to get evaporation and heat transfer equations (Brutsaert, 1982).

(c) Combination method

The Penman and Priestley-Taylor equation has been used for the last 50 years to estimate evaporation from water, vegetation (Penman, 1948). A table has been presented by Linarce (1993) comparing the monthly and annual measurements of evaporation with Penman estimates for a wide range of water bodies (Finch & Hall, 2001; Gorjizade et al., 2014). Penman has combined the mass transfer and energy budget methods and eliminated the requirements for surface temperature to obtain this expression for estimation of evaporation from open water as (Finch & Hall, 2001):

$$E = \frac{\Delta R_n}{\Delta + \gamma} + \frac{\gamma f_{(u)}(e_a * - e)}{\Delta + \gamma} \quad [3]$$

Where *E* is evaporation rate, R_n is the net radiation in units of equivalent depth of water, Δ is the slope of the saturated vapour pressure-temperature curve, and γ is the psychometric coefficient, $f_{(u)}$ is the function of the wind speed, $e_a *$ and e are the saturated vapour pressure of the air at the water surface temperature and vapour pressure of the air at the

reference height. This method assumes that the evaporating surface temperature is equal to the water surface temperature (Finch & Hall, 2001).

(d) Isotopic mass-balance method

This method uses mass-balance equations of isotopic tracers to provide independent hydrological information for estimating evaporation and water balance parameters (Bowser et al., 1990; Alazard et al., 2015). Natural spatial and temporal variations in these isotopic tracers are common features used in most hydrological systems and they arise due to changing atmospheric conditions, differentially affecting the transport of heavy versus light isotopes in atmospheric moisture to a given region at a given time (Bowser et al., 1990; Krabbenhoft et al., 1990; Alazard et al., 2015). The isotopic balance relationship describes the changes in isotopic composition occurring in response to the evaporative enrichment when the water body is well mixed (Saadi et al., 2018). This method has been very successful in semi-arid regions which are often characterised by a lack of available data, and this method is able to provide an in depth understanding of the hydrological cycle with less amounts of data and can contribute useful information to other estimation methods (Bowser et al., 1990; Yagbasan, 2016). It is also useful in providing help to delineate the origin and evaporative history of any water body (Najmaddin et al., 2017). Furthermore, it has enabled continental-scale assessments of evaporation/transpiration ratios which can be used in turn with precipitation rates for volumetric estimates of vapour loss from a given catchment or surface water body (Simpson et al., 1992).

2.1.2 Evapotranspiration

The term “evapotranspiration” was first defined by Thornwaite in (1944), and was later adopted by Penman and Monteith from their successful efforts of estimating the amount of water lost to the atmosphere using standard climate measurements (Liou & Kar, 2014). Yang et al. (2016) has defined evapotranspiration (ET) as the total water loss or transfer from a unit land surface area to the atmosphere. It includes water vapour evaporating from the surface of the soil and from free water on plant surfaces, and from water transpiring from within plant surfaces (Wang et al., 2014; Yang et al., 2016). According to Beamer et al. (2013) evapotranspiration is the rate at which water is transferred from land and plant surface to the atmosphere. It is a function of the at-surface radiative and advective energy, and varies in time and space depending on various factors, such as vegetation type and density, soil type and moisture, and local-to-regional meteorological factors such as, humidity and precipitation (Beamer et al., 2013).

ET constitutes a significant percentage and forms an integral component of the precipitation formation cycle, and is found to be the largest component of the hydrological cycle and the main component of the water balance at irrigated fields (Anderson et al., 2011; Najmaddin et al., 2017; V. Kumar et al., 2018). Furthermore, ET plays an important role in the water budget, and can be used to diagnose climate variability and change. ET also plays a critical role as the driving force of weather patterns at local scale, affecting turbulences, cloud formation and

convection (Fisher et al., 2017). It is the most challenging component of the hydrological cycle to estimate especially in arid and semi-arid regions and is affected by the type of vegetation cover (Beamer et al., 2013). Hydrographic areas characterised by deep groundwater, and limited surface water resources, water loss through evapotranspiration will be limited to local precipitation amount. However, in shallow groundwater basins, evapotranspiration rates often exceed precipitation rates (Beamer et al., 2013). The majority of the water loss due to evapotranspiration is expected to happen in summer months and growing seasons, with little or no evapotranspiration loss expected in winter months or periods (Balasubramanian & Nagaraju, 1994). There are two terms used to denote these conditions, namely actual, and potential evapotranspiration (Balasubramanian & Nagaraju, 1994). Actual evapotranspiration can be defined as the amount of water that is removed from the surface by evaporation and transpiration processes, and potential evapotranspiration is defined as the measure of the ability of the atmosphere to remove water from the surface through evaporation and transpiration processes (Gu et al., 2017). Scientists need to consider these evapotranspiration processes for the practical purpose of water resource management (Gu et al., 2017).

The comparison between the magnitude of ET, and precipitation can be used to determine the specific climatic conditions for different areas (Mendicino & Senatore, 2012; Yang et al., 2016). At local and global scale, ET is a dominant controlling factor of climate and hydrology, and mass and energy exchange between the atmosphere and terrestrial ecosystem (Beamer et al., 2013; Yang et al., 2016). It also plays an important role in controlling the amount of water that is recharged into aquifers, and relative to groundwater fluctuations (Fiorillo, 2011), it continues to extract a substantial percentage of the water that falls from precipitation, thus reducing recharge to groundwater systems (Najmaddin et al., 2017).

The rate of ET is controlled by a combination of factors such as warmer temperature, reduced bulk canopy conductance associated with increasing CO_2 concentrations, and large-scale land use changes (Fiorillo, 2011), and by several climatic, hydrological, soils, geomorphological conditions of a region (Balasubramanian & Nagaraju, 1994). Generally, here are two remote sensing approaches which have been have been widely used to estimate spatial distributions of evapotranspiration, a surface energy balance (SEB), and vegetation index (VI) (Liou & Kar, 2014). The SEB method uses surface reflectance and surface temperature data to formulate a solution of the surface energy budget, whereas, the VI approach allows point estimates of annual ET using seasonally averaged or peak annual VI values to be spatially distributed over the total discharge area. These relationships can be used across large areas with multiple sensor systems, such as MODIS or LANDSAT satellites (Beamer et al., 2013; Liou & Kar, 2014).

However, quantification of ET is a difficult task, and requires improved techniques for its accurate quantification on a field, watershed, and regional scale for efficient use of water resources (Fisher et al., 2017). Land-use is important in ET processes, particularly the type and distribution of the vegetable cover (Scan et al., 2007; Fiorillo, 2011). In agriculture, ET is related to water demand, and losses due to ET in agriculture can be used to ensure that best conditions for agricultural needs are met, especially when water resource management is correctly planned and implemented (Scanlon et al., 2005; Mendicino & Senatore, 2012). Additionally, ET is very important for the correct quantification of water requirements for

crops which assists with water management (Balasubramanian & Nagaraju, 1994), and to calculate water balance at various scales to partition the ET into soil evaporation and plant transpiration in order to understand water dynamics and soil-plant-atmosphere interactions (Mendicino & Senatore, 2012).

2.1.2.1 Factors affecting evapotranspiration

(a) Weather parameters

Weather parameters affecting ET are radiation, air temperature, humidity and wind speed (Liu et al., 2020). The amount of energy available for evaporation is dictated by weather conditions, and these therefore play an important role in determining ET rates (Gao et al., 2017; Awe et al., 2020). Solar radiation is the meteorological parameter that has the greatest impact on ET, as it contributes large amounts of energy to vegetation in the desert (Novák & Novák, 2012; Saadi et al., 2018). The wind plays two major roles, firstly, transporting heat building up on adjacent surfaces, such as dry vegetation accelerating evaporation. Secondly, accelerating evaporation by enhancing turbulent transfer of water vapour from the vegetation to the dry atmosphere (Novák & Novák, 2012). Moist air located within and just above the plant canopy with dry air above is constantly replaced by wind (Mendicino & Senatore, 2012). Temperature also has major impacts on ET rates through its impact in vapour pressure deficits and advection. ET is expected to be higher for warm as compared to cool vegetation due to less energy required to evaporate water from warm vegetation (Awe et al., 2020). Winds impacts ET more at low temperatures (Fisher et al., 2017).

(b) Crop type

Different types of crops produce different ET levels due to differences in resistance to transpiration, crop height, roughness of the crop, reflection, groundcover and crop rooting characteristics under identical environmental conditions (Liu et al., 2020). Crop type, varieties and development stages should be considered when assessing the ET from crops grown in well-managed fields (Novák & Novák, 2012). The type of species or variety of plant being grown can greatly influence the rate of ET (Awe et al., 2020).

(c) Management and environmental conditions

ET rates can also be affected or reduced by factors such as soil salinity, poor land fertility, limited application of fertilizers, the presence of hard or impenetrable soil horizons, and poor soil management which limit the crop development. These factors need to be considered when assessing the rate of ET of a particular catchment (Novák & Novák, 2012). When assessing ET, the other factors that need to be considered are the type of ground cover, density of the plant and size, and the soil water content (Varoufakis, 1998). The effect of soil water content on ET is conditioned by the magnitude of water deficit and type of soil (Mata, 2014), therefore ET losses must be determined based on the vegetation types for different climatic regimes and soil types (Awal et al., 2020).

2.1.2.2 Methods of estimating evapotranspiration

Estimation of ET has become the main objective for many scientific disciplines, and is essential for water management in areas where water is scarce (Najmaddin et al., 2017). ET estimates are also crucial in the long term terrestrial water balance, and the knowledge of ET has become very important because of increased use of irrigation of farmlands (Mata, 2014; Awal et al., 2020; Liu et al., 2020). However, it is a difficult process to measure, especially in arid and semi-arid regions where losses of water are spatially and temporally highly variable (Najmaddin et al., 2017; Awe et al., 2020). Methods and instruments to estimate or measure ET are available, and they depend upon different approaches (Kidston et al., 2010). These methods and techniques that are recognized and acknowledged should give approximate estimates, and be simple to apply. The attempts made by any or all of the methods should enable comparative results (Kidston et al., 2010). However, the application of some of the methods may be restricted in many locations since they require a number of weather parameters such as radiation, air temperature, air humidity and wind speed that may not be available (Gao et al., 2017; Awal et al., 2020). Obtaining these weather data is problematic due to limitations of installing expensive and complicated weather stations. The ET estimating methods should be compared to get the most correct value of ET, and to reduce uncertainties of each method (Flerchinger & Seyfried, 2014). Most commonly used ET estimation methods are differentiated between direct and indirect approaches (Allen et al., 1998).

(i) Direct approaches

(a) Lysimeter method

Lysimeter is a direct measurement approach extensively used to monitor evapotranspiration of agricultural soils (Gao et al., 2017; Awe et al., 2020). They are considered to be the most accurate for ET estimation when vegetation is grown in a large soil tank which allows the rainfall input together with the water loss through the soil to be easily calculated (Mata, 2014). They consist of a mass of soil in an enclosed container which can be accurately weighted to determine the amount of water that is gained or lost per unit time (Mata, 2014). They are very useful in research where partitioning evaporation, and transpiration are studied separately (Najmaddin et al., 2017). They are designed to be representative of the surrounding field so that the measured Lysimeter ET closely mimics the field ET, if the surrounding field is properly managed (Gao et al., 2017). ET can be estimated as (Mata, 2014):

$$E_T = R_W + I_W - Q_D \pm \Delta S \quad [4]$$

Where E_T is evapotranspiration, R_W is the rainfall water, I_W is irrigation water, Q_D is quantity of water demand, and ΔS is the surface and subsurface change in storage. This method can be very accurate in estimating ET but is very expensive, and requires knowledge and experience to obtain the best ET measurement (Najmaddin et al., 2017). Under freezing temperatures of winter, where snow cover is present, certain difficulties may be encountered

when operating this method, but these discrepancies can be ignored since evaporation losses are very low and often negligible under these conditions (Novák & Novák, 2012).

(b) Water balance method

The water balance method has been widely used to estimate ET, especially in production agriculture in the practise of irrigation scheduling (Fisher et al., 2017). This method tracks ET from the fields when applying the water balance (Saadi et al., 2018). In arid and semi-arid regions where precipitation does not meet crop water requirements and is supplemented by irrigation, it is important that additions of water irrigation are accounted for (Fisher et al., 2017). In drier climates, the soil moisture change between the growing seasons is minor, and, in such cases, precipitation and irrigation are the main water inputs (Gao et al., 2017). The water balance can be determined using the equation (Novák & Novák, 2012):

$$\Delta S = P - ET - R - D \quad [5]$$

Where ΔS the change in soil moisture, P is precipitation, R is the sum of run off and run on, D is the drainage, and ET is evapotranspiration. Seasonal ET estimates can be modelled with the water balance method by obtaining the volumetric water content from soil samples at the beginning and end of a growing season (Saadi et al., 2018). If precipitation and irrigation are measured, the change in soil moisture is then used to calculate seasonal ET using this method (Gibson et al., 1993). However, it is often difficult to determine drainage and runoff using the water balance approach (Saadi et al., 2018). Drainage and runoff are commonly miniscule in arid and semi-arid regions, but to get the greatest accuracy in ET estimation they would need to be accounted for (Gao et al., 2017).

(c) Stable isotope mass-balance method

Gibson et al. (1993) suggested that the stable-isotope-mass balance method is very useful in providing water balance information for ungauged catchments. Isotopic monitoring of ungauged catchments using the isotope-mass-balance method is best suited for longer term studies encompassing complete annual cycles, and to approximate conditions of consistent water balance. This method is suited for arid and semi-arid areas and can offer significant potential to supplement the information obtained from conventional hydrometeorological monitoring to aid in understanding and managing of local and regional water resources (Mata, 2014). This method has enabled continental-scale assessments of transpiration/evaporation ratios (Evaristo et al., 2015), and these ratios can be combined in turn with precipitation or hydrometric data to make volumetric estimates of vapour loss from a catchment or surface water body (Fisher et al., 2017). The stable-isotope-mass balance method is not constrained by extensive in situ measurements, but relies instead on isotopic labelling of water as it passes through the hydrological cycle (Saadi et al., 2018). The main strength of this method lies in the ability to derive useful water balance information in the absence of detailed hydrometeorological information (Flerchinger & Seyfried, 2014).

(ii) Indirect approaches

(a) Blaney-Criddle method

This method was developed by Blaney-Criddle (1950) from their observations that the amount of water consumed by crops during their growing seasons was closely correlated with monthly temperatures and daylight hours during the growing season (Gao et al., 2017). This method is simple, uses readily available data, and thus is the best for estimating evapotranspiration (Mata, 2014; Saadi et al., 2018; Fisher et al., 2017). The correlation coefficients can be used in areas where only climatic data is available to determine ET. Using the Blaney-Criddle method, ET can be expressed as (Mata, 2014):

$$E_T = 0.46P(T + 17.8) \quad [6]$$

Where E_T is evapotranspiration, P is the percentage of daylight in hours in a year, and T is the temperature in degrees celsius. This method only requires the use of two factors, the temperature measured by the weather stations and daylight hours, based on the latitude of the place (Mata, 2014). However, this method does not account for most of the climatic parameters which greatly influence ET (Novák & Novák, 2012).

(b) Remote sensing

This method can be used to provide estimates of meteorological variables required to calculate ET at different scales. The estimation of ET in this method is based on the evaluation of the surface energy balance (Mata, 2014; Awe et al., 2020), and it has been successful in arid and semi-arid regions in support for sustainable use of water for agriculture (Fisher et al., 2017). It has also been successful in providing spatially continuous and temporal recurrent estimates of ET over a regional to global scale (Saadi et al., 2018). This method has been widely used for monitoring agricultural water resources at different spatial and temporal scales, and can cover large geographical areas enabling monitoring of vegetation dynamics through vegetation indexes (Gao et al., 2017). It is also useful in detecting water stresses through the land surface temperature which is a crucial factor controlling ET (Saadi et al., 2018). Remote sensing can be used with weather data from nearby weather stations, however, satellite data used to generate ET maps may have poor spatial and temporal resolution. Furthermore, the capabilities of remote sensing working below the ground surface and to detect groundwater conditions directly are limited (Gao et al., 2017).

2.1.3 Groundwater flow systems

Groundwater flow systems are part of the complex dynamic hydrological system, and they are paramount to the development of sustainable strategies to better manage groundwater extraction. They should also be an integral part of any administration framework aimed at minimizing, and controlling related negative environmental impacts (Zhou & Li, 2011). These systems are a three dimensional entities that have a recharge point where water enters the

system, a discharge point where water leaves the system, and boundary conditions and physical dimensions (Toth, 1970; Carrillo-Rivera & Cardona, 2012). They are controlled by topography, geology and climate, and hence these systems should be reached through an integrated approach from circumstantial evidence that features isotopic, chemical, vegetation, soil, and groundwater characterization (Carrillo-Rivera & Cardona, 2012). The expected continuous population increase and production in arid and semi-arid regions indicate extra pressure on existing groundwater flow systems, and depiction of those groundwater flow systems may be a valuable tool in defining vulnerability of groundwater to climate change at different scales (Carrillo-Rivera & Cardona, 2012). Understanding their hierarchical positions in an area can assist in planning and controlling groundwater extractions, and assist in developing appropriate strategies that can sustain and protect local flows and take advantage of regional and intermediate flows which have the lowest response to climate change (Zhou & Li, 2011). In addition to this, stable isotopic composition of rainfall can be used as a tracer to understand storm elevation and evaporation effects, and to describe the paths involved from the recharge zone to discharge zone. This will also help in providing information about the natural flow systems and to help with water functioning and recharge processes (Flow et al., 2019). Toth (1963) has divided these systems into, local, intermediate/sub-regional and regional flow systems (Fig. 2).

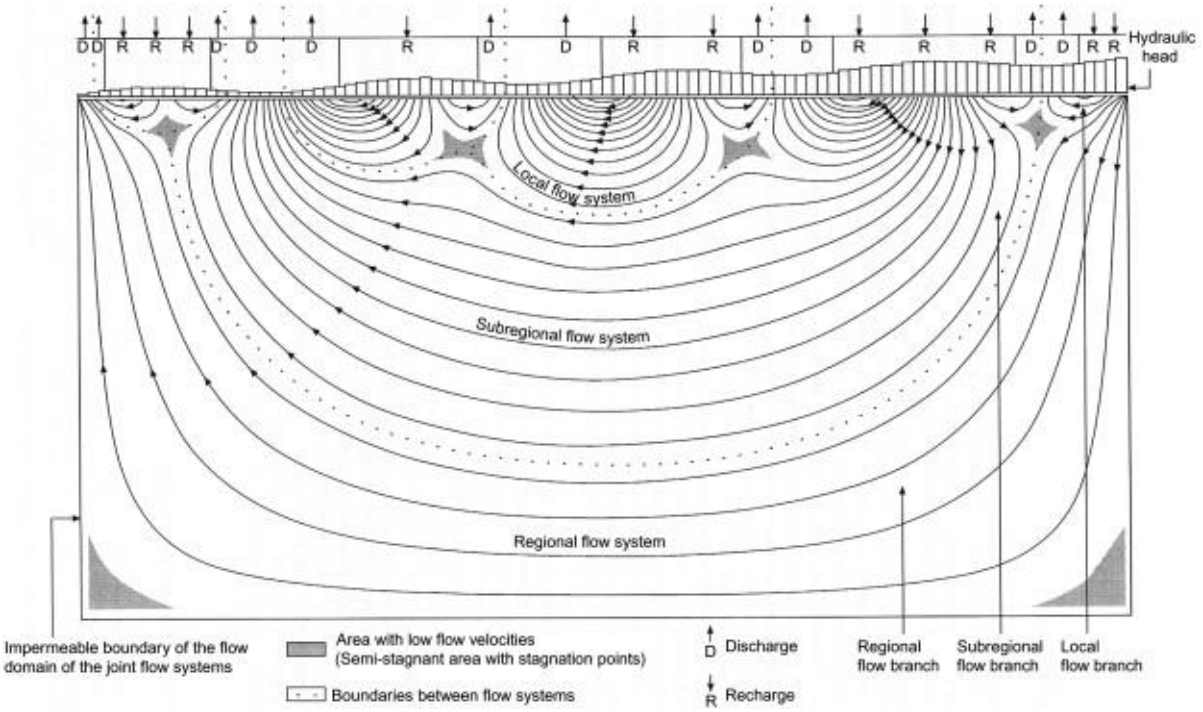

Figure 2: Schematic diagram of the different groundwater flow systems (Engelen and Kloosterman, 1996).

Local flow systems are shallow, unsteady, fast, and they have the greatest variability when interacting with surface water (Zhou & Li, 2011). Water can take longer to travel between the

recharge point and its discharge zone, but may travel for shorter distances between the recharging and discharging points at the same valley (Zhou & Li, 2011). Recharge occurs in high topographic areas and discharge to an adjacent low, thus topographic features such as slope and depression are the key controlling factors (Carrillo-Rivera & Cardona, 2012). A reduction in the amount of precipitation reduces recharge and rapidly diminishes the amount of stored water, causing the local flow system to be vulnerable to alterations in climatic conditions (Flow et al., 2019). Contamination from human activities are also common in this groundwater flow system.

Intermediate/sub-regional and regional flow systems are deep, steady, slow, and water travels for longer and deeper distances (Flow et al., 2019). They are characterised by smaller recharge rates, but discharge to large streams, and are continuous throughout the year (Flow et al., 2019). These system result in areas of local recharge as well as springs or other discharge features within the larger systems (Carrillo-Rivera & Cardona, 2012). They have no contact with surface after recharge, and they are often recharged at the divide between two catchments (Carrillo-Rivera & Cardona, 2012). Recharge processes are located in zones away from the discharge zone.

2.2 Application of stable isotopes in hydrological cycle

Stable isotopes of water play an important role in the study of the global hydrological cycle. This is based on the process of “fractionation” during phase changes associated with water during the hydrological cycle (Mook, 2001; Kumar, 2013). These process involve evaporation of water from the ocean and surface, and evapotranspiration from surrounding vegetation. As the water moves through different processes in the hydrological cycle (e.g., evaporation or evapotranspiration and infiltration) it undergoes small but measurable changes in the relative abundance of different isotopes through the fractionation process (Mook, 2001), (Fig. 3). Hence, different degree of fractionation caused by different processes can result in a wide range in stable isotope ratios used to understand the hydrological system (Terzer et al., 2013; Eslamian, 2014; Tian et al., 2018). The “fractionation” process occurs naturally through evaporation, evapotranspiration, and condensation processes, during which the lighter isotopes evaporate faster, and the heavier isotopes condense faster, leaving precipitation enriched in the light isotopes (Fig. 3). During the fractionation process distinct isotopic signatures of water develop in various components or processes, and these variations can be used to understand these hydrological processes (Yeh et al., 2009; Maria et al., 2017). Additionally, these isotope signatures can be used in providing information for tracing the provenance and movement of water in the hydrological cycle (Adomako et al., 2010; Tian et al., 2018). In particular, the journey of a water molecule can be traced from its sources for a given catchment using the different isotope ratios (Gat, 2002).

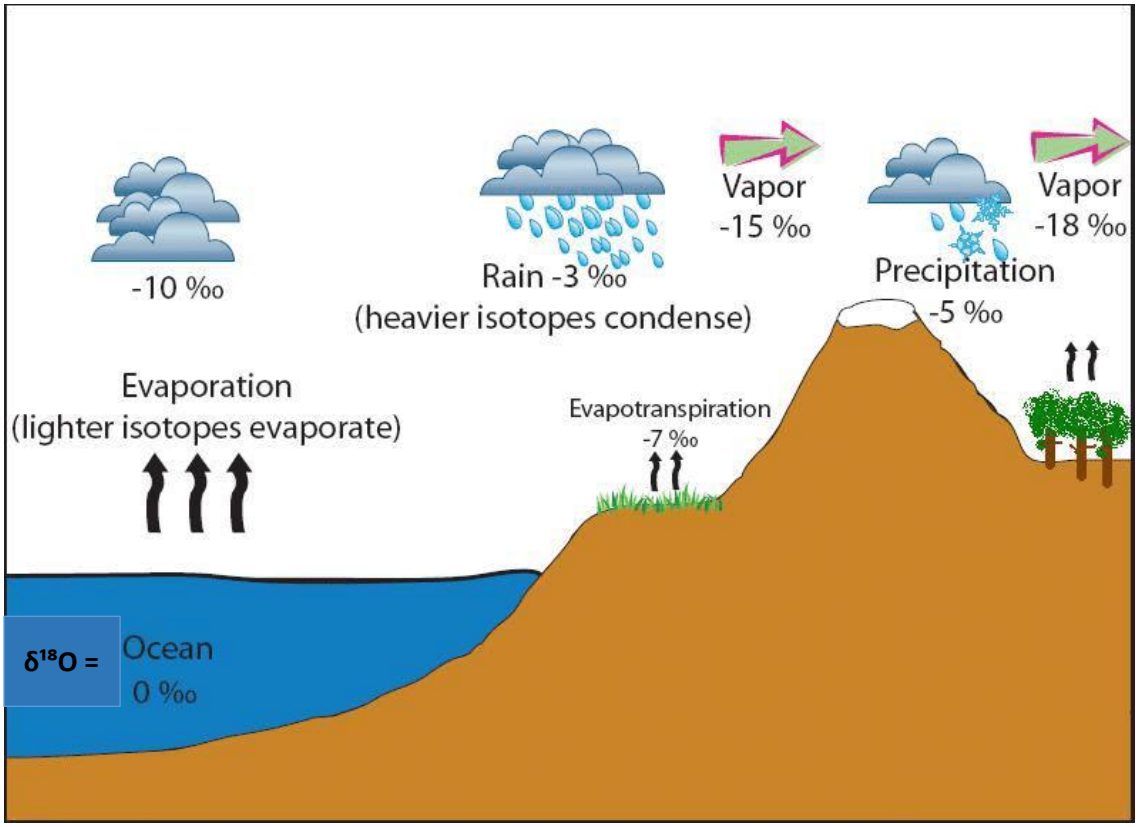

Figure 3: Schematic diagram of $\delta^{18}O$ fractionation by evaporation, condensation and evapotranspiration (Mook, 2001).

The stable isotope technique has increasingly been used to trace provenance of groundwater (Thomas & Rose, 2003; Sharma et al., 2015). It has proven to be very effective in identifying processes that cause a depletion or enrichment in isotopic composition of rainfall prior to infiltration, such as evaporation, evapotranspiration, and mixing of water (West et al., 2014). Furthermore, waters of different sources such as precipitation, rivers, and groundwater produce different isotopic compositions/signatures that can be used to understand the relationship between these components (Gat, 2002). These stable isotopes are ideal conservative tracers of water movement, and can be used to locate groundwater discharge locations, and distinguish the sources of groundwater recharge (West et al., 2014).

2.2.1 Stable isotopic notation

The stable isotopic compositions in hydrology are reported as δ (delta) values in parts per thousand expressed as parts per mil (‰). They can be expressed as ratios using the δ notation (Gat, 2002):

$$\delta = \left(\frac{R_{sample}}{R_{standard}} - 1\right) \times 1000 \qquad [7]$$

R is the isotopic ratio of heavy to light isotopes in the sample or standard. A positive delta (δ) value means that the sample has an isotopic ratio that is enriched in heavy isotopes (higher

than that of the standard), and negative delta (δ) value means that the isotopic ratio of the sample is depleted in heavy isotopes (lower than that of the standard). The stable isotopic compositions are reported relative to SMOW (Standard Mean Ocean Water) or VSMOW (Vienna-Standard Mean Ocean Water) international reference standards.

In practice, all laboratories have their own set of standards which are calibrated relative to the international standards. Measured isotopic ratio of a sample is compared to the standards which have been set by the laboratory, and recalculated to the VSMOW scale.

2.2.2 The Global Meteoric Water Line (GMWL)

The Global Meteoric Water Line (GMWL) was developed by Craig (1961), and has been used to describe the relationship between the behaviour of heavy to light isotopes of oxygen in comparison to the behaviour of heavy to light isotopes of hydrogen. It has also been used to provide a reference by which local differences in water can be compared, and can thus provide assistance on the interpretations of the origin of water (McGuire, 2004; Craig & Lal, 1960). The GMWL has also been widely used to track water masses in the hydrogeology field, and is expressed as (Craig & Lal, 1960):

$$\delta^2 H = 8 \times \delta 18O + 10 \qquad [8]$$

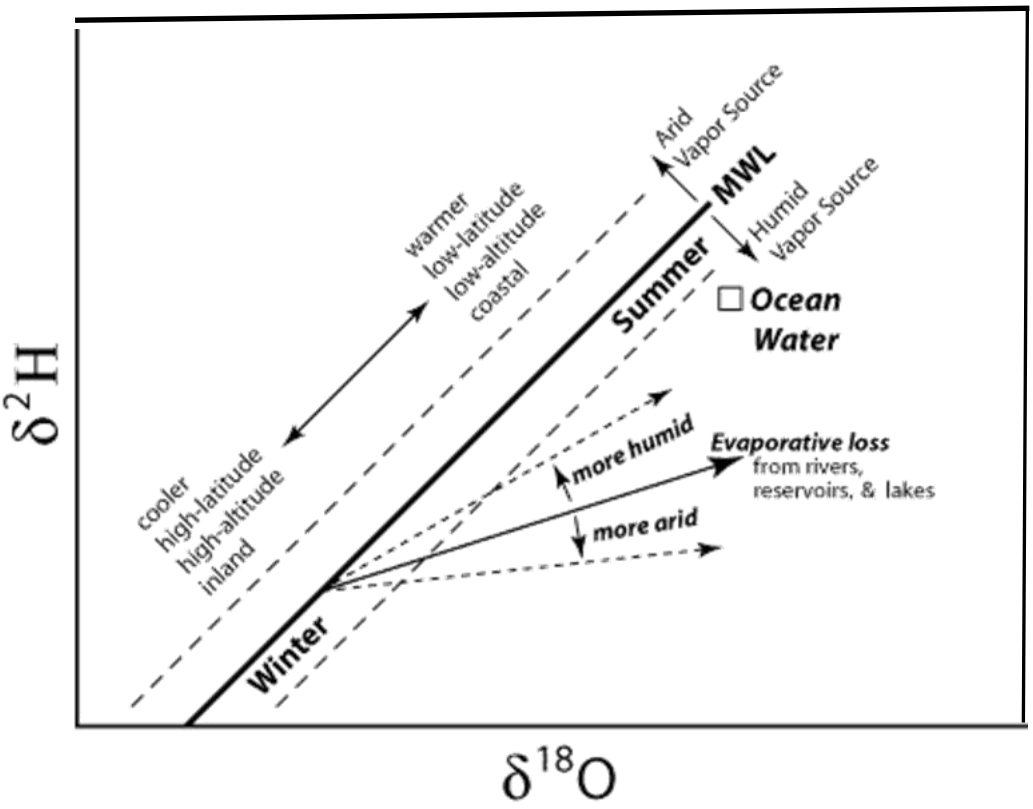

Figure 4: Schematic meteoric water line showing factors causing deviations from δ^2H vs δ^{18} relationship (adopted from SAHRA, 2005).

Generally, the most negative values that lie on the meteoric water line are indicative of localized recharge by large rainfall events or passing of a cloud mass across continents (Yeh et al., 2014). Furthermore, isotopic compositions of groundwater and rainwater that lie to the right or have deviated from the meteoric water line are indicative of evaporation during recharge either at the surface or within the soil zone, and for a given rainfall regime the further away a sample lies to the right of the MWL, the lower the recharge rate (Yeh et al., 2014), (Fig. 4). This may be caused by non-equilibrium kinetic effects occurring under evaporative conditions that cause fractionation of $\delta^{2}H$ and $\delta^{18}O$ proportions (McGuire, 2004). As a result of this fractionation process, water often develops unique fingerprints that can be used to understand the processes and the conditions under which they have formed and their sources (Fig. 4).

The stable isotopic composition ratios of precipitation reaching groundwater depends on several factors:

(i) Latitude

Is based on the observation of gradually depleted isotope signals in precipitation towards higher altitudes. With increasing latitude, the more depleted precipitation becomes in heavy isotopes ($\delta^{18}O$).

(ii) Altitude

Isotopic composition of precipitation becomes more and more depleted in $\delta^{18}O$ with increasing altitude. The altitude effect is related to the temperature, because condensation is caused by temperature drop due to increasing temperature.

(iii) Continental effect (Distance from the coast/ocean)

Land masses have an effect of forcing rainout from the vapour mass. As the vapour mass moves from is source region across a continent, its isotopic composition evolves more rapidly due to topographical effects and the temperature range of the continent. Coastal precipitation is isotopically enriched compared to the inner continental regions. $\delta^{18}O$ in precipitation is strongly correlated with temperature and is expected to decrease with increasing distance from the ocean, and also depends on topography and the climate of a region. Thus, isotopic ratios decrease with increasing distance from the coast.

(iv) Seasonal effect

Greater seasonal changes in temperature as well as moisture source generate strong seasonal variation in isotopes of precipitation. This variation is helpful in determining the rate of groundwater circulation, watershed response to precipitation, and the time of the year when recharge occurs. This also has an effect on the isotopic composition ratios, as temperature, particularly in hot summer months, may cause rainfall to experience evaporation before reaching the ground.

(v) Rainfall amount effect

The isotopic signature is affected by the intensity and duration of rainfall, and thus produces different isotopic ratios. Small amounts of rain are enriched in heavy isotopes along evaporation lines, especially in the more semi-arid and arid regions.

Due to all these factors, local precipitation can have variable relationships between $\delta^{18}O$ and $\delta^{2}H$. Thus, it is very important that local precipitation is sampled over time to develop a Local Meteoric Water Line (LMWL) against which a comparison can be made with isotopic values from water in other parts of the hydrological cycle (Gat, 2002). The $\delta^{18}O$ and $\delta^{2}H$ values of groundwater and its relationship to the MWL can be used to determine the recharge type (delayed, immediate), and to determine processes that have altered the isotopic composition of precipitation before recharging the groundwater (West et al., 2014)

2.2.3 ^{17}O-excess

Experimental developments made it possible to get an accurate measurement of $\delta^{17}O$ abundance, and this led to the definition of a new tracer in the water cycle, ^{17}O-excess (Barkan & Luz, 2007; Landais et al., 2008). Despite its low abundancy, ^{17}O has the potential to provide information on additional constraints on the precipitation formation mechanisms (Tian et al., 2018). However, it requires high precision analytical methods (i.e. water fluorination technique), but recent developments have made it possible to measure this low abundant isotope(Risi et al., 2010; Tian et al., 2018). It was first demonstrated by Luz & Barkan (2000) that the relationship between $\delta^{17}O$ and $\delta^{18}O$ is different in evaporation than in equilibrium controlled processes that affect meteoric waters. These demonstrations led to the suggestions that the relationship between these two variables may yield unique information on past relative humidity independently of temperature (Angert et al., 2004). Luz & Barkan (2010) suggested that the use of ^{17}O-excess can provide a better understanding of the atmospheric conditions, the mechanisms of multiple hydrological, and meteorological processes. It can also be used to investigate the hydrological system, adding information over the "traditional" deuterium excess because it is much less sensitive to changes in temperature. This isotope tracer is indicative of evaporation and evapotranspiration conditions at the moisture sources, the controls on precipitation in different regions, and can be expressed as (Luz & Barkan, 2010):

$$^{17}O - excess = \ln(\delta^{17}O + 1) - 0.528 \times \ln(\delta^{18}O + 1) \quad [9]$$

Uemura et al. (2010) measured ^{17}O-excess in the marine water vapor, and found it to be negatively correlated with relative humidity, while in polar ice cores it provided valuable information of past changes in global hydrological cycle, such as large scale variations in relative humidity over the ocean or the moisture origin of precipitation sites.

2.2.4 Deuterium excess (d-excess)

Deuterium excess is also sensitive to evaporation/transpiration of water of the ocean (Gat, 2002). Furthermore, it can be measured in meteoric water to understand both sources of precipitation, sub-cloud processes, and the evolution of moisture during transport (Yeh et al., 2014). It can potentially trace past and present precipitation processes in climate studies, and can reflect prevailing conditions during the evolution and interaction of mixing of air masses *en route* to the precipitation site (Froehlich et al., 2002). Deuterium excess is expressed as (Gat, 2002):

$$d - excess = \delta^2 H - 8 \times \delta^{18} O \quad [10]$$

.

2.3 Groundwater recharge

One of the key challenges in determining the sustainable yield of many aquifers in semi-arid zones, is the lack of groundwater recharge information (de Vries & Simmers, 2002; Vázquez-Suñé et al., 2010; Islam et al., 2016; Souissi et al., 2018). In these regions, recharge rates are difficult to determine precisely because they are generally low in comparison with average annual rainfall or evapotranspiration (Sophocleous, 2005). Groundwater recharge is fundamental to understanding the water balance of any watershed, and to meet the expanding urban, industrial, agricultural water requirements, particularly in semi-arid regions (De Souza et al., 2019).

Groundwater recharge can be defined as water that percolates down through the unsaturated zone and enters the dynamic-water flow system, contributing to the replenishment of the groundwater reservoir (Scanlon et al., 2002). This addition of water to the reservoir may be affected by various factors such as precipitation (intensity, frequency, duration), topography, vegetation, soil and subsoil types, flow mechanisms in the unsaturated zone, bedrock geology, and availability of groundwater storage (Jacks & Traoré, 2014). These factors may control groundwater recharge processes in different ways across climates. The rates of groundwater recharge are greatest when rainfall inputs through the soil exceed evapotranspiration losses (de Vries & Simmers, 2002).

In many aquifers, groundwater levels have fallen drastically due to above ground diversions of water sources as well as excessive groundwater mining for irrigation (Misstear, 2000). Thus, a better understanding of recharge processes and aquifer responses to a changing future are necessary (Walker et al., 2019).

2.3.1 Groundwater recharge mechanisms

Groundwater recharge mechanisms have been classified by Lerner et al. (1990) into three fundamental mechanisms, (1) direct (diffuse) recharge which can be defined as water added to the groundwater reservoir in excess of soil moisture deficit and evapotranspiration by direct vertical through the unsaturated zone (Xu and Beekman, 2003), (2) indirect (non-diffuse) recharge which is the percolation of water to the water table through riverbeds and defined channels, and (3) localised recharge which can be defined as recharge that is concentrated in small depressions, joints and cracks (de Vries & Simmers, 2002).

In humid regions characterized by shallow water tables and gaining rivers, direct (diffuse) recharge dominates, whereas, in arid regions with deep water tables and losing rivers, recharge is usually focused along the river corridors with rates generally controlled by surface water availability (Scanlon et al., 2002).

Arid and semi-arid regions are commonly dominated by deep water tables and losing streams. In these regions evapotranspiration often exceeds rainfall, so that groundwater recharge depends on high intensity concentrations of rainfall (Sophocleous, 2005). This limits aquifer recharge, and with these aquifers being the most accessible water sources in these regions, they are prone to depletion under projected future climate trends (de Vries & Simmers, 2002). However, recent findings by Seddon et al. (2021) have shown that future climate change will increase groundwater recharge in these regions.

In arid and semi-arid regions groundwater recharge is more susceptible to near surface conditions. Poor vegetation cover on a permeable soil or fractured porous bedrock near the surface, together with high rainfall intensity also creates favourable conditions for aquifer recharge (Walker et al., 2019). Semi-arid regions are often characterized by high evapotranspiration from dense vegetation during dry seasons that dictate the amount of water that can pass the root zone to contribute to aquifer recharge (Lerner et al., 1990). Recharge can also be hampered by thick alluvial soils in (semi-)arid regions which allow high retention storage during wet seasons and vegetation that subsequently extracts soil water in the dry season (Misstear, 2000).

2.3.2 Groundwater recharge estimation techniques

There are various methods available to estimate groundwater recharge, and these methods have been properly outlined by Scanlon et al. (2002), de Vries & Simmers (2002), Lerner et al. (1990), Xu and Beekman (2003). Groundwater recharge estimation is a fundamental part of groundwater resource management, and for the calculation of water availability, especially in arid and semi-arid regions where there is a high demand for water resources (Jacks & Traoré, 2014). These methods are applicable in surface water, saturated zone, and unsaturated zone studies. Methods based on data from surface water and unsaturated zones provide potential recharge estimates, and those based on data from groundwater can provide actual recharge estimates (Scanlon et al., 2002). Groundwater recharge estimates vary

between methods due to uncertainties inherent with each method, the different spatio-temporal scales at which they operate, and the type of recharge they represent (Scanlon et al., 2002).

Furthermore, the available recharge estimation methods have their own limitations and applicability. These methods should be related to the aquifer target for development, and to increase reliability of the results, multiple methods should be used (Scanlon et al., 2002). Groundwater recharge estimation methods are divided into physical and tracer methods (Bredenkamp et al., 1995).

2.3.2.1 Physical methods

Physical methods attempt to estimate recharge from water balances calculated either from hydro-meteoric measurements, direct estimates of soil water fluxes based on soil physics or changes in the aquifers saturated volume based on water table fluctuations.

(a) Water Table Fluctuation (WTB) method

The application of this method is based on the assumption that the rise in the groundwater level with respect to time in unconfined aquifers is indicative of recharge water arriving at the water table (Xu & Van Tonder, 2001). This method can be applied over longer time intervals (seasonal or annual) to estimate the change in subsurface storage (Adomako et al., 2010), and over short time periods in regions with shallow water tables with rapid rise and decline in water levels (Scanlon et al., 2002). Recharge can be estimated using this method as (Scanlon et al., 2002):

$$R = S_y \frac{\Delta h}{\Delta t} \qquad [11]$$

Where S_y is the specific yield, Δh is the water table rise, and Δt is the time within which rise takes place. It is simple to apply in unconfined aquifers, but cannot account for steady state conditions, and difficulties may arise from calculation of specific yield (Misstear, 2000).

(b) Cumulative Rainfall Departure (CRD)

This method is based on the assumption that water level fluctuations are a result of rainfall events, and it has been revised to accommodate for trends in rainfall time series (Xu & Van Tonder, 2001). This method has been applied extensively with success in South Africa by Bredenkamp et al. (1995). Recharge can be estimated as (Xu & Van Tonder, 2001):

$$R_r = rCRD_i = S_y \left[\Delta h_i + \frac{Q_{pi} + Q_{out}}{AS_y} \right] \qquad [12]$$

With

$$CRD_i = \sum_{i=1}^{N} P_i - (2 - \frac{1}{P_{av}} \sum_{t=1}^{N} P_t) i P_i \quad [12.1]$$

Where r is the fraction CRD which contributes to recharge, S_y is the specific yield, Δh is water level change during month i, Q_{pi} is groundwater abstraction, Q_{out} is the natural outflow, A is recharge area, P_i is rainfall for month i, and P_t is the threshold value representing aquifer boundary conditions. This method is not applicable in areas or regions with no groundwater level fluctuations (Xu & Van Tonder, 2001).

2.3.2.2 Tracer methods

These methods are based on the distribution of natural tracers present in rainfall (^{2}H, ^{3}H, ^{14}C, ^{18}O and Cl) in the saturated and unsaturated zone.

(a) Chloride Mass Balance (CMB)

The application of this method requires mean annual precipitation, chloride concentration of that precipitation, and the chloride concentration of groundwater (Scanlon et al., 2002). It assumes that chloride within the groundwater originates from precipitation, and that there are no alternative chloride sources (Xu & Van Tonder, 2001). This method is independent of whether recharge is focused or diffuse, and it integrates recharge rates both spatially across a region and temporally over long periods (Sophocleous, 2005). The basic equation applicable for estimating recharge using this method is (Scanlon et al., 2002):

$$R = \frac{(P_{eff})(Cl_{wap})}{Cl_{gw}} \quad [13]$$

Where R is the annual recharge, P_{eff} is average annual effective precipitation, Cl_{wap} is the weigh-average chloride concentration in precipitation including dry deposition, and Cl_{gw} is the average chloride concentration in groundwater. The CMB cannot be applied in areas underlain by evaporates or where there is mixing of saline waters, and there should a great caution in applying this method in areas close to the sea where the rainfall chloride contents are highly variable (Scanlon et al., 2002). The application of this method in South Africa is limited by the lack of long term rainfall quality data in sites across the region.

(b) Groundwater dating

These can be referred to as historical or event markers from their ability to date the age of groundwater to estimate groundwater recharge rates (Scanlon et al., 2002). The most widely used tracers to estimate the age of groundwater are Chloroflourocarbons (CFCs), ^{14}C, ^{3}H, and ^{3}He. The range of recharge rates that can be estimated from dating of groundwater depends on the range of ages that can be determine (Scanlon et al., 2002). In this context, age is defines as the time since water has entered the saturated zone, and groundwater ages can be readily estimated by comparing the concentration of these tracers found in groundwater to those

found in precipitation (Adomako et al., 2010). The age of groundwater can be estimated from $^{3}H/^{3}He$ data using (Scanlon et al., 2002):

$$t = -\frac{1}{\lambda} \ln \left[1 + \frac{3_{He}}{3_{H}}\right] \quad [14]$$

Where $\lambda(\frac{ln2}{t^{\frac{1}{2}}})$ is the decay constant, $t^{\frac{1}{2}}$ is the ^{3}H half-life (12.43 years), and ^{3}He is tritiogenic ^{3}H. CFCs and $^{3}H/^{3}He$ can be applied in estimating recharge rates in unconfined, shallow aquifers with water tables less than 10 m deep which are dominated by vertical groundwater flows, and can be used to determine groundwater ages up to 50 years, with a precision of 2 to 3 years (Scanlon et al., 2002). Recharge rates determined using groundwater dating spatially integrate recharge over an area up-gradient from the measurement point, and are average rates over the time period represented by the groundwater age (Xu & Van Tonder, 2001). $^{3}H/^{3}He$ can be used to determine groundwater recharge rates of 100 to 1000mm/year, but can be difficult to estimate recharge rates of less than 30mm/year due to the diffusion of ^{3}He into the unsaturated zone, and the difficulty of obtaining discrete samples near the water table (Misstear, 2000). Recharge rates in confined and deeper aquifers with groundwater ages of 200 to 2000 years can be estimated using the radioactive decay of ^{14}C (Cook & Solomon, 1997).

The groundwater age indicators are becoming more established as a reliable tool/technique for estimating recharge rates in semi-arid regions in unsaturated zone moisture profiles. An example of a successful use of this technique was in the deserts of Senegal, where the sandy dunes and deserts were closely studied in conjunction with the incidence and intensity of rainfall events. The findings of this study verified that recharge had occurred (Edmunds, 1992).

(c) Isotopic tracers (stable isotopes of oxygen and hydrogen)

Stable isotopes have been used extensively in catchment studies to determine groundwater recharge, transit time and water flow paths, as they are transported conservatively in shallow aquifers (Sophocleous, 2005). These isotope tracers are very useful in providing information about the soil water fluxes (evaporation, transpiration, and downward infiltration) that is difficult to determine by other techniques (Adomako et al., 2010). They maintain the same combinations of the meteoric water, and record the status of the initial formed meteoric water making them permanent tracers (De Souza et al., 2019). These isotopes are naturally abundant in precipitation but due to the process of fractionation, seasonal variability in water isotopes occurs. This seasonal variability is then attenuated by transport processes in the subsurface, and can be reflected in shallow groundwater systems allowing the identification of the physical processes that may have altered the isotopic composition (Adomako et al., 2010). The fractionation process that exist between heavy and light isotopes supports the applicability of these isotopes to identify groundwater infiltration at high altitude regions, and as well as where evaporation has occurred prior to recharge (Bredenkamp et al., 1995).

Stable isotopes offer insight into the groundwater system's recharge and flow since they make up the actual water molecule, and their composition remains the same unless the flow

path is subjected to phase changes or fractionation. This makes it possible to trace recharge water sources, physical processes and flow path by examining the differences in isotopic signatures of various different waters. Groundwater isotopic composition content is dependent on the recharge isotopic composition content (Islam et al., 2016).

Stables isotopes can provide an extensive visual understanding of the water cycle, and could contribute important information to other estimation techniques. Developments of more sophisticated and automated instrumentation for a very precise isotopic measurement, stable isotopes have become a vital component for hydrological studies (Bredenkamp et al., 1995). This method is well-established, straight forward, inexpensive, and it has both technological and economic benefits for water resources (Barbieri, 2019; Islam et al., 2016). Furthermore, a single stable isotope analysis can yield a considerable amount of information on the hydrological processes, hence this method would be best for the purpose of the project.

3. ENVIRONMENTAL SETTING

The Verlorenvlei catchment with an estimated area of 1832 km^2 is situated within the Sandveld area in South Africa, and is the most important and largest natural wetland in West Coast region of South Africa. The Verlorenvlei area is known for its intensive agricultural activities which support 15 % of the country's potato industry (Watson et al., 2018). As such agriculture is the dominant water user in the catchment with an estimated usage of 20 % of the total recharge (DWAF, 2003; Conrad et al., 2004). This has caused the Verlorenvlei area to be highly dependent on groundwater, as surface water resources are scarce. The catchments consists of the Pieketberg Mountains (1446m) in the east, which receive average annual rainfall of ~790 mm/year. Rainfall amount decreases moving to the western parts of the catchment from the Pieketberg Mountains and reaches a low of ~210 mm/year at the mouth of the Verlorenvlei (Lynch, 2004). The dominant feature of the catchment is the Verlorenvlei estuarine lake, situated between Redelinghys and Elandsbay, with an approximate size of 15 km^2. The estuarine lake is fed by four main tributaries namely, Kruismans, Bergvallei, Hol, and Krom Antonies rivers (Miller et al., 2018). The Krom Antonies tributary originates in the Pieketberg Mountains where average annual precipitation exceeds that of the lower lying areas of the catchment. The Hol and Kruismans are variably saline (Eilers, 2018). The lake is host to a variety of natural vegetation, including the Strandveld, Karroid and Fynbos biomes that are sensitive to reduced freshwater inflows (Helme, 2007). The lake has been RAMSAR listed due to its unique biodiversity that has been derived from the interaction between fresh and marine water (Miller et al., 2018). The environment has adapted to low rainfall conditions (Watson et al., 2018), and these rainfall distributions and volumes as well as high groundwater abstractions in the catchment have had a negative impact on the on the water quality and the level of water within the lake resulting in saline conditions (Miller et al., 2018).

3.1 Geology

The geology of the catchment consists of the Neoprotozoic Malmesbury Group (~760 Ma) which is the oldest of the major groups found in the catchment (Watson et al., 2018). This group has been divided into three terranes and three major groups. The three terranes are namely the, Northeastern Boland terrane, Central Swaartland terrane, and Southwestern Tygerberg terrane, with their formation controlled by tectonic processes (Hartnady et al.,

1974). The tectonic processes which have been formed the three terranes form part of the Pan African Orogeny, where the Malmesbury group has formed part of a low-grade Saldanha Belt, and a north-westerly striking fault zone (Gresse et al., 2006). The Pieketberg-Wellington Fault which lies at South-Eastern parts of boundary catchment, has caused a separation between north eastern Boland and Central Swaartland terranes (Eilers, 2018). The Redelinghys fault, which runs through the centre of the catchment, is believed to be associated with the Pieketberg-Wellington Fault and a product of Pan-African tectonics (De Beer, 2003).

The Verlorenvlei lies in the Boland terrane, with a small portion of the Moreesburg Formation of the Swaartland terrane outcropping on the eastern edge of the catchment where greywacke and phyllites dominant (Gresse et al., 2006). The sediments of the Malmesbury Group are thought to have been deposited on a passive continental margin (Rozendaal et al., 1994). This group is represented by the Pieketberg Formation of the Boland terrane which occur between Pieketberg and Redelinghys, and is composed of highly foliated and lineated rocks comprising of quartzite, sericitic schist, greywacke, conglomerate and limestone (Rozendaal & Gresse, 1994). The Porterville Formation covers a large area in the eastern parts of the catchment, and consists of greywacke and phyllites (Gresse et al., 2006).

The Malmesbury Group has been intruded between Redelinghys and Pieketberg by the Riviera Pluton of the Cape Granite Suite (Watson et al., 2018). The Malmesbury Group and the Cape Granite Suite are unconformably overlain by the sedimentary rocks of the Palaeozoic Table Mountain Group (TMG), which represent the youngest rocks in the catchment and outcrops the Redelinghys area, and they dominantly make up the high elevation mountains around the catchment (Miller et al., 2018). Quartzose sandstones of the TMG form the part of the Pieketberg and Cederberg mountain ranges that flank through the eastern ridges of the Sandveld, and their depositional environments may range from shallow marine to glacial deposits with hard and resilient nature that contrasts with the easily weathered rocks of the surrounding Malmesbury Group (Eilers, 2018). The TMG group is comprised of three major formations, the oldest being the Piekenirskloof Formation which is dominant in the Sandveld region, consisting of varying amounts of conglomerate, and coarse grained sandstone with small patches of mudrock and can reach a maximum thickness of ~900m (De Beer, 2003; Thamm and Johnson, 2006). The Piekenirskloof Formation is overlain by the Graafwater Formation consisting of sandstone, siltstone, and shale. The sandstone components of the Graafwater Formation may vary between 50% and 100% of the total formation (De Beer, 2003). This formation may reach thicknesses of up to 430m (Thamm and Johnson, 2006). The Graafwater Formation is overlain by the Peninsula Formation (~2000m) and is dominated by quartz arenite minor shale and conglomerates (Rozendaal et al., 1994; Thamm and Johnson, 2006). This formation is also characterised by bedding planes which may vary between 1m and 4m (De Beer, 2003). The Sandveld Group of the Cenozoic deposits is the youngest geological unit covering the south-western coast from False Bay to Elandsbay (Rozendaal et al., 1994).

3.2 Soils

The catchment is classified as a zone of littoral sands with nine different types of soils (arensols, leptosols, solonetzs, fluviols, planosols, regosols, lixisols, cambisols, and luvisols), and is generally characterised by fine sandy soils, with isolated sections classified as rocks and undifferentiated lithosols on the southern shores, extending from Elandsbay to Redelinghys (CSIR, 2009). The coastal lowlands of the catchment consist of sands and conglomerates with low water retaining capacity (Johnson et al., 2006). The soils are relatively infertile nearer to the coast, variably saline, and alkaline with a distinct horizon of lime accumulation, that may reflect water logging (CSIR, 2009). A large dune field is also present in the catchment towards the north of the estuary mouth and towards Elandsbay, and several patches of drift sand and bare dunes away from the coast have originated mostly from the mismanagement of the veld (CSIR, 2009).

3.3 Hydrogeology

The catchment consists of three aquifer units, (1) the unconsolidated-primary porosity aquifer on the west on the catchment characterised by high yields and is made up of coarse-grained clean sand ~15m thick, (2) the fractured-rock secondary-porosity aquifer which underlies the primary-porosity aquifer, with visible geological features such as weathering zones, bedding surfaces and faults controlling the flow of groundwater, and is made up of Malmesbury Group shale with varying transmissivity of between 0.07m^2/d and 7m^2/d (Watson et al., 2018; Miller et al., 2018), and (3) the TMG aquifer which is also a fractured-rock aquifer system (Miller et al., 2018). The fractured-rock secondary-porosity aquifer is also said to be associated with high yielding boreholes and good groundwater quality, especially where the Krom Antonies river is located (Eilers, 2018). The primary aquifer is prone to contamination from anthropogenic activities due to its shallowness and unconfined nature, and its salinity increases towards the coast (SRK, 2009). The TMG rocks that make up the Pieketberg Mountains in the hinterland to the Verlorenvlei lake also constitute an important fractured rock aquifer system, where transmissivity estimates for the Peninsula Formation vary between 15m^2/d and 200m^2/d (Weaver et al., 1999). There is a strong hydrological connection between the primary and secondary aquifers as shown by the recharge relationship between the two aquifers, and the high piezometric head suggesting that the secondary aquifer may discharge into the primary aquifer (Watson et al., 2018). Groundwater recharge primarily occurs within the high relief areas where the TMG aquifer dominates, similar to other high lying areas within the Western Cape (Watson et al., 2018). The primary aquifer is thought to have been recharged directly from rainfall, while the secondary aquifer shows much more limited response from rainfall (Watson et al., 2018). This has led to suggestions that the secondary aquifer may be recharged by the overlying TMG aquifer at the top of the Moutonshoek sub-catchment as evident from the high hydraulic gradient and the groundwater flow that is controlled by the faults (Watson et al., 2018). This has also been supported by the high potential evaporation which limits vertical recharge from rainfall in the valleys (Watson et al., 2018).

3.4 Hydrology

The Verlorenvlei comprises four quaternary catchments (G30B, G30C, G30D, and G30E), (Fig. 5) (CSIR, 2009), that drain the low relief sandy coastal plain with most the water originating in the eastern edges of the Cape Fold Belt in the upper reaches of the Verlorenvlei river (DWAF, 2003). These gauging stations have not been operational since 2009, but water level monitoring is still active within the Verlorenvlei estuarine lake towards Elandsbay (Watson et al., 2018). During dry periods, the water level in the lake can drop significantly causing the water to become stagnant and saline resulting in the growth of algae (Watson et al., 2018; DWAF, 2003). These low water levels are caused by the changes in rainfall patterns, but also agricultural abstractions that are likely to reduce the flow water flow in the lake's major feeding rivers (Watson et al., 2018).

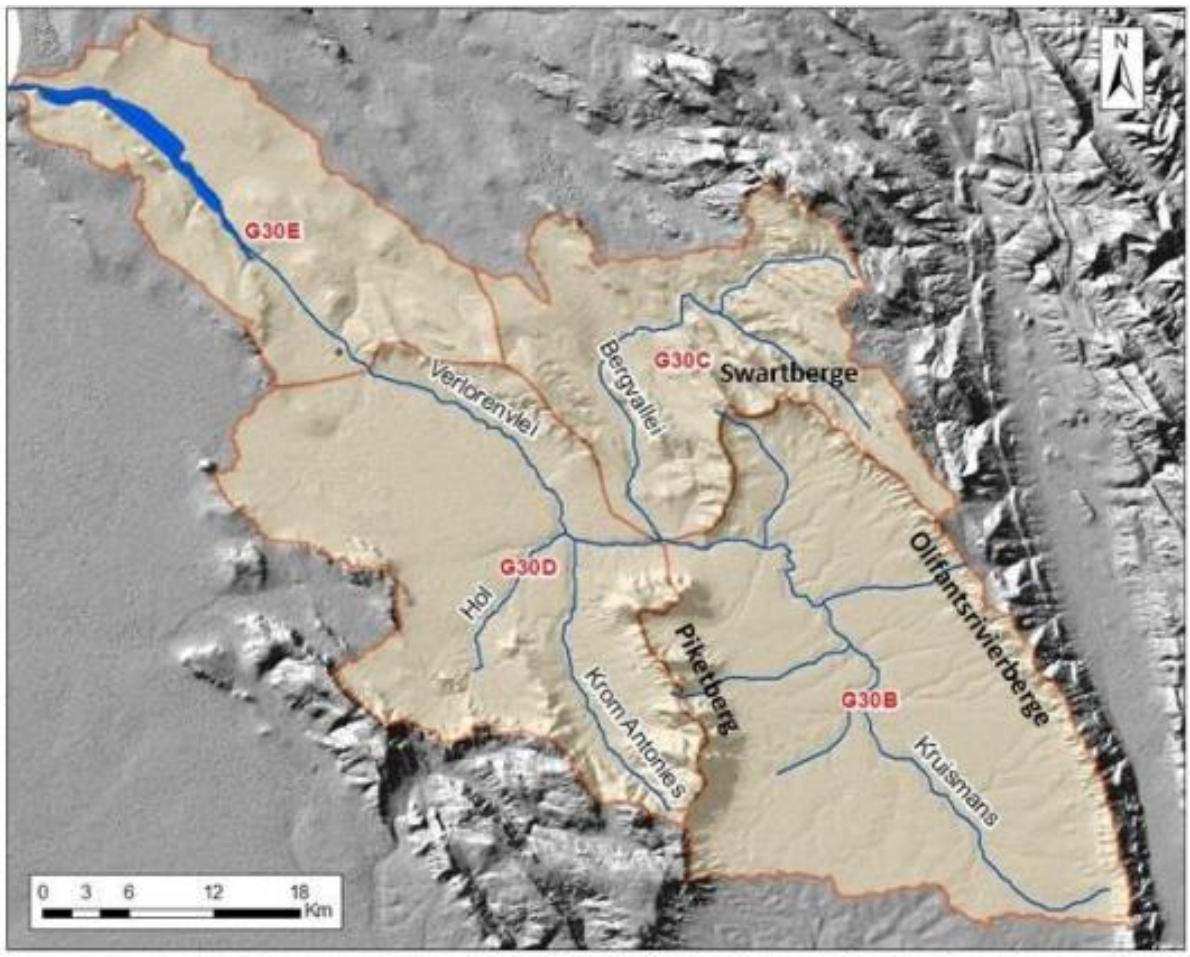

Figure 5: Showing the Quaternary catchment of the Verlorenvlei (Eilers, 2018).

The Krom Antonies river is the most significant contributor of both quantity and quality of flow into the lake, and it receives its water from the highest areas of the Pieketberg mountains (Watson et al., 2018). The Kruismans River is the longest tributary and originates from the eastern parts of the Pieketberg Mountains, where it drains the extensive low lying Kruismans basin between the Olifansrivier Mountains and the Pieketberg Mountains (Eilers, 2018) and

a large relatively flat agricultural region (Watson et al., 2018). As it passes through the wide neck in the eastern part of the Pieketberg mountains, it joins up with the south draining Bergvallei river (Watson et al., 2018). The point on the Kruismans river after these three rivers have joined is known as the confluence (Miller et al., 2018). The river below the confluence is the Verloren river, which drains westwards until the beginning of the actual lake west of Redelinghys. The Verlorenvlei river flows mainly in winter and early summer, and contributes fresh water input to the estuarine system (Eilers, 2018). The Bergvallei River is mostly dry with a lack of surface water flow, resulting in parts of the river bed being ploughed for agriculture. It drains the Swaartberg and flows into the Kruismans river (Eilers, 2018). The Krom Antonies River is the most significant in terms of freshwater input into the Verlorenvlei. The Hol river only flows sporadically after good long rains but is more saline than the other tributaries into the Verloren River (Eilers, 2018).

3.5 Climate and Vegetation

The Verlorenvlei catchment has a Mediterranean climate, with 80% of its rainfall generated by cut-offs lows and low pressure systems during the winter months (April-September) (CSIR, 2009; Holloway et al., 2010). The highest amounts of rainfall (~790mm/year) occur in the Pieketberg Mountains where the Krom Antonies river originates (Fig. 6), southeast of the catchment (Eilers, 2018), and decreases moving northwest from the Pieketberg mountains reaching a low of 210mm/year at the mouth of the Verlorenvlei at around 50m above sea level (Watson et al., 2018). The summer daily average temperatures are between 17 and 23 ^{0}C, and are associated with increased mean annual evaporation rates ranging between 5.5 and 7.35 mm/d, whereas in winter average daily temperatures are between 8 and 13 ^{0}C, with low mean annual evaporation rates ranging between 1.5 and 2.3 mm/d (Schuzle et al., 2007).

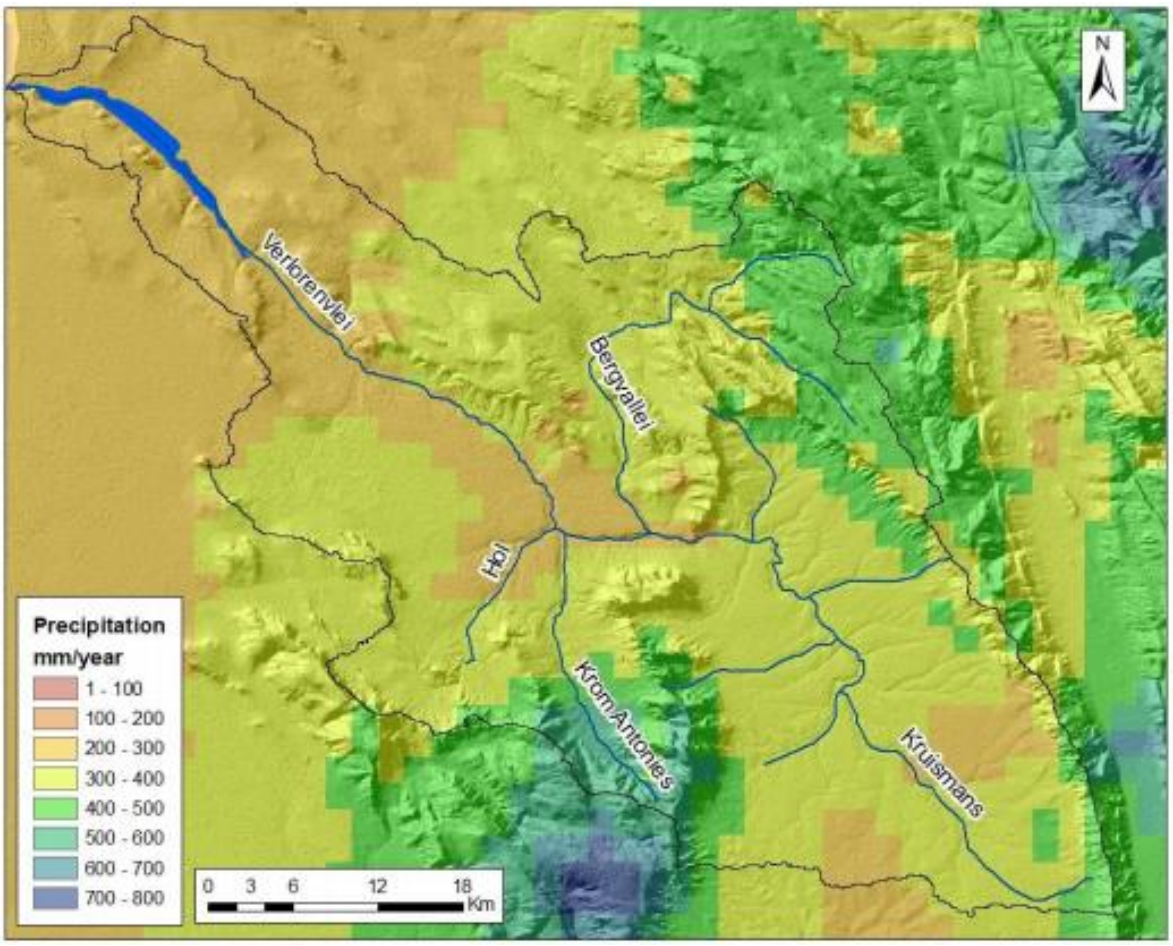

Figure 6: Showing the mean annual precipitation of the Verlorenvlei catchment (Watson et al., 2020).

The vegetation types in the catchment have adapted to the low rainfall environments, making soil evaporation more important than transpiration, even though these have not been well constrained within the catchment (Watson et al., 2018). Most indigenous vegetation present in the catchment is the Sandveld, a semi-succulent vegetation transitioning between Coastal Fynbos, and Succulent Karoo vegetation (CSIR, 2009). Both these biomes are ecologically important, thus have been identified as the top conservative sites by the South African government (CSIR, 2009).

3.6 Land use and land cover

Agriculture in the Sandveld region is the major water user, accounting for more than 80% of the total water demand (Watson et al., 2018). Potatoes in the Sandveld are the major primary food crop grown, accounting for over 6600 ha of land, and can use up to 20% of the total recharge (DWAF, 2003). These potatoes are usually grown in sandy soils and may result in high yields, but require large amounts of water and fertilizers to grow successfully (Watson et al., 2018). Tea is also grown in the sandy soils of the Sandveld area, making it the second most grown crop in the catchment accounting for more than 5000 ha. Tea is rain fed in the catchment, and requires less amounts of water for processing and has limited impact on

groundwater resources (Watson et al., 2018). Some fields in the southern shores of the area have been left bare between crop rotation resulting in soil erosion, and the greatest pasts Verlorenvlei wetlands used as grazing lands for livestock (CSIR, 2009). Other high water use agricultural activities in the Sandveld includes is the production of citrus and viticulture in the upper reaches of the Moutonshoek as well as in the Kruismans basin (Watson et al., 2018).

4. METHODOLOGY

4.1 Study Area

The Verlorenvlei catchment is situated on the west coast of South Africa, and within the Sandveld area. For the purpose of this project, 10 locations (farms) were selected namely, Doornfontein, Kruispad, Sebulon, Eagles Rest, Kardoesie, Farawayfields, Padstal, Beaverlac, Olifants Doorn and Volgenvontein (Fig. 7). Kruispad, Sebulon and Doornfontein are located in the lower catchment, Eagles Rest, Farawayfields, Eagles Rest, Kardoesie and Padstal are located in the middle catchment, with Volgenvontein, Olifants Doorn and Beaverlac situated in the upper catchment (See Fig. 7 for the distribution of the locations). These sites were selected in such a way that they cover a larger area of the catchment, and to the lower parts of the catchment (close to Redelinghys) where less sampling and research has been done. Groundwater samples were collected from Doornfontein, Sebulon, Eagles Rest, Kardoesie, Farawayfields, Padstal, Beaverlarc, and Farawayfields. Riverwater samples and springwater samples were collected from Kruispad and Olifants Doorn respectively. A total of 100 groundwater samples, 2 springwater samples, 9 riverwater samples, and 75 precipitation samples from all the sites were collected from July 2019 to January 2020.

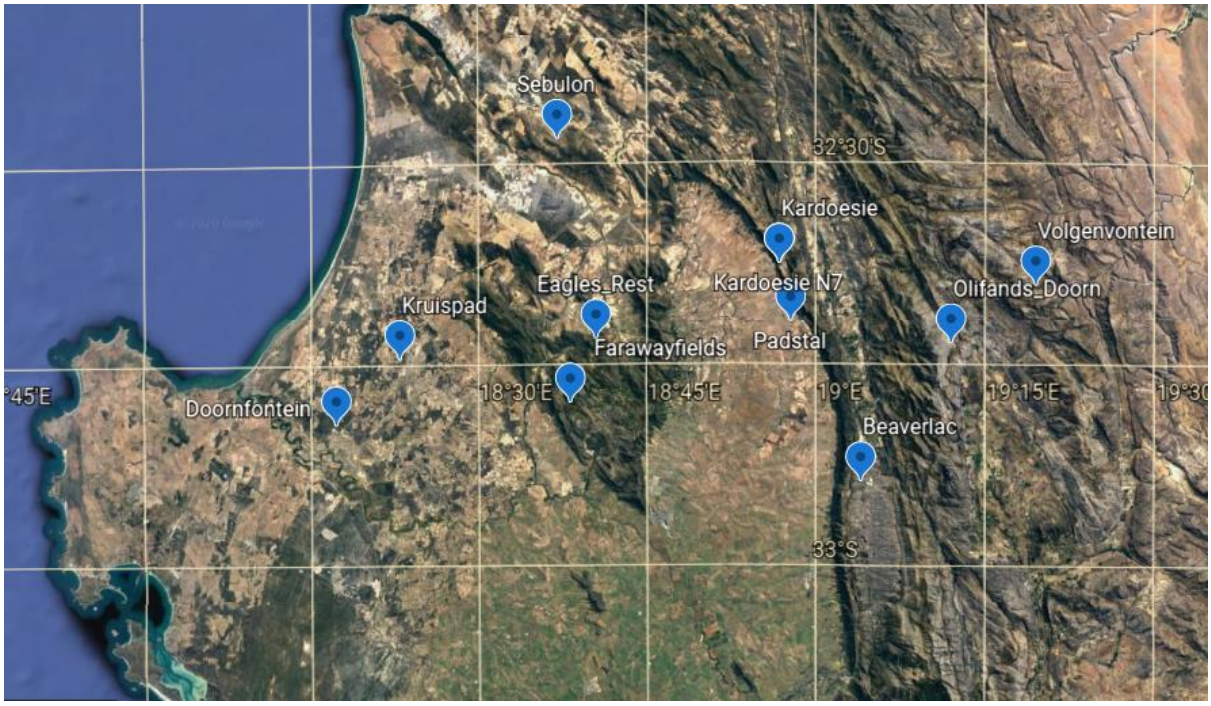

Figure 7: Distribution of groundwater and precipitation sample locations in the Verlorenvlei catchment (taken from Google Earth).

4.2. Field sampling

A reconnaissance field visit was undertaken in July 2019, to assess the catchment and to identify local farmers who would be willing to assist with rainwater, river water, spring water and groundwater sample collection. A total of 10 (farmers) locations were selected and which agreed to assist with the collection of samples, all of them expected to start sampling in August. A follow up visit was undertaken later in July 2019 to deliver the sample bottles to the identified farms and the farmers were instructed on the correct sampling and labelling protocol (Date, location, sample type (groundwater or rainwater), time), and to keep the samples cool (avoid high temperatures or direct sunlight) until collection during the next visit (5 site visits were made). The farmers were instructed to collect weekly groundwater samples, river water at the same location and depth and one rainwater sample after each rainfall event for a year (August 2019-August 2020). 50ml PP tubes were provided to collect the samples from the 10 sites.

4.2.1 Groundwater collection

The farmers were instructed to purge their boreholes before collecting the sample to get a fresh groundwater sample (Fig. 8b), and also instructed to sample the groundwater on the same day each week (if collected on a Wednesday, it has to be every Wednesday).

Table 1: Number of groundwater samples collected per location (farmer) for a particular sampling period

Location	**Sampling period**	**No. of groundwater samples collected**
Padstal	August2019-October 2019	7
Sebulon	September 2019-November 2019	8
Volgenfontein	September 2019-October 2019	9
Beaverlarc	September 2019-October 2019	11
Doornfontein	August 2019-January 2020	22
Farawayfields	August 2019-January 2020	23
Kardoesie	August 2019-January 2020	14
Eagles rest	July 2019 to January 2020	6

There was an obvious difference in the collection patterns between the locations (farmers) which resulted to a huge difference in the number of samples being collected. These differences were caused by: (1) the 50 ml PP tubes used to collect groundwater samples were not delivered at the same time, hence the difference in the sampling period, (2) the farmers are so big, the people that have volunteered to collect the samples work in different locations within the farmers, so they forget to collect the samples, (3) some farmers who were collecting the samples themselves ended up going on holidays, and others going out of town (for working purposes), and this has greatly affected the number of samples being collected, (4) Covid-19 has had a huge impact, as many samples could not be collected because the country was shut down due to the safety regulations that were put in place. These reasons also affected the collection of riverwater, springwater, and rainfall.

4.2.2 Riverwater collection

The riverwater samples were collected at Kruispad, recording a total number of 9 riverwater samples. The samples were collected from September to October 2019. The farmers were instructed to take weekly direct measurements of river water at the same depth. The correct sampling and labelling protocol was explained.

4.2.3 Spring water collection

At Olifants Doorn 2 springwater samples were collected, with sampling starting from November to December, and the farmers were instructed to take direct measurement of spring water (Fig. 8a). The farmers were also instructed to take weekly spring water samples,

and the correct sampling (rinsing the sampling bottle 3 times before taking a sample) and labelling protocol was explained.

Figure 8: (a) Springwater sampling (OD-SP - Olifants Doorn) and (b) Groundwater sampling (ER - Eagle's Rest).

4.2.4 Rainwater collection

A total of 75 rainfall samples were collected from the 10 sites (Table 1)., and the correct collection procedure was explained (labelling the tube with date, time, and location), also the transferring of rainwater from the rain gauge to a clean 50ml PP tube was explained.

Table 2: Number of rainfall samples collected per location (farmer)

Location	**No. of rainfall samples collected**
Padstal	2
Sebulon	1
Volgenvontein	3
Beaverlarc	5
Doornfontein	9
Kruispad	2
Farawayfields	21
Kardoesie	16
Eagles rest	15
Olifants Doorn	1

Rainwater water samples were collected using normal rain gauges at 9 locations, and a Hellmann rain gauge (Fig. 9) was used at Olifants Doorn to measure rainfall.

Figure 9: Hellmann rain gauge used to measure rainfall at Olifants Doorn.

4.3 Sampling Limitations

The impact of Covid 19 has had a huge impact on the number of groundwater, rainwater, spring water and rainwater samples that were collected for the purpose of this project. Although a proper methodology has been set up for this project, the number of samples that the project ended up with were not enough or the farmers/people who have volunteered did not get as many samples the project has thought they would, although weekly follow ups were made to understand if the farmers were facing any difficulties or if anything was unclear regarding the sampling procedures. Distance between the farmers was another limiting factor, this led to the 50 ml PP tubes used to collect the samples to be delivered at different types, and this has greatly affected the start of the sampling. There also could be a number of limiting factors that have led to the inadequate number of samples, from the farmer's workloads to some time away from the farm during holidays.

The last batch of samples could not be collected from February to June, due to the lockdown restrictions that were put in place, and this has forced the project to make analysis based on the limited number samples that was already collected. During the December, January, and February months, the area receives less amounts of rainfall, and this is a result of the high temperatures during these months. The West Coast receives most of its rainfall during the winter months. So, when this period ended or when it started raining, the lockdown happened, and has led to the other rainfall samples to not be collected, hence the inadequate number of rainfall samples from all the sites.

4.4 Analysis of O and H Stable Isotope Ratios

Oxygen and hydrogen isotope analysis was conducted for all the samples (100 groundwater, 75 rainwater, 2 springwater samples, and 9 river water samples). The oxygen and hydrogen isotope values were analysed relative to the SMOW (Standard Mean Ocean Water) standard. The results were reported as δ- values in parts per mil, which can also be expressed as ratios using δ notation:

$$\delta^2 H = \left[\frac{\left(\frac{^2H}{^1H}\right) sample}{\left(\frac{^2H}{^1H}\right) standard} - 1 \right] * 1000\ (‰) \qquad [15]$$

$$\delta^{18} O = \left[\frac{\left(\frac{^{18}O}{^{16}O}\right) sample}{\left(\frac{^{18}O}{^{16}O}\right) standard} - 1 \right] * 1000\ (‰) \qquad [16]$$

All the samples were analysed in the University of Lausanne (Geoscience Department), in Switzerland, using a Picarro Cavity Ring-Down Laser Spectroscopy System (model G1102-i). The Picarro analysis enables simultaneous measurement of $\delta^{18}O$, $\delta^{17}O$, and $\delta^{2}H$ in solids, liquids and vapor. The results have an analytical precision of 0.008 ‰ for $\delta^{17}O$, 0.004 ‰ for $\delta^{18}O$ and <1 ‰ for $\delta^{2}H$ (30-second measurements), with samples repeatedly measured several times.

^{17}O-excess was calculated according to (Luz & Barkan, 2010) using equation 9While deuterium excess (*d-excess*) was calculated according to equation 10

5. RESULTS

5.1 Precipitation Stable Isotope Data

The $\delta^{18}O$ and $\delta^{2}H$ ratios for the rainwater samples collected for the sites across the Verlorenvlei catchment range from -8.24 ‰ to 7.80 ‰, and -53.2 ‰ to 43.0 ‰, with simple means of -2.20 ‰ and -3.76 ‰ respectively for the sampling period (Refer to the Appendix page). The $\delta^{18}O$ and $\delta^{2}H$ ratios show similar distribution patterns with elevation across the catchment, albeit with $\delta^{2}H$ ratios showing greater variation compared to the $\delta^{18}O$ ratios. Good spatial variations in both δ^{18} and $\delta^{2}H$ occurs at Kardoesie, Doornfontein, Beaverlarc, and Farawayfields (Fig. 10). More positive $\delta^{18}O$ and $\delta^{2}H$ ratios are associated with lower elevations (e.g. Padstal) while lower$\delta^{18}O$ and $\delta^{2}H$ ratios are observed at higher elevations (e.g. Eagles Rest, Beaverlarc, and Eagles Rest) (Fig. 11). Eagles Rest and Volgenvontein have the same $\delta^{18}O$ ratio, with Volgenvontein and Olifants Doorn showing the same $\delta^{2}H$ ratios.

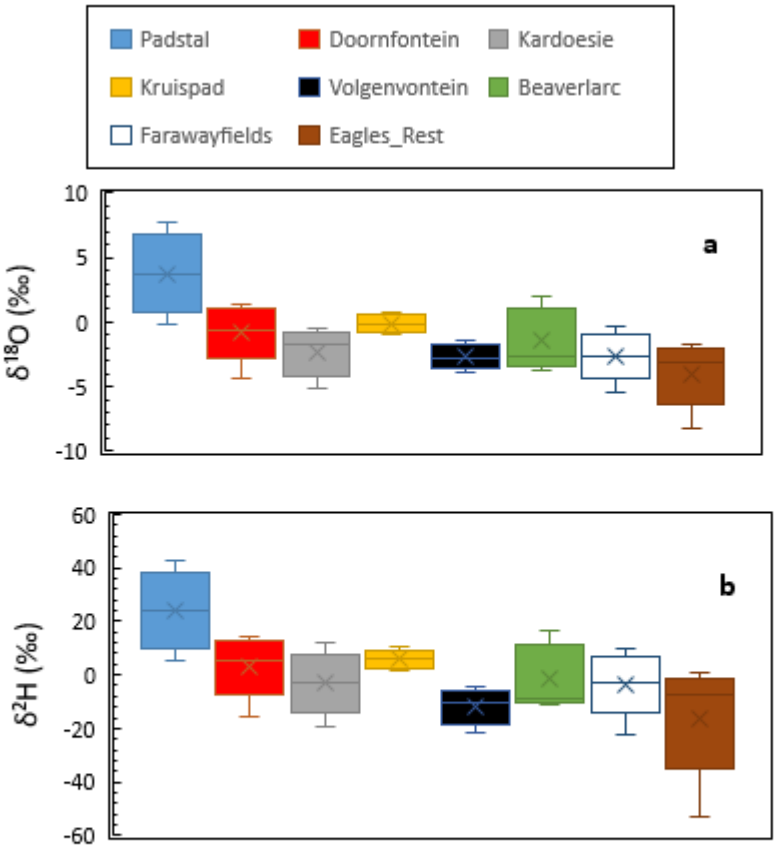

Figure 10: Variation in (a) $\delta^{18}O$ and (b) $\delta^{2}H$ in rainwater samples collected from the catchment across altitudinal gradient.

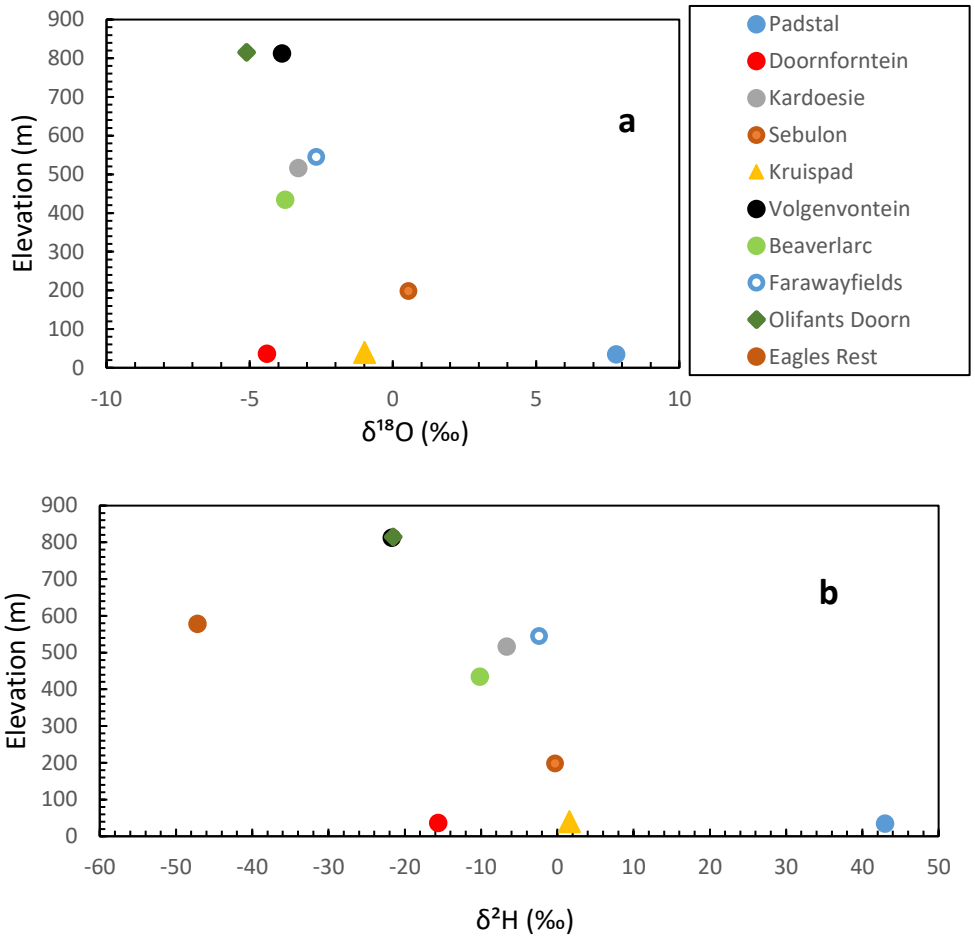

Figure 11: Variation of (a) $\delta^{18}O$ and (b) $\delta^{2}H$ in rainwater samples with elevation for each location site.

More positive $\delta^{18}O$ and $\delta^{2}H$ ratios occur in summer and most negative $\delta^{18}O$ and $\delta^{2}H$ ratios occurring in winter. The LMWL for this study, based on all data collected and not weighted to rainfall amount was determined to be $\delta^{2}H = 5.45\ \delta^{18}O + 8.27$, which shows a slight evaporation relative to the GMWL ($\delta^{2}H = 8\ \delta^{18}O + 10$) and the slope defined by Watson et al. (2020) ($\delta^{2}H = 6.48\ \delta^{18}O + 9.48$) (Fig. 11). The slope of the winter LMWL ($\delta^{2}H = 5.87\ \delta^{18}O + 9.21$) is higher than the slope of the LMWL ($\delta^{2}H = 5.45\ \delta^{18}O + 8.27$) and the summer LMWL ($\delta^{2}H = 5.00\ \delta^{18}O + 7.58$), but lower than slope (6.48) obtained by Watson et al. (2020). The slope of the general LMWL of this study is lower than the slope obtained by (Diamond & Harris, 1997) ($\delta^{2}H = 6.2\ \delta^{18}O + 10.6$). These results are based on the number samples that were collected, and this study also acknowledges that the total number samples presented may not be adequate. This will be further explained under the discussion section.

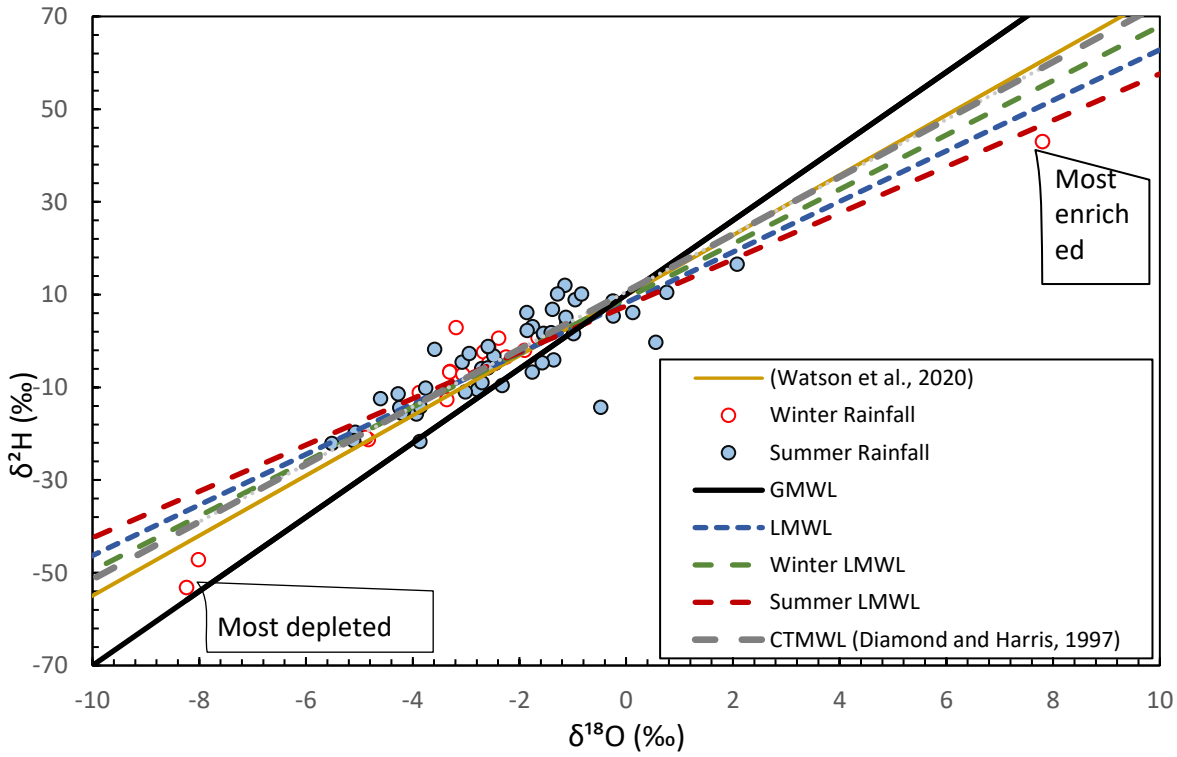

Figure 12: $\delta^{18}O$ vs $\delta^{2}H$ of the rainwater samples collected from the Verlorenvlei Catchment, and the slope of the LMWLs: Local Meteoric Water Line, Winter LMWL, Summer LMWL in comparison with the slope obtained by Watson et al. (2020); GMWL: Global Meteoric Water Line, and the CTMWL: Cape Town Meteoric Water Line by Diamond and Harris (1997).

The isotopic composition of the rainwater records effects of the changing seasons (Fig. 12). The summer LMWL shows a slight evaporative trend relative to the GMWL and the winter LMWL. The LMWLs observed for the two seasons are: $\delta^2\mathrm{H} = 5.87 \times \delta^{18}\mathrm{O} + 9.21$ for winter and $\delta^2\mathrm{H} = 5.00 \times \delta^{18}\mathrm{O} + 7.58$ for summer.

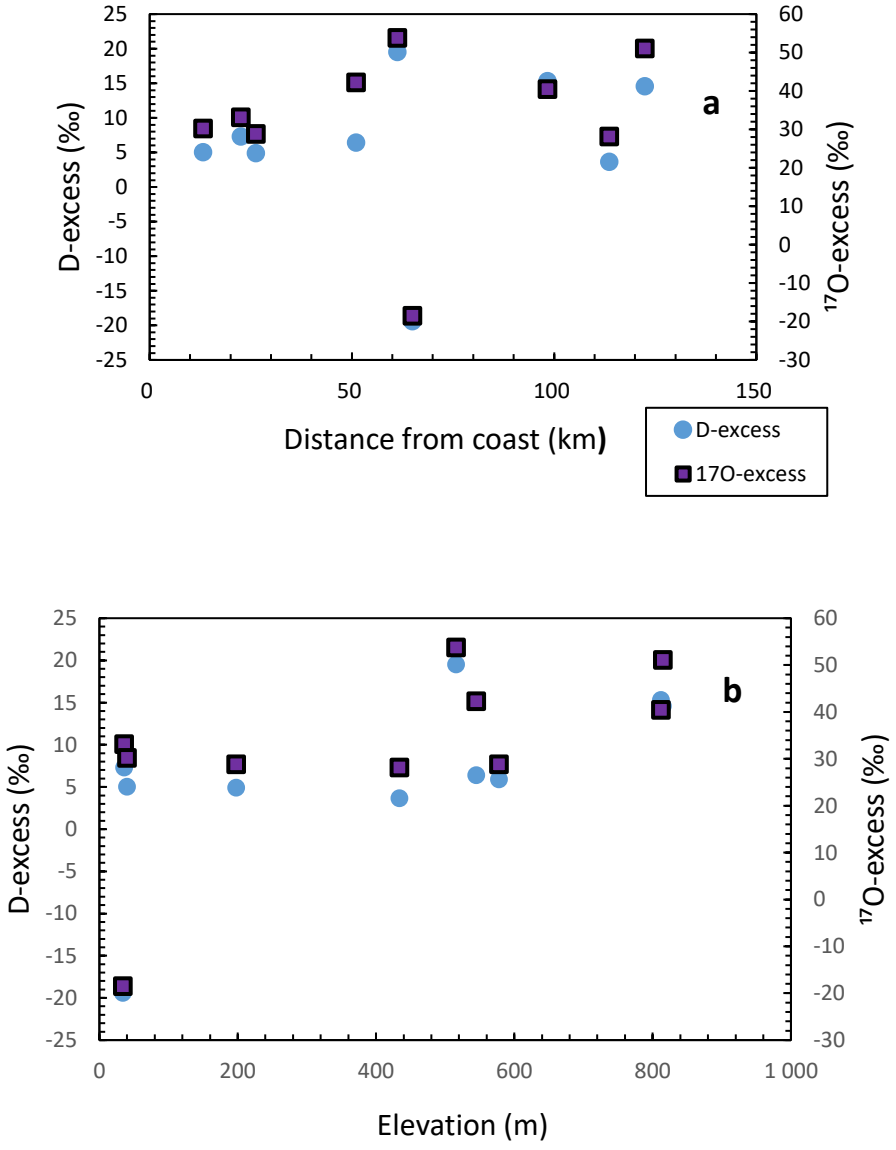

Figure 13: Variation of δ^{17}O-excess and D-excess in rainwater with (a) increasing distance from the coast/ocean and (b) elevation. See Fig. 7 for sample locations.

Deuterium excess (calculated using equation 10) and ^{17}O-excess (calculated using equation 9), for the rainfall samples collected, ranges from -19.4 ‰ to 28.4 ‰ and -18.5 ‰ to 76.7 ‰

respectively (Refer to the Appendix page). Both values show no correlation with increasing distance from the coast/ocean, with r^2 = 0.07 for deuterium excess and r^2 = 0.08 for δ^{17}O-excess (Fig. 13). D-excess and δ^{17}O-excess show moderate correlation with elevation, with r^2 = 0.39 for D-excess, and r^2 = 0.38 for ^{17}O-excess. They do not show similar spatial distribution patterns. The δ^{18}O and δ^{2}H ratios in rainwater show no correlation with increasing distance from the coast/ocean, r^2 = 0.007 for δ^{18}O and r^2 = 0.0001 for δ^{2}H. Both δ^{18}O and δ^{2}H ratios show similar spatial distribution patterns across the catchment (Fig. 14).

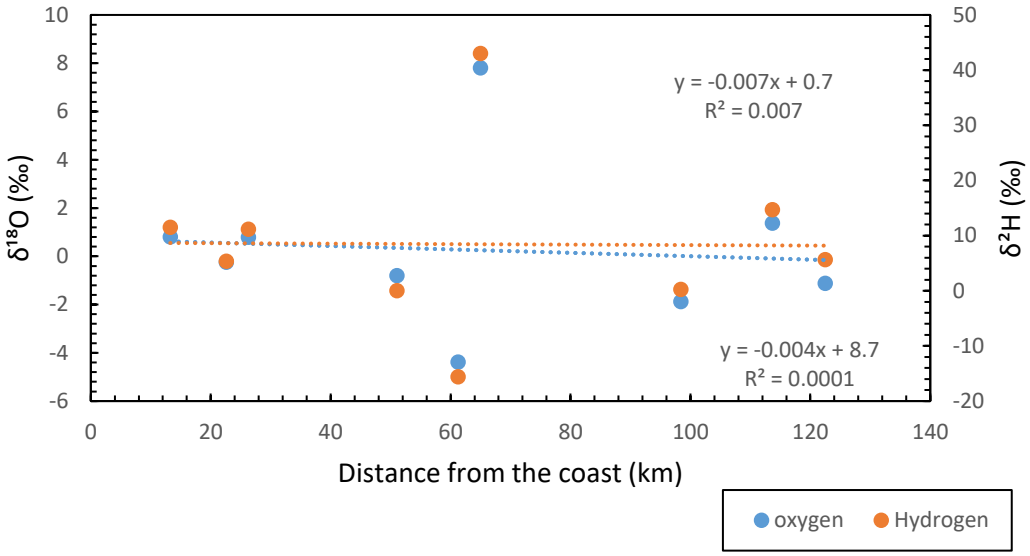

Figure 14: Variation of δ^{18}O and δ^{2}H ratios in rainwater with increasing distance from the coast/ocean.

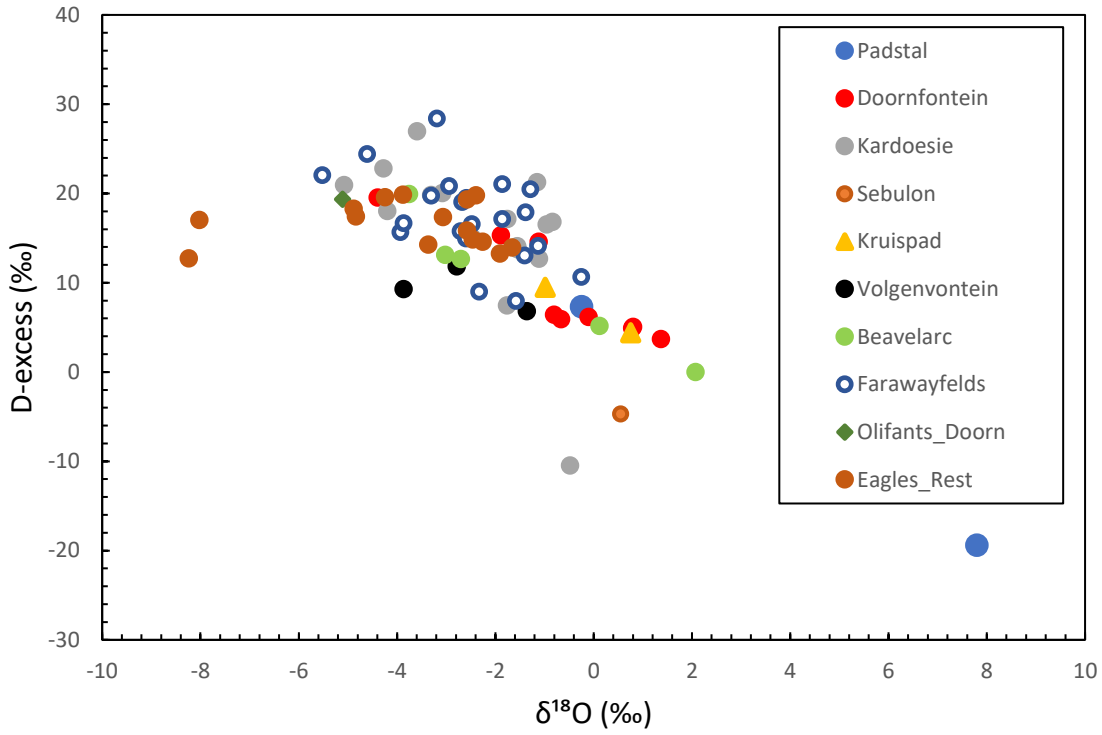

Figure 15: Relationship between d-excess and $\delta^{18}O$ for the rainwater collected from the Verlorenvlei catchment. See Fig. 7 for sample locations.

The distribution of d-excess and $\delta^{18}O$ show a moderately strong negative correlation (r^2 = 0.52), the higher the $\delta^{18}O$ value the lower the d-excess value. Most samples show a similar variation between d-excess and $\delta^{18}O$. One sample at Padstal recorded a significantly different and more positive $\delta^{18}O$ ratio and more negative d-excess value.

^{17}O-excess and δ^{18}O show a moderate negative correlation (r^2 = 0.4). (Fig. 16), similar to the trend seen between d-excess and δ^{18}O in Fig. 15. Increasing ^{17}O-excess values are indicative of low humidity, less evaporation influences, and possibly strong evapotranspiration influences. This is also evident from the isotopic depletion in δ^{18}O from the rainwater samples collected from the catchment. Isotopic depletion of the rainwater samples is associated with an increase in ^{17}O-excess values with a similar trend observed in Fig. 15. The higher the ^{17}O-excess values, the lower the δ^{18}O values (Fig. 16).

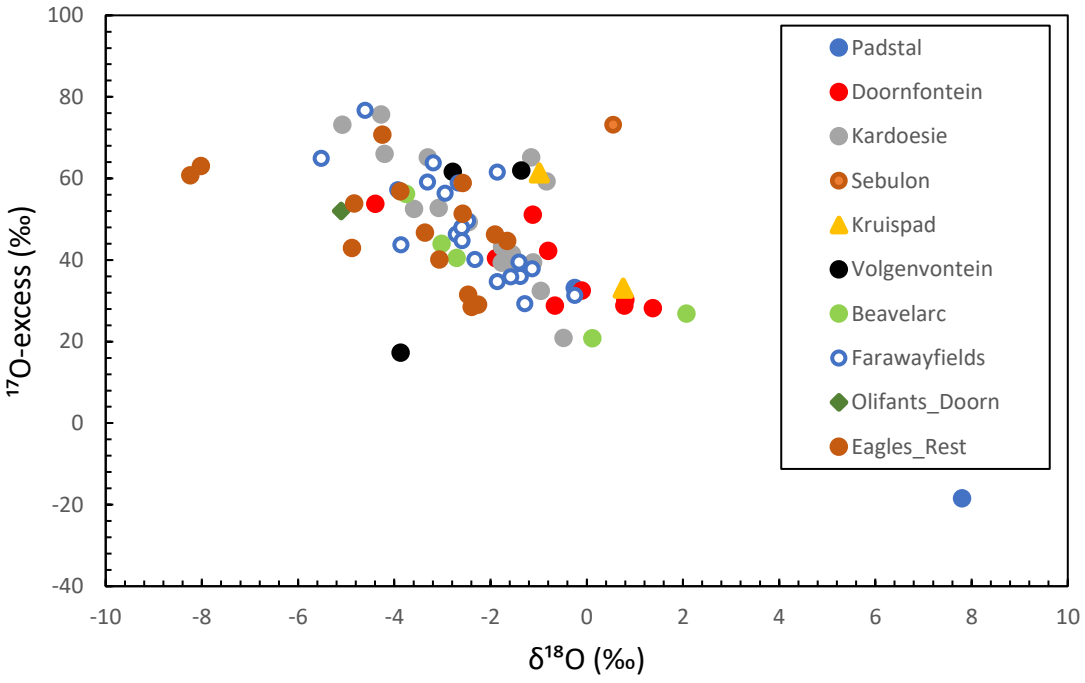

Figure 16: Showing relationship between ^{17}O-excess and δ^{18}O for the rainwater samples collected from the catchment.

5.2 Precipitation amounts

Tables 3, 4, and 5 shows how the $\delta^{18}O$ and $\delta^{2}H$ ratios in rainwater vary with rainfall volume/amounts at Kardoesie, Farawayfields, and Eagles Rest.

Table 3: Showing stable isotopic variation with rainfall amount for Kardoesie.

	Kardoesie		
Date	**$\delta^{18}O$ (‰)**	**$\delta^{2}H$ (‰)**	**Rainfall amount (mm)**
31/8/2019	-3.3	-6.6	1
12/9/2019	-4.2	-15.6	15
13/9/2019	-4.3	-11.4	4
21/9/2019	-1.0	8.9	4
29/9/2019	-1.5	1.4	3
9/10/2019	-1.8	3.1	4
26/10/2019	-1.8	-6.7	10
27/10/2019	-5.1	-19.7	9
28/10/2019	-3.6	-1.8	5
6/11/2019	-1.1	3.8	1.5
3/12/2019	-3.1	-4.6	8
14/12/2019	-1.6	1.7	5
18/12/2020	-1.2	12.0	4
19/12/2019	-0.8	10.1	3
7/1/2020	-0.5	-14.3	3.5
25/1/2020	-2.5	-4.7	10

Both $\delta^{18}O$ and $\delta^{2}H$ ratios in rainwater show a moderate negative correlation with the rainfall volumes/amounts, r^2= 0.2 for $\delta^{18}O$, and r^2= 0.3 for $\delta^{2}H$ (Fig. 17). $\delta^{2}H$ values show the greatest variation.

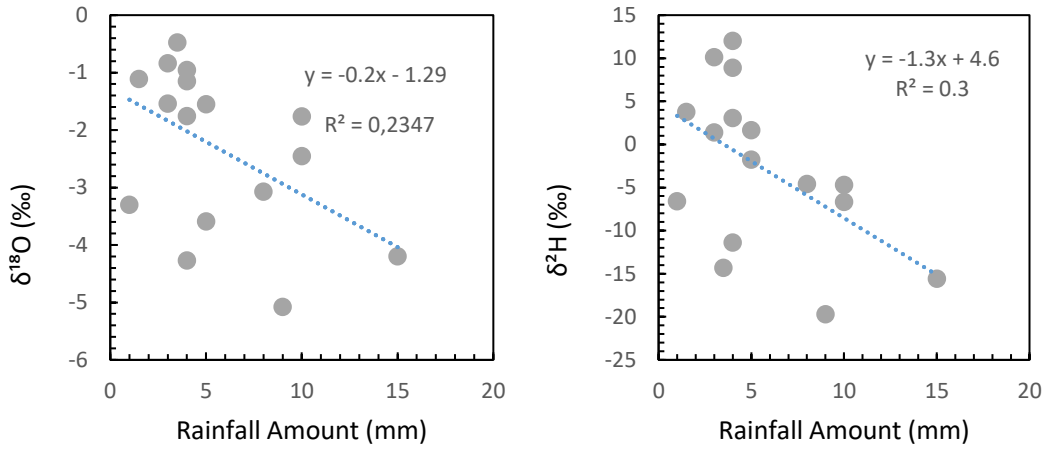

Figure 17: Variation of $\delta^{18}O$ and $\delta^{2}H$ ratios with rainfall amount from samples collected at Kardoesie.

Table 4: Showing stable isotopic variation with rainfall amount for Farawayfields.

	Farawayfields		
Date	**$\delta^{18}O$ (‰)**	**$\delta^{2}H$ (‰)**	**Rainfall amount (mm)**
26/8/2019	-2.7	-2.4	5.5
27/8/2019	-3.2	2.9	2.5
30/8/2019	-3.3	-6.7	4
12/9/2019	-3.9	-15.8	10
13/9/2019	-5.5	-22.1	7.5
21/9/2019	-2.5	-3.3	17
29/9/2019	-2.7	-5.9	12
9/10/2019	-1.9	2.3	5
25/10/2019	-2.3	-9.6	20
27/10/2019	-1.9	6.1	16
28/10/2019	-4.6	-12.5	9.4
6/11/2019	-3.9	-14.2	0.5
7/11/2020	-1.3	10.1	1
12/11/2019	-0.2	8.6	1
3/12/2019	-2.6	-1.2	10
14/12/2019	-1.1	5.1	10
18/12/2019	-1.4	6.8	9
21/12/2019	-1.6	-4.7	3.5
26/12/2019	-2.9	-2.7	3.5
8/1/2019	-1.4	1.8	2
20/12020	-2.6	-5.8	2

$\delta^{18}O$ and $\delta^{2}H$ ratios in rainwater from samples collected at Farawayfields are weakly correlated, r^2= 0.006 for $\delta^{18}O$, and r^2= 0.02 $\delta^{2}H$. $\delta^{18}O$ ratios have more negative values compared to the $\delta^{2}H$ ratios, whereas $\delta^{2}H$ ratios have more positive values (Fig. 18).

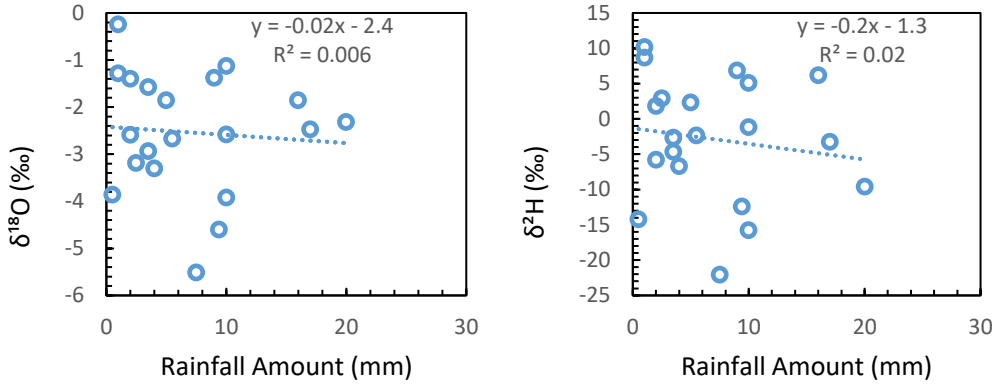

Figure 18: Variation of $\delta^{18}O$ and $\delta^{2}H$ ratios with rainfall amounts from samples collected at Farawayfields.

Table 5: Showing stable isotopic variation with rainfall amount for Eagles Rest.

	Eagles Rest		
Date	**$\delta^{18}O$ (‰)**	**$\delta^{2}H$ (‰)**	**Rainfall amount (mm)**
22/6/2019	-8.0	-47.1	4
23/6/2019	-4.8	-21.3	8
28/6/2019	-2.6	-1.3	16
29/6/2019	-2.4	0.6	7
1/7/2019	-8.2	-53.2	25
6/7/2019	-2.5	-4.9	42
19/7/2019	-1.9	-2.0	14
20/7/2019	-3.4	-12.6	1
23/7/2019	-4.9	-20.8	14
30/7/2019	-2.3	-3.5	65

5/8/2019	-2.6	-4.8	16
7/8/2019	-3.1	-7.2	14
11/8/2019	-1.7	0.7	10
30/8/2019	-3.9	-11.1	7
12/9/2019	-4.2	-14.4	3

Both $\delta^{18}O$ (r^2= 0.002) and $\delta^{2}H$ (r^2= 0.0002) ratios are poorly correlated with rainfall amount (Fig. 19).

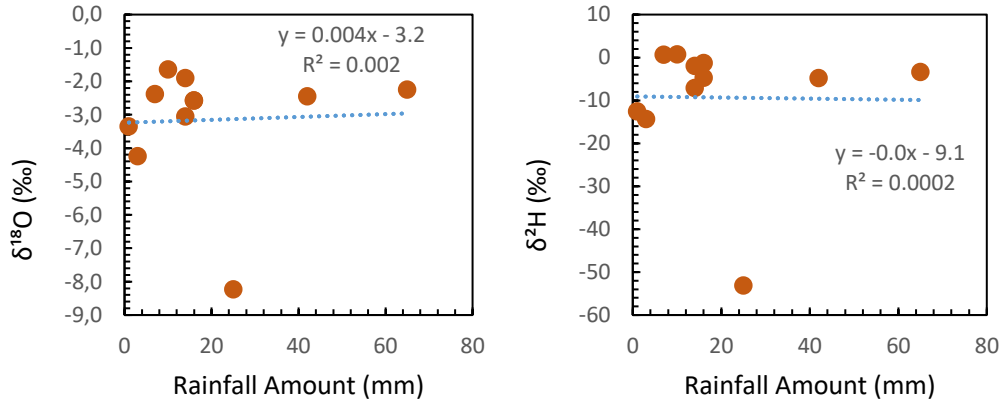

Figure 19: Variation of $\delta^{18}O$ and $\delta^{2}H$ ratios with rainfall amounts from samples collected Eagles Rest.

5.3 Groundwater Stable Isotope Data

The $\delta^{18}O$ and $\delta^{2}H$ ratios for the groundwater samples collected from the catchment range from -6.03 ‰ to 8.69 ‰ for $\delta^{18}O$ and -35.3 ‰ to 4.6 ‰ for $\delta^{2}H$. Groundwater samples show greater variation in $\delta^{18}O$ and $\delta^{2}H$ compared to the rainwater samples. The widest range of isotopic values occurs at Padstal, with high values of both $\delta^{18}O$ and $\delta^{2}H$, as seen in Fig. 20. Kruispad and Eagles Rest show a good isotopic variation in both $\delta^{18}O$ and $\delta^{2}H$ across the catchment as seen in Fig. 20. Most of the samples show similar $\delta^{18}O$ and $\delta^{2}H$ ratios falling within the ratios of the rainwater samples collected from the catchment (Fig. 21 Fig. 22a, c, d, e and Fig. 23a, b). The isotopic composition of groundwater from samples collected from high altitude areas and those from low lying areas show similar composition (Fig. 22 and 23). $\delta^{2}H$ shows the greatest variation of the two variables. Very small variations in both $\delta^{18}O$ and $\delta^{2}H$ can be seen at Olifants Doorn, Beaverlarc, Kardoesie, and Volgenvontein. Most of the samples fall on the LMWL and closer to the GMWL, with samples collected from Padstal showing evaporative enrichment as seen in Fig. 21, and Fig. 23c with a slope of 4.04. Please refer to the tables (Table 6 and 7) for the $\delta^{18}O$ and $\delta^{2}H$ values in groundwater for the groundwater samples collected from the Verlorenvlei catchment:

Table 6: Summary of the $\delta^{18}O$ values from the groundwater samples collected from the Verlorenvlei catchment.

PDL (Padstal), DFN (Doornfontein), VVN (Volgenvontein), SBN (Sebulon), BVL (Beaverlarc), FAF (Farawayfields), ER (Eagles Rest), KSP (Kruispad, River Water), and OD (Olifants Doorn, Spring Water). See Fig. 7 for sample locations.

	PDL	**DFN**	**VVN**	**SBN**	**KDS**	**BVL**	**FAF**	**ER**	**KSP (RW)**	**OD (Spring)**
	$\delta^{18}O$ (‰)									
Min.	1.75	-4.27	-6.03	-2.91	-4.32	-3.92	-4.38	-3.55	-2.38	-5.58
Max.	8.69	-2.63	-5.81	-2.77	-4.20	-3.73	-2.82	-0.86	1.19	-5.52
Average	5.47	-3.13	-5.93	-2.82	-4.27	-3.79	-4.18	-2.61	-0.80	-5.55

Table 7: Summary of the $\delta^{2}H$ values from the groundwater samples collected from the catchment. See Table 1 for explanation of abbreviations.

	PDL	**DFN**	**VVN**	**SBN**	**KDS**	**BVL**	**FAF**	**ER**	**KSP (RW)**	**OD (Spring)**
	$\delta^{2}H$ (‰)									
Min.	10.3	-20.0	-35.3	-14.4	-21.7	-18.2	-21.1	-15.2	-8.12	-28.2
Max.	41.1	-11.8	-32.5	-11.9	-19.7	-15.8	-5.2	4.00	6.70	-27.6
Average	26.0	-14.3	-34.0	-12.4	-20.1	-16.3	-18.3	-6.7	-1.90	-5.55

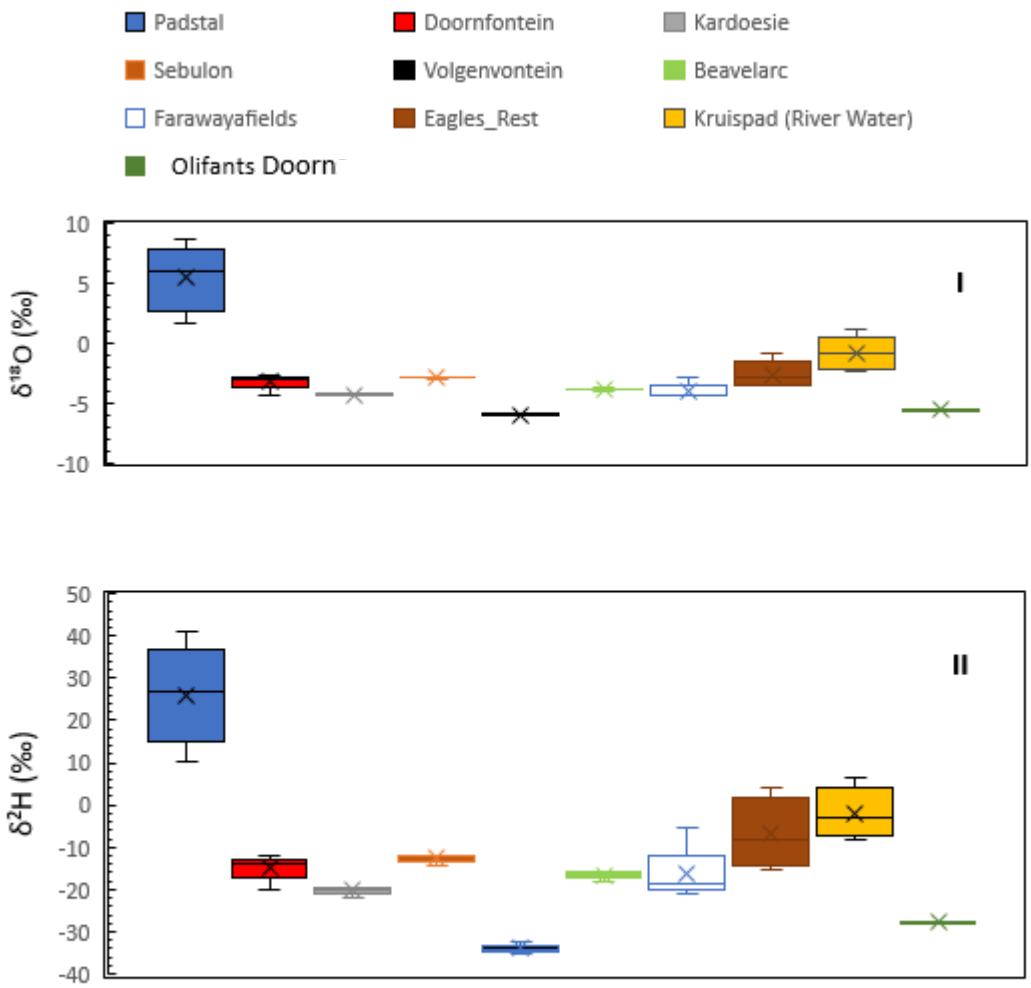

Figure 20: Showing the variation of (I) $\delta^{18}O$ and (II) $\delta^{2}H$ in groundwater samples collected from the catchment.

The groundwater samples collected at Padstal show a strong evaporative trend (r = 0.9) and a slope of 4.04 according to $\delta^{2}H = 4.04*\delta^{18}O + 3.90$ as seen in Fig. 21 and 23c, with high deuterium excess values compared to the other samples taken from the other sites. The riverwater samples taken at Kruispad show a slight influence of evaporation as seen in Fig. 21 and 24a.

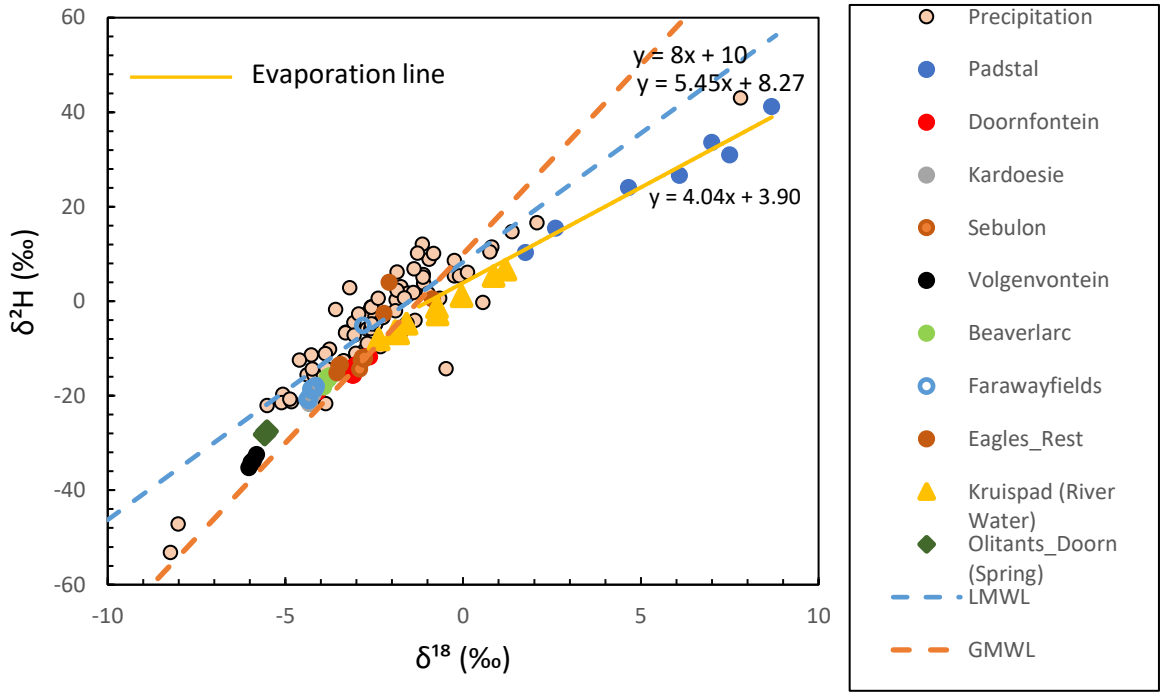

Figure 21: Stable isotopic composition of all groundwater, spring water and riverwater samples collected in comparison with rainwater values from the Verlorenvlei catchment, LMWL and GMWL.

The groundwater samples taken from both the high altitude areas and the low lying areas of the catchment fall close/on the LMWL, with samples from Eagles Rest and Farawayfields falling above the GMWL as seen in Fig. 21, Fig. 22d and Fig. 22e. Riverwater samples from Kruispad fall below the LMWL as seen in Fig. 21 and Fig. 24a. Samples from Kruispad and Padstal have the highest $\delta^{18}O$ and $\delta^{2}H$ values, with lowest values from Volgenvontein (Fig. 21 and Fig. 22b). Spring water samples collected at Olifants Doorn fall above the GMWL but below the LMWL (Fig. 21 and Fig 24b).

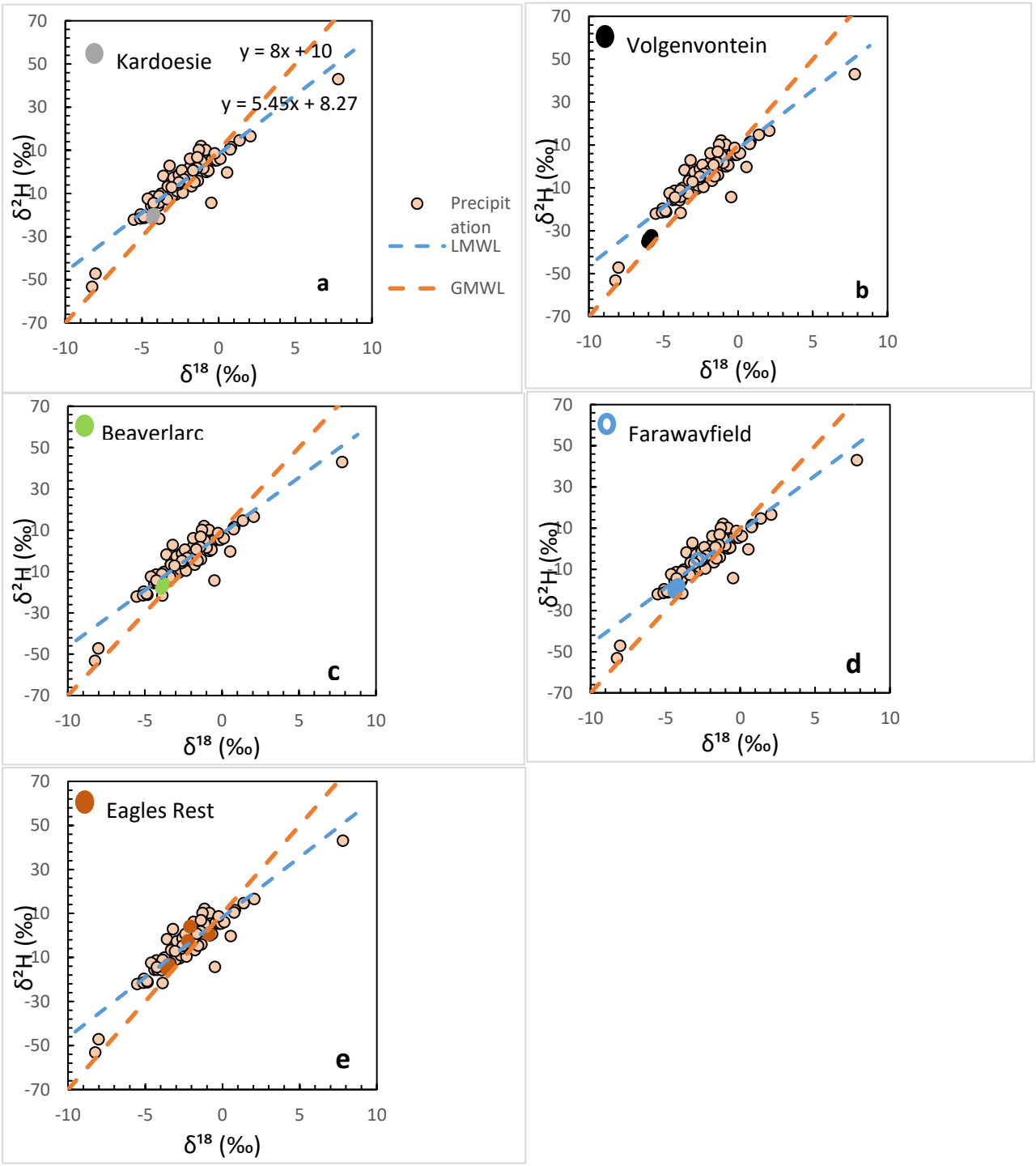

Figure 22: Variation in O and H isotope composition of groundwater samples from high altitude areas of the Verlorenvlei catchment. Groundwater samples from (a) Kardoesie, (b) Volgenvontein, (c) Beaverlarc, (d) Farawayfields, and (e) Eagles Rest, in comparison with the LMWL and GMWL.

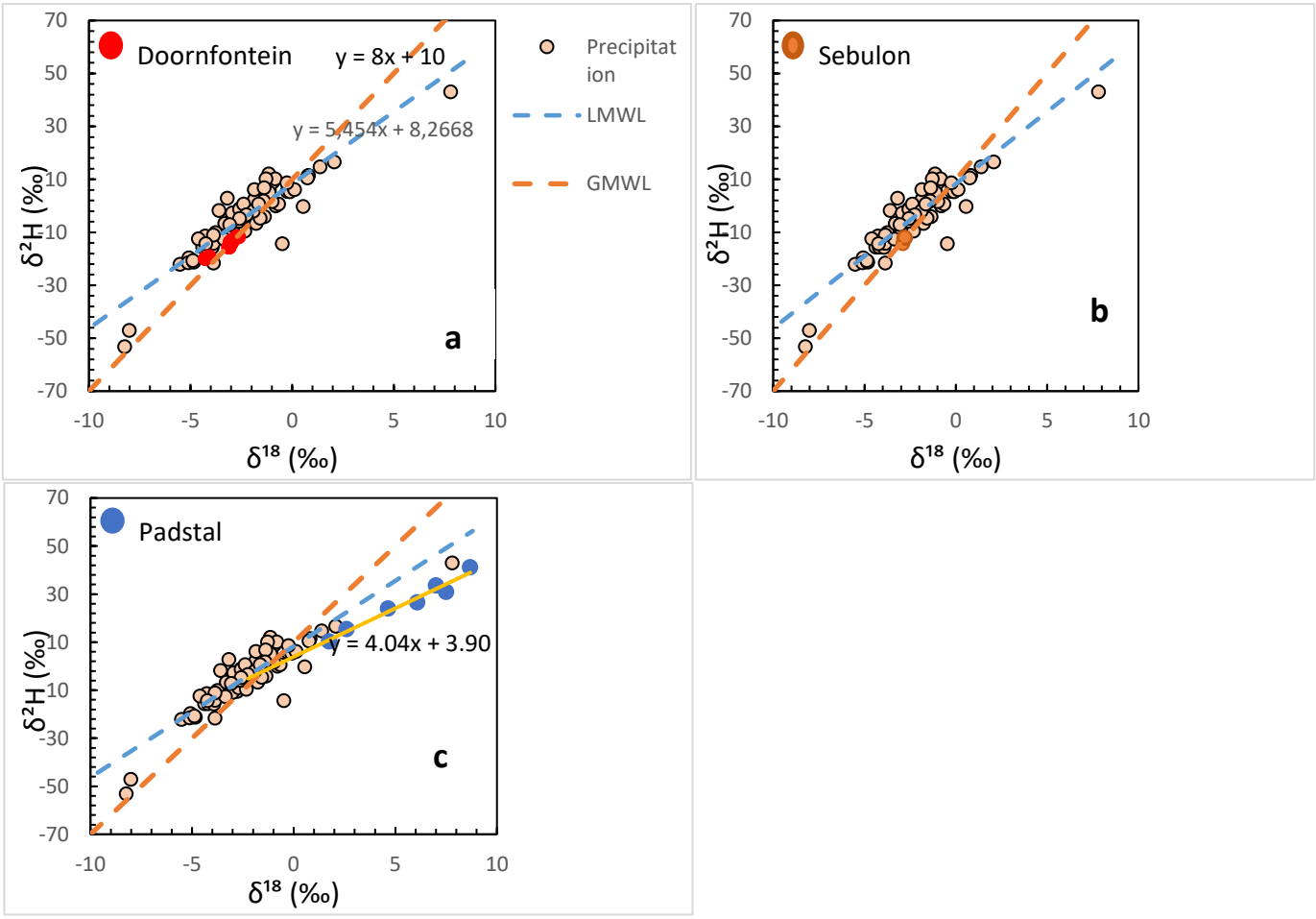

Figure 23: Showing the variation of stable isotopic composition of groundwater samples from lower lying areas of the Verlorenvlei catchment. Groundwater samples from (a) Doornfontein, (b) Sebulon, and (c) Padstal, in comparison with the LMWL and GMWL.

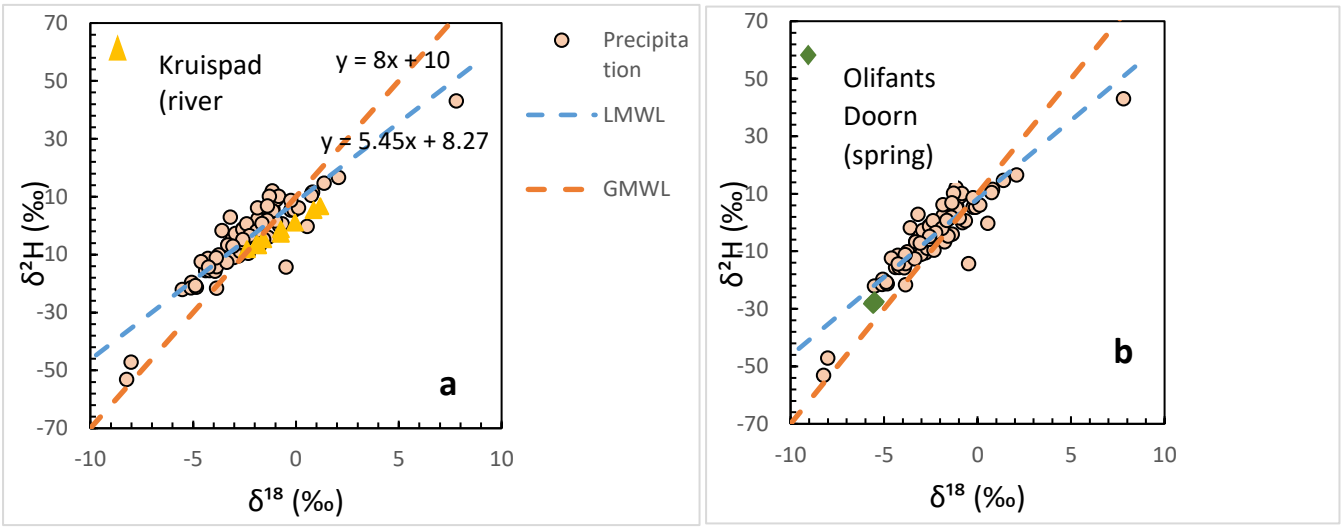

Figure 24: Variation of stable isotopic composition of (a) Kruispad (river water) and (b) Olifants Doorn (spring water) samples from the Verlorenvlei catchment, in comparison with the LMWL and GMWL.

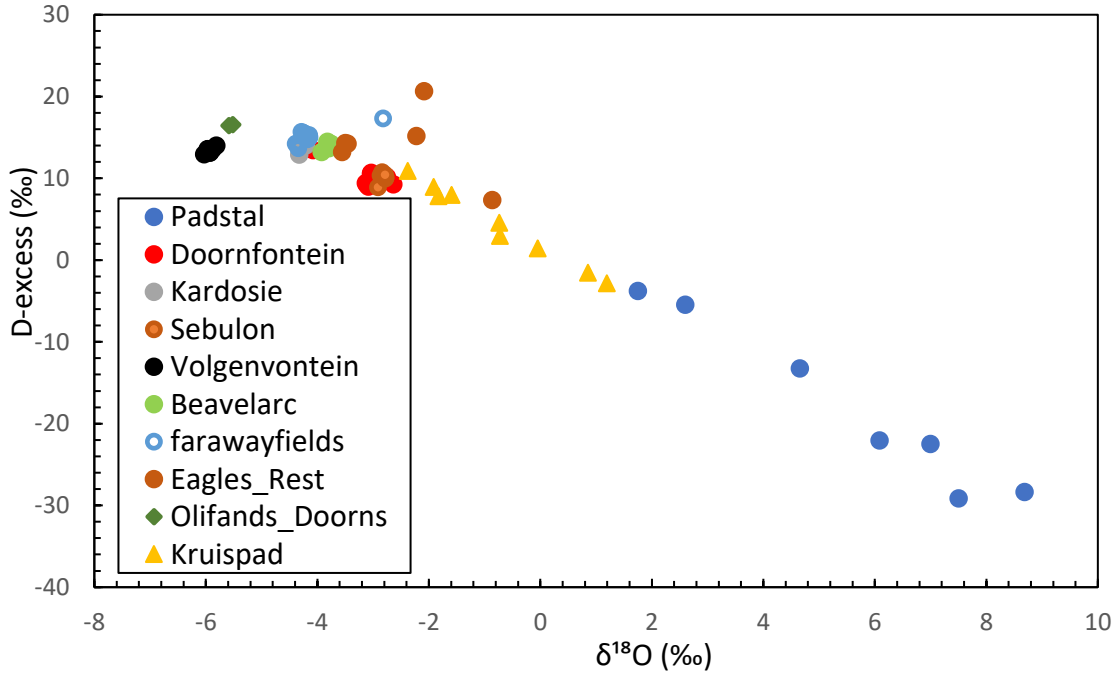

Figure 25: Relationship between d-excess and $\delta^{18}O$ for all samples collected from the Verlorenvlei catchment.

For all the groundwater samples collected from the Verlorenvlei catchment, deuterium excess varies from -2.83 ‰ to 20.6 ‰ whilst, ^{17}O-excess varies between -26.0 ‰ to 92.91 ‰. As seen

from Fig. 25 and Fig. 26 most of the sites show similar variation between d-excess and ^{17}O-excess values with that of δ^{18}O. Figure 25 shows a decrease in d-excess is associated with an increase in δ^{18}O, with similar trend observed with that ^{17}O-excess and δ^{18}O in. Samples collected at Padstal and Kruispad show decreasing or low values of d-excess and ^{17}O-excess with increasing δ^{18}O values, and this is due to strong evaporation influence in these sites as seen in Fig. 23c and Fig. 24a. The δ^{17}O and δ^{18}O ratios for all the samples collected in the catchment range from -3.16 ‰ to 4.56 ‰ for δ^{17}O and -6.03 ‰ to 8.69 ‰ for δ^{18}O. Evaporation process causes a systematic decrease in d-excess and ^{17}O-excess values and increase in δ^{18}O values, and this can be seen in Fig. 25 and Fig. 26 at Padstal from the great spread/variation/increase in δ^{18}O values. Groundwater samples from Farawayfields, Sebulon, Kardoesie and Volgenvontein show weak correlations between ^{17}O-excess and δ^{18}O, as increasing ^{17}O-excess does not influence the δ^{18}O values (Fig. 26). The variation in δ^{18}O for Volgenvontein, Farawayfields, Beaverlarc, and Doornfontein is very small compared to the δ^{18}O variation for Padstal and Kruispad (Fig. 26, Appendix page)

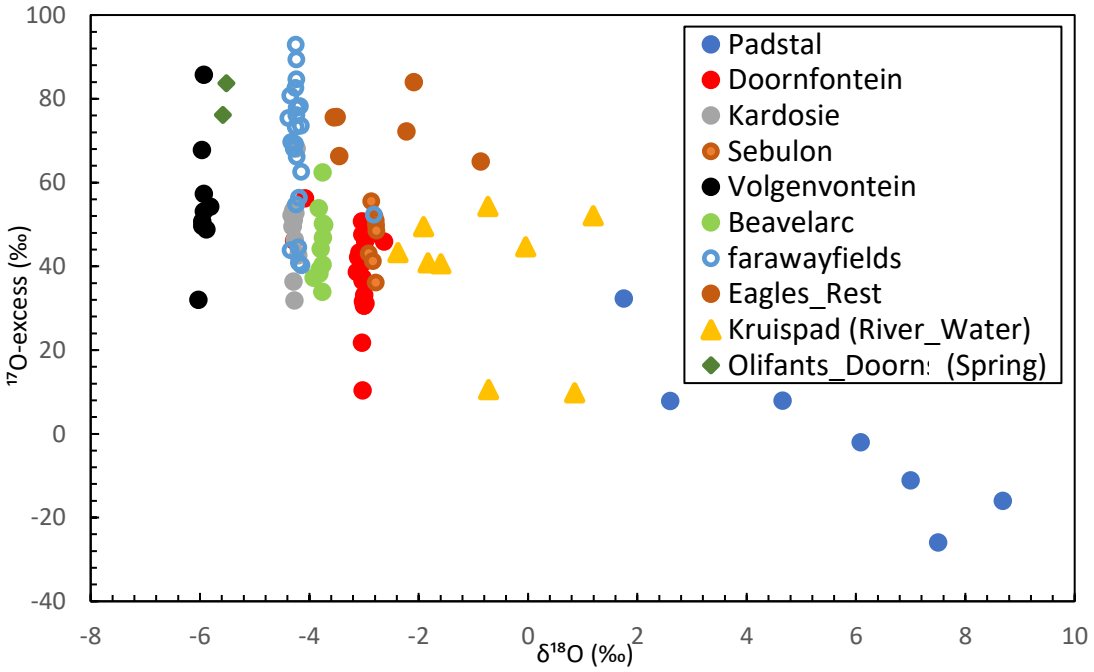

Figure 26: Relationship between ^{17}O-excess and δ^{18}O for all groundwater samples collected from the Verlorenvlei catchment.

6. DISCUSSION

The variation in stable isotope data suggests that there are processes and factors that are responsible for these variations at local scale that need to be discussed. To understand these factors and processes, the evolution of water mass from its original source, through its flow paths, and recharge processes and ending to an aquifer needs to be traced. This would a provide a better understanding of rainfall formation mechanisms, make it possible to explore various processes that might explain the variation in isotopic compositions along the flow paths in both rainwater and groundwater, and to provide an insight and an integrated view on the possible factors responsible for these variations. Furthermore, understanding these variations would make it easier to identify trends/signatures associated with evaporation and evapotranspiration processes and their role in rainfall formation and groundwater recharge.

6.2 Precipitation sources

The concept of "variations in d-excess" values in rainfall data are useful in determining relative moisture sources and moisture recycling, as d-excess values depend upon the temperature and humidity conditions at the sea surface where moisture is generated (Durowoju et al., 2019; Lai & Ehleringer, 2011; Otte et al., 2017). The average d-excess of this study is ~14 ‰, and this result shown that the source of rainfall in the region is from the Sea which has a similar Sea Surface Temperature as that of the Mediterranean sea (Appendix page), and this can also be attributed to the low values in isotopic composition in the rainfall samples. The data has also revealed that upper lying areas (high elevation) tend to have higher d-excess values with depleted isotopic composition compared to those in the lower lying areas (low elevation), this is likely indicative of re-evaporated moisture transport from low lying areas to upper lying areas. With the catchment dominated by natural vegetation, these increased d-excess values could also be a result of recycled local inland moisture from vegetation and water bodies around in the region. This has also been evident from the increased ^{17}O-excess values (Appendix page), a decrease in δ^{18}O values, and an increase in d-excess values. There were minor influences of evaporation on the rainfall; with rainfall samples collected at Padstal showing these evaporation trends/signatures and this is also supported by the excessive evaporation that occurs at Padstal, resulting in decreased ^{17}O-excess and increased δ^{18}O values (Fig. 16). The gradual increase in ^{17}O-excess (Fig. 16) could be attributed to evapotranspiration processes from the moisture sources resulting possibly from the natural vegetation present in the study area. This is to be expected, as you move to the upper regions, the catchment is covered with natural vegetation, and these might have an impact on the increased ^{17}O-excess values observed at these areas. This has also resulted in a decrease in δ^{18}O values. These evapotranspiration signals across the catchment are supported by the sudden increase in ^{17}O-excess values. Higher ^{17}O-excess values are found in the winter months, than in the summer months, and this is evident from the isotopic depletion of the rainfall samples. ^{17}O-excess values tend to decrease during the summer months, when evaporation is more common.

6.3 Geographic and Climatic factors

The stable isotopic composition of precipitation depends on several factors, such as temperature, rainfall amount, seasonality, continentality, latitude and altitude, and moisture sources may vary on seasonal scale (Dansgard, 1964; Hussain et al., 2015). The stable isotopic composition of rainwater is variable across the catchment. Seasonality effect is apparent in the study area, with most depleted $\delta^{18}O$ and $\delta^{2}H$ values occurring in winter and more enriched values in summer (Fig.12). The depletion of $\delta^{18}O$ and $\delta^{2}H$ ratios in winter may be attributed to air mass travel distances, where Mediterranean air masses travel longer distances inland than the summer air masses from the Indian ocean, resulting in depleted isotopic compositions in winter, i.e. low temperatures with long distance travel results in depleted winter precipitation (Hussain et al., 2015). The variation in stable isotopic composition may also be caused by seasonal shifts in moisture sources. Although the most enriched values are found in the winter months, this enrichment can be attributed to seasonal temperature differences and incloud re-evaporation prior to rainfall formation. This causes heavy isotopes to condense and lighter isotopes to fall as rainfall that evaporate below the cloud, resulting in heavy isotope values in rainfall reaching the surface (Lai & Ehleringer, 2011). The depletion in $\delta^{18}O$ and $\delta^{2}H$ values during the winter months can also be linked to the temperature effect, i.e., lower the temperature, the more depleted the isotopic composition ratio becomes. As large amounts of rainfall in the Western Cape are expected during the winter months (Diamond & Harris, 2019), these colder temperatures with high latitude rainfall may cause depletion in $\delta^{18}O$ values. There has also been an effect of elevation differences, where samples collected from higher elevation are expected to be isotopically depleted than those areas in lower elevation (Dansgard, 1964) (Fig. 11). These elevation differences have also had an effect on the variability of the ^{17}O-excess across the catchment, with sites situated at higher elevations showing higher ^{17}O-excess values than those at lower areas. Precipitation across the catchment has shown strong trends of evapotranspiration effects than evaporation, making evapotranspiration process a more dominant source of precipitation formation. This is supported by the systematic increase in ^{17}O-excess values from the rainfall samples collected.

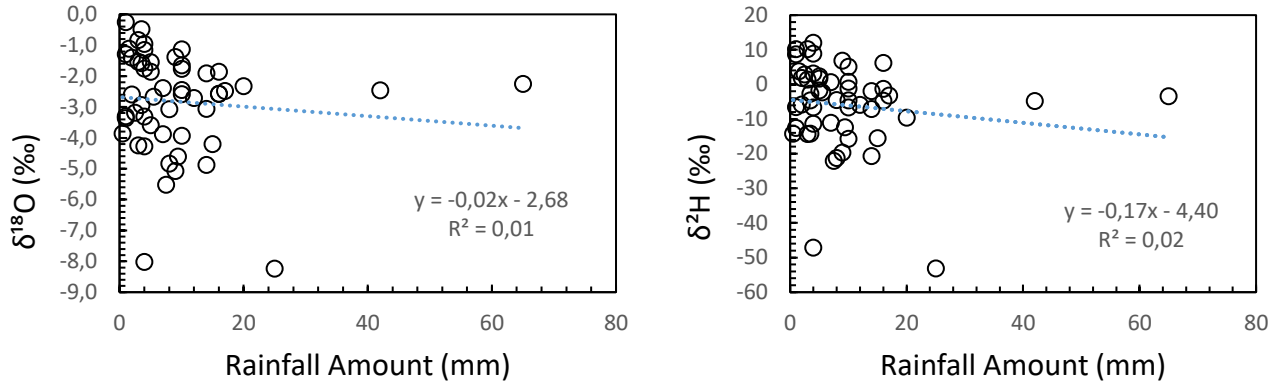

Figure 27: Variation of $\delta^{18}O$ and $\delta^{2}H$ ratios with rainfall amounts from all the samples collected.

Figures (17, 18, 19 and 27), show that there has been minimal "rainfall amount effect, where it is expected that an increase in rainfall amount should relate to a depletion in heavy isotopes ($\delta^{18}O$), while small rainfall amounts are related to the enrichment in heavy isotopes ($\delta^{18}O$). This concept is related to the fact that during the rainfall formation process, water bodies are evaporated leaving the water bodies enriched in isotopic composition, and during the condensation process this process is reversed (heavy isotopes are condensed first) (Dansgard, 1964). However, this has not been the case for Farawayfields and Eagles Rest, this effect was only evident at Kardoesie, where high rainfall volumes are characterised by a depletion in$\delta^{18}O$.

Factors such as variable rainfall patterns, temperature and wind conditions, all contribute to different climatic conditions from one place to another, and this results in a subtle variations in the LMWL relative to the GMWL (Dansgard, 1964; Harris et al., 2010). This is evident from Fig.12, where the general LMWL of the study, winter LMWL and summer LMWL are less than that of GMWL and the one observed from (Watson et al., 2020). The winter LMWL (slope = 5.87, intercept = 9.85), summer LMWL (slope = 5.00, intercept = 8.27), and the general LMWL (slope = 5.45, intercept = 7.58) for this study are lower than the GMWL, with relatively small intercepts, and this is indicative of seasonal temperature differences that occurs during the different seasons. Summer LMWL is expected to be lower than that of winter, as temperatures during the summer seasons tend to have increased temperatures resulting in possible evaporation influences, hence causing a lower slope with more enrichment in heavy isotopes ($\delta^{18}O$). This suggests that the rainfall formation processes occurred as a result of kinetic fractionation and low humidity conditions, and this is supported by the increasing d-excess value and depleted $\delta^{18}O$ values. During kinetic fractionation, the clouds became enriched in lighter isotopes, and when in-cloud re-evaporation occurred the clouds were enriched in heavy isotopes causing the resulting rainfall collected to be depleted in $\delta^{18}O$ (Appendix page). The difference in the slope of the summer LMWL may be attributed to

partial evaporation under warm and dry conditions, and the increase in temperatures as we approach the summer months (Dansgard, 1964; Han et al., 2020) (Fig. 12).

There was a partial "continental effect" on the isotopic composition of the rainfall data. Moving inland has caused a partial variation in the isotope composition of rainfall. With the "continental effect", isotopic composition is expected to be lighter (more negative) as you move away from the ocean/coast (Fig. 14). This can attributed to moisture re-cycling, resulting in variable isotopic composition in rainwater across the catchment. The "altitude effect" was common with areas in the high lying areas (higher altitude) becoming more depleted in isotopic composition than those in the lower parts of the catchment. This may probably be caused by uplift and cooling of air masses along the mountain slopes/higher areas.

6.4 Groundwater recharge pathways

Comparing the isotopic character of precipitation with that of the groundwater allows basic inferences of how precipitation and groundwater are linked. The groundwater isotopic composition shows similar isotopic composition to that of the rainwater composition (Fig. 28). The groundwater and spring samples fit around the LMWL, indicating that the samples are of meteoric origin, because of their low $\delta^{2}H$ and $\delta^{18}O$ values, thus infiltrating down to the lower lying areas resulting in an increase in $\delta^{18}O$ values in groundwater. The decrease in $\delta^{2}H$ and $\delta^{18}O$ values of the spring water could be a result of mixing processes or a common source between the groundwater and springwater, resulting in the same range of isotopic values or similar isotopic composition. The river water samples and groundwater samples have similar isotopic composition, and they both show evaporative enrichment in stable isotopic composition suggesting that they may be hydrologically connected, and the river may be fed by the groundwater. This can also be as a result of bulk precipitation falling on solid grounds, and pushed via piston flow from the unsaturated zone to the saturated zone, which then pushes the water from the saturated zone into the river system. Hence, river water has stable isotopic composition similar to that of the groundwater. This could also be a result of mixing processes that might occur as a result of riverwater being pushed through fractures and reaching the groundwater, causing the groundwater and riverwater to have similar isotopic composition.

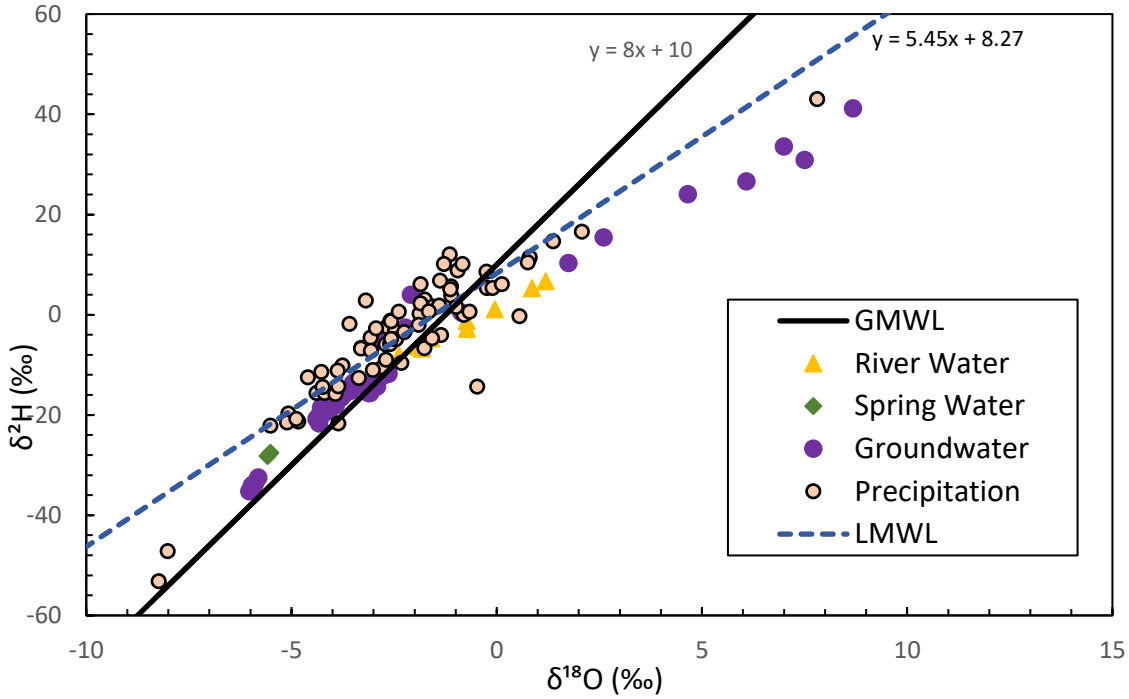

Figure 28: Stable isotope composition of groundwater, river water, and spring water in comparison with precipitation, LMWL, and GMWL.

This is also evident from the low d-excess values (<10‰), resulting from monsoonal recharge (Florea et al., 2017). High d-excess values (>10‰), are indicative of high latitude recharge processes associated with sources of recycled moisture. It is noticeable that the d-excess values from ground compared to rain water show similar range of values, which suggests that groundwater is recharged from local rain water. Based on the groundwater sample data (Appendix page), there has been evaporative influences prior to infiltration, in the groundwater samples collected at Padstal, and this is also supported by the low d-excess values. Where there's high degree of evaporation influences, d-excess values are expected to decrease (Fig. 25). Although Fig. 28 shows evaporation of water prior to infiltration, this evaporative trend is caused by the samples that have been collected at Padstal, and this is clearly shown in Fig. 21 and Fig. 23c. Samples from Padstal have shown evaporation signals that might have influenced groundwater prior to its infiltration which could lead to low recharge rates, and these trends have been transferred from rainfall to the groundwater at Padstal. Samples collected at Volgenvontein show the most negative isotopic values and are indicative of high latitude recharge from large rainfall events. Groundwater samples from Eagles Rest and Farawayfields lie slightly above the LMWL, and this indicates that there has been rapid infiltration of rainwater before it evaporated, resulting in low isotopic values in both these sites (Fig. 21). There has been minor evaporation influences to the fraction of precipitation that has been recharged in the catchment, while there has not been any evidence of evapotranspiration influences based on the observed ^{17}O-excess trends/signals observed from the groundwater data. Although it would have been better to represent rainwater isotope data as a weighted average mean to clearly see the recharge mechanism in the catchment, but there's limited data to calculate it. This leaves a room for other methods to be explored to better understand the evapotranspiration influences on the amount of

precipitation that becomes groundwater. Conclusive results could not be drawn on whether evapotranspiration process has had an effect or has had any influence on groundwater due to the small variations in ^{17}O-excess for groundwater samples collected in the catchment. But based on Fig. 16 and Fig.26, evapotranspiration signals from rainfall were not observed in in the groundwater system. The method used in this study needs to be evaluated to better understand the effects of this process on the groundwater system.

7. CONCLUSION

7.1 General Conclusions

The aim of the project was to provide an understanding of how stable isotopes can be used to understand relative contributions of evaporation and evapotranspiration on groundwater recharge, and how these processes may affect the stable isotopic compositions of groundwater and rainwater. Based on the findings of this project, the rainfall isotopic composition was affected by the "seasonal effect which has resulted in different isotopic compositions between the winter and summer seasons. The seasonality effect was also evident as a result of temperature difference between the two seasons. The rainfall was not heavily influenced by evaporation prior to its formation. This is evident from the relatively low $\delta^{2}H$ and $\delta^{18}O$ values from all the samples collected from the catchment. The isotopic composition in some of the areas (e.g Kardoesie) was also affected by the rainfall amount, where in rainfall with high volumes have produces isotopically depleted rainfall, and small rainfall volumes have produces isotopically enriched rainfall. In other areas where this has not been the case, it could be attributed to atmospheric moisture recycling. The rainfall was not influenced by the continentality effect, which states that as you move away from the ocean/moisture source the rainfall becomes isotopically depleted, and isotopically enriched as you move closer to the moisture source/ocean.

The high d-excess and $\delta^{17}O$-excess values in rainfall the catchment indicates a local moisture source, and evapotranspiration influences. Low $\delta^{17}O$-excess values are indicative of evaporation influences, whereas very high $\delta^{17}O$-excess are indicative of the effects of evapotranspiration from the surrounding natural vegetation and agricultural fields which have provided moisture for rainwater. High altitudes areas had isotopically enriched rainfall

compared to those in the lower lying areas, and this has suggests that there is moisture transport from lower lying areas to upper lying areas in the catchment.

The groundwater isotopic composition was similar to that of the rainwater and spring, suggesting a similar source. This is evident from the similar range of $\delta^{2}H$ and $\delta^{18}O$ ratios. Groundwater in the catchment was recharged from local precipitation, with minimal evaporative influences. The samples collected as Padstal have had an evaporative influence prior to infiltration. Based on the d-excess (>10‰) values obtained from the groundwater samples, groundwater may have been recharged by local precipitation in high altitude areas. The low isotopic values of the spring water indicates mixing processes. The groundwater and river water have shown a hydrological connection, with groundwater feeding the river water, which subsequently evaporates resulting in evaporative enrichment, and this has been evident from their isotopic composition.

For the purpose of this study, stable isotopes techniques proved to be a vital tool in investigating evaporation processes, but has not been very successful in addressing the evapotranspiration component of the project. Although literature has proven stable isotopes to be very effective for implementing proper water management strategies, but they have been unsuccessful in understanding the complex processes, such evapotranspiration of the hydrological cycle. This study suggests that the stable isotope technique be used in conjunction with other available methods to understand complex processes that influence groundwater recharge. Future research in the area should focus on detailed inspection on vegetation/plant water isotope to understand contributions of ET on groundwater recharge.

7.2 Limitations of the project

7.2.1 Covid 19

This study was seriously impacted by the Covid 19 pandemic, and the regulations that were put in place. These resulted in a large number of samples not being collected. As a result of this, some research questions could not be answered.

7.2.2 Data collection process

This study really relied on citizen science, engagement from farmers and communities, which has proven to be very effective in some studies, because it is allows participants to gain scientific skills, and for data collection in areas and in quantities that individuals/researchers/scientist could not achieve. However, for this study it has not been the case, with inconsistent sampling and inadequate number of samples. It was not worth doing for this study.

7.2.3 Analysis method used

Even though the samples were collected or there were enough samples, it wouldn't have been possible to understand the influences of evapotranspiration process on groundwater recharge, as this is a complex process which requires many parameters and aspects to be taken into account.

7.2.4 Sample size

The number samples used was too small for a proper analysis to be made. This has made it difficult to find significant relationships from the data set. Larger data could have generated more accurate results, and sample size is of great importance in a quantitative based project.

7.2.5 Limited access to literature and lack of studies in the research area

There has not been enough research done on the area that focuses on ET processes and how they affect groundwater and there has been little research done in this topic.

7.3 Recommendations

- Provided that there are enough funds for the project to cover the transport expenses, I would suggest that citizen science should not be relied on, rather do the weekly visits to the sites or get continuous samplers, without having to rely on local people.
- The stable isotope technique should be used together with other available methods, such as the water balance methods and model based approaches to understand complex processes, such as ET.
- ET is a combination process of transpiration and evaporation, water from soils and plants/vegetation/plant stems should also be analysed when assessing this process's influence on groundwater recharge.
- For this study to be successful in the future, additional isotope data collection of groundwater, springwater, surface water, and rainfall is required for the refinement of the baseline values, and for the establishment of long-term trends.
- Rainfall collector design needs to be improved, and an expansion of the spatial distribution of these collectors is needed to increase efficiency.

REFERENCE LIST

Adelana, S. M., Allinson, G., Kitching, M., Ii, H., Salzman, S., Mcnamara, E., … Shelley, B. (2015). Flow , Recharge and Mixing Processes in the Werribee Basin (Australia) Using Natural Environmental Isotope Geochemistry : Implications for Water Resources Management. In *Groundwater*.

Adelana, S. M. A., & Olasehinde, P. I. (2005). *Isotopes Techniques As Tools for Sustainable Ground Water Isotopes Techniques As Tools for Sustainable Ground*. (September 2014), 7–9.

Adomako, D., Maloszewski, P., Stumpp, C., Osae, S., & Akiti, T. T. (2010). Estimation de la recharge des eaux souterraines à partir des profils en profondeur des isotopes de l'eau (d2H, d18O) dans le bassin de la Rivière Densu, Ghana. *Hydrological Sciences Journal*, *55*(8), 1405–1416. https://doi.org/10.1080/02626667.2010.527847.

Alazard, M., Leduc, C., Travi, Y., Boulet, G., & Ben Salem, A. (2015). Estimating evaporation in semi-arid areas facing data scarcity: Example of the El Haouareb dam (Merguellil catchment, Central Tunisia). *Journal of Hydrology: Regional Studies*, *3*, 265–284. https://doi.org/10.1016/j.ejrh.2014.11.007.

Allen, R.G., Pruitt, W.O., 1991. FAO-24 reference evapotranspiration factors. J. Irrig. Drain. Eng. 117, 758–773. https://doi.org/10.1061/(ASCE)0733-9437(1991) 117:5(758).

Allison, G.B., Cook, P.G., Barnett, S.R., Walker, J.R., Jolly, I.D., and Hughes, M.W. (1990). Land clearance and river salinization in the western Murray basin, Australia. J Hydrol. 9: 1-20.

Althoff, D., Rodrigues, L. N., & Silva, D. D. da. (2019). Evaluating evaporation methods for estimating small reservoir water surface evaporation in the Brazilian savannah. *Water (Switzerland)*, *11*(9). https://doi.org/10.3390/w11091942.

Anderson, M. C., et al. (2011), Mapping daily evapotranspiration at field to continental scales using geostationary and polar orbiting satel- lite imagery, Hydrol. Earth Syst. Sci., 15, 223–239.

Angert A., Cappa C. D. and DePaolo D. J. (2004) Kinetic 17O effects in the hydrologic cycle: indirect evidence and implica- tions. Geochim. Cosmochim. Acta 68, 3487–3495.

Awal, R., Habibi, H., Fares, A., & Deb, S. (2020). Estimating reference crop evapotranspiration under limited climate data in West Texas. *Journal of Hydrology: Regional Studies*, *28*(February), 100677. https://doi.org/10.1016/j.ejrh.2020.100677.

Awe, G. O., Akomolafe, T. N., Umam, J., & Ayuba, M. B. (2020). Efficiency of small pan evaporimeter in monitoring evapotranspiration under poly-covered house and open-field conditions in a hot, tropical region of Nigeria. *Journal of Hydrology: Regional Studies*, *32*(September), 100735. https://doi.org/10.1016/j.ejrh.2020.100735.

Balasubramanian, A., & Nagaraju, D. (1994). The Hydrologic Cycle. *International Geophysics*, *56*(C), 115–135. https://doi.org/10.1016/S0074-6142(08)60562-8.

Ball, P. (2000). The hydrological cycle. *Nature*. https://doi.org/10.1038/news000127-12.

Barbieri, M., Boschetti, T., Petitta, M., & Tallini, M. (2005). Stable isotope (2H, 18O and 87Sr/86Sr) and hydrochemistry monitoring for groundwater hydrodynamics analysis in a karst aquifer (Gran Sasso, Central Italy). *Applied Geochemistry*, *20*(11), 2063–2081. https://doi.org/10.1016/j.apgeochem.2005.07.008.

Barbieri, M. (2019). Isotopes in hydrology and hydrogeology. *Water (Switzerland)*, *11*(2). https://doi.org/10.3390/w11020291.

Barkan, E., and B. Luz (2007), Diffusivity fractionations of H2 16O/H2 17O and H216O/H2 18O in air and their implications for isotope hydrology, Rapid Commun. Mass Spectrom., 21, 2999–3005.

Beamer, J. P., Huntington, J. L., Morton, C. G., & Pohll, G. M. (2013). Estimating Annual Groundwater Evapotranspiration from Phreatophytes in the Great Basin Using Landsat and Flux Tower Measurements. *Journal of the American Water Resources Association*, *49*(3), 518–533. https://doi.org/10.1111/jawr.12058.

Benettin, P., Volkmann, T. H. M., Von Freyberg, J., Frentress, J., Penna, D., Dawson, T. E., & Kirchner, J. W. (2018). Effects of climatic seasonality on the isotopic composition of evaporating soil waters. *Hydrology and Earth System Sciences*, *22*(5), 2881–2890. https://doi.org/10.5194/hess-22-2881-2018.

Biran, A., Pedahzur, R., Buchinger, S., Reifferscheid, G., & Belkin, S. (2009). *for Genotoxicity Assessment*. 161–186. https://doi.org/10.1007/698.

Bowser, C. J., Anderson, M. P., & Valley, J. W. (1990). *Estimating groundwater exchange with lakes : 1 . The stable isotope mass balance method Estimating Groundwater Exchange With Lakes 1 . The Stable Isotope Mass Balance Method*. (September 2015). https://doi.org/10.1029/WR026i010p02445.

Braune, E., & Xu, Y. (2009). Groundwater management issues in Southern Africa - An IWRM perspective. *Water SA*, *34*(6), 699–706. https://doi.org/10.4314/wsa.v34i6.183672.

Bredenkamp, D.B., L.J. Botha, G.J. Van Tonder, and H.J. Van Rensburg. 1995. Manual on quantitative estimation of groundwater recharge and aquifer storarivity. Water Research Commision Report TT 73/95.

Brutsaert, W. (1982) Evaporation into the atmosphere - theory, history and applications, Dordrecht, Holland: D Reidel Publishing Company.

Carrillo-Rivera, J. J., & Cardona, A. (2012). Groundwater flow systems and their response to Climate change: A need for a water-system view approach. *American Journal of Environmental Sciences*, *8*(3), 220–235. https://doi.org/10.3844/ajessp.2012.220.235.

Casellas, E., Latron, J., Cayuela, C., Bech, J., Udina, M., Sola, Y., … Llorens, P. (2019). Moisture origin and characteristics of the isotopic signature of rainfall in a Mediterranean mountain catchment (Vallcebre , eastern Pyrenees). *Journal of Hydrology*, *575*(December 2018), 767–779. https://doi.org/10.1016/j.jhydrol.2019.05.060.

Conrad, J., Nel, J., and Wentzel, J.: The challenges and implications of assessing groundwater recharge: A case study-northern Sand- veld, Western Cape, South Africa, Water SA, 30,

75–81, 2004.

Cook, P. G., & Solomon, D. K. (1997) Recent advances in dating young groundwater: Chlorofluorocarbons, 3H/3He and 85Kr, Journal of Hydrology, 191, pp. 245–265.

Craig, B. H., & Lal, D. (1960). *The Production Rate*. *2*. https://doi.org/10.1111/j.2153-3490.1961.tb00068.x.

CSIR. (2009). *Development of the Verlorenvlei estuarine management plan: Situation assessment. Report prepared for the C.A.P.E. Estuaries Programme*. 142. Retrieved from http://fred.csir.co.za/project/CAPE_Estuaries/documents/Verlorenvlei Situation Assesment_Final Draft_Oct2009.pdf.

Currell, M. J., Cartwright, I., Bradley, D. C., & Han, D. (2010). Recharge history and controls on groundwater quality in the Yuncheng Basin, north China. *Journal of Hydrology*, *385*(1–4), 216–229. https://doi.org/10.1016/j.jhydrol.2010.02.022.

Dansgard, B. W. (1964). *Stable isotopes in precipitation*.

De Beer, C. H. (2003) *The geology of the Sandveld area between Lambert's Bay and Piketberg*: *CGS Report No. 2003-0032*. Bellville: Council for Geosciences, Western Cape Unit.

De Souza, E., Pontes, L. M., Fernandes Filho, E. I., Schaefer, C. E. G. R., & Dos Santos, E. E. (2019). Spatial and temporal potential groundwater recharge: The case of the doce river basin, Brazil. *Revista Brasileira de Ciencia Do Solo*, *43*, 1–27. https://doi.org/10.1590/18069657rbcs20180010.

de Vries, J. J., & Simmers, I. (2002). Groundwater recharge: An overview of process and challenges. *Hydrogeology Journal*, *10*(1), 5–17. https://doi.org/10.1007/s10040-001-0171-7.

Diamond, R. E., & Harris, C. (2019). *Annual shifts in O- and H-isotope composition as measures of recharge : the case of the Table Mountain springs , Cape Town , South Africa*.

Durowoju, O. S., Odiyo, J. O., & Ekosse, G. E. (2019). *Determination of isotopic composition of rainwater to generate local meteoric water line in Thohoyandou , Limpopo Province , South Africa*. *45*(2), 183–189.

DWAF (2003) *Sandveld preliminary (rapid) reserve determinations. Langvlei, Jakkals and Verlorenvlei Rivers. Olifants-Doorn WMA G30*. Surface Volume 1: Final Report Reserve Specifications. DWAF Project Number 2002-227.

Edmunds, W. M. (1992). *Mechanisms, Timing and Quantities of Recharge to Groundwater in Semi-Arid and Tropical Regions*. (Custodio), 77–88.

Eilers, A. (2018). *Deep groundwater characterisation and recharge estimation in the Verlorenvlei catchment*. (March), 92.

Elliot, T. (2014). Environmental tracers. *Water (Switzerland)*, *6*(11), 3264–3269. https://doi.org/10.3390/w6113264.

Engelen, G.B., Kloosterman, F.H., 1996. Hydrological system analysis: methods and application. In: Water Science and Technology Library, vol. 20. Kluwer Academic Publishers, p. 149.

Engman, E. T., Gurney, R. J., Engman, E. T., & Gurney, R. J. (1991). Hydrologic cycle. *Remote Sensing in Hydrology*, 1–9. https://doi.org/10.1007/978-94-009-0407-1_1.

Eslamian, S. (2014). Handbook of engineering hydrology: Fundamentals and applications. *Handbook of Engineering Hydrology: Fundamentals and Applications*, 1–604. https://doi.org/10.1201/b15625.

Evaristo, J., Jasechko, S., & McDonnell, J. J. (2015). Global separation of plant transpiration from groundwater and streamflow. *Nature*, *525*(7567), 91–94. https://doi.org/10.1038/nature14983.

Finch, J. W., & Hall, R. L. (2001). Estimation of Open Water Evaporation. *Report*, 155.

Fiorillo, F. (2011). The Role of the Evapotranspiration in the Aquifer Recharge Processes of Mediterranean Areas. *Evapotranspiration - From Measurements to Agricultural and Environmental Applications*. https://doi.org/10.5772/17065.

Fisher, J. B., Melton, F., Middleton, E., Hain, C., Anderson, M., Allen, R., … Wood, E. F. (2017). The future of evapotranspiration: Global requirements for ecosystem functioning, carbon and climate feedbacks, agricultural management, and water resources. *Water Resources Research*, *53*(4), 2618–2626. https://doi.org/10.1002/2016WR020175.

Fleischer, M., Kralisch, S., Fink, M., Pfennig, B., & Butchart-kuhlmann, D. (2016). *Water Use and Management in Semiarid Regions – A Distributed Modelling Approach in the Verlorenvlei Catchment , South Africa*. *18*(July 2019), 6123.

Fleitmann, D., & Leuenberger, M. (2015). *Triple isotope (d D , d 17 O , d 18 O) study on precipitation , drip water and speleothem fl uid inclusions for a Western Central European cave*. *127*. https://doi.org/10.1016/j.quascirev.2015.08.030.

Flerchinger, G. N., & Seyfried, M. S. (2014). Comparison of Methods for Estimating Evapotranspiration in a Small Rangeland Catchment. *Vadose Zone Journal*, *13*(4), vzj2013.08.0152. https://doi.org/10.2136/vzj2013.08.0152.

Florea, L., Bird, B., Lau, J. K., Wang, L., Lei, Y., Yao, T., & Thompson, L. G. (2017). Stable isotopes of river water and groundwater along altitudinal gradients in the High Himalayas and the Eastern Nyainqentanghla Mountains. *Journal of Hydrology: Regional Studies*, *14*(September), 37–48. https://doi.org/10.1016/j.ejrh.2017.10.003.

Flow, G., Zone, H., Khan, H. H., & Khan, A. (2019). *Groundwater-Surface Water Interac- tion Groundwater and Surface Water Inter- action*.

Froehlich, K., Gibson, J. J., & Aggarwal, P. (2002). Deuterium excess in precipitation and its climatological significance. *Journal of Geophysical Research-Atmospheres*, (July 2002), 1–23.

Gao, F., Feng, G., Ouyang, Y., Wang, H., Fisher, D., Adeli, A., & Jenkins, J. (2017). Evaluation of Reference Evapotranspiration Methods in Arid, Semiarid, and Humid Regions. *Journal of the American Water Resources Association*, *53*(4), 791–808. https://doi.org/10.1111/1752-1688.12530.

Gat, J. R. (2002). Oxygen and Hydrogen Isotopes in the Hydrologic Cycle. *Annual Review of Earth and Planetary Sciences*, *24*(1), 225–262.

https://doi.org/10.1146/annurev.earth.24.1.225.

Gibson, J. J., Edwards, T. W. D., Bursey, G. G., & Prowse, T. D. (1993). Estimating Evaporation Using Stable Isotopes : Two catchments in Northern Canada. *Nordic Hydrology*, *24*, 79–94.

Good, S. P. (2019). *isotopes*. https://doi.org/10.1007/s00442-018-4192-5.Inferring.

Gorjizade, A., Akhondali, A. M., Zarei, H., & Kaboli, H. S. (2014). Evaluation of Eight Evaporation Estimation Methods in a Semi-arid Region (Dez reservoir, Iran). *International Journal of Advanced Biological and Biomedical Research*, *2*(5), 1823–1836. https://doi.org/10.13140/RG.2.1.4700.1122.

Gresse, P. G., von Veh, M. W. and Frimmel, H. E. (2006) Namibian (Neoproterozoic) to early Cambrian successions, in Johnson, M. R., Anhaeusser, C. R., and Thomas, R. J. (eds) *The Geology of South Africa*. Johannesburg: Geological Society of South Africa, pp. 395– 420.

Gu, L., Hu, Z., Yao, J., & Sun, G. (2017). Actual and reference evapotranspiration in a cornfield in the Zhangye oasis, Northwestern China. *Water (Switzerland)*, *9*(7), 4–6. https://doi.org/10.3390/w9070499.

Han, T., Zhang, M., Wang, S., Qu, D., & Du, Q. (2020). Sub-hourly variability of stable isotopes in precipitation in the marginal zone of East Asian monsoon. *Water (Switzerland)*, *12*(8). https://doi.org/10.3390/W12082145.

Harris, C., Burgers, C., Miller, J., & Rawoot, F. (2010). O- and H-isotope record of Cape Town rainfall from 1996 to 2008, and its application to recharge studies of table mountain groundwater, South Africa. *South African Journal of Geology*, *113*(1), 33–56. https://doi.org/10.2113/gssajg.113.1.33.

Harris, C., Oom, B.M. and Diamond, R.E. 1999. A preliminary investigation of the urban isotope hydrology of the Cape Town area. Water SA, 25, 15–24.

Hartnady, C. J. H., Newton, A. R. and Theron, J. N. (1974) The stratigraphy and structure of the Malmesbury Group in the southwestern Cape, Bulletin of the Precambrian Research Unit, University of Cape Town, 15, pp. 193–213.

Healy, R.W., & Cooke, P.G., 2002, Using groundwater levels to estimate recharge: Hydrogeology Journal, v. 10, p. 91- 109.

Helme, N.: Botanical report: Fine Scale vegetation mapping in the Sandveld, as part of the C.A.P.E programme, Report for Cape Nature, Scarborough, 2007.

Holloway, A., Fortune, G., Chasi, V., 2010. RADAR Western Cape risk and development annual review disaster mitigation for sustainable livelihoods programme. PeriPeri Publications, Rondebosch.

Houghton-Carr, H., & Matt, F. R. Y. (2006). The decline of hydrological data collection for development of integrated water resource management tools in Southern Africa. *IAHS-AISH Publication*, (308), 51–55.

Hussain, S., Xianfang, S., Hussain, I., Jianrong, L., Dong Mei, H., Li Hu, Y., & Huang, W. (2015). Controlling Factors of the Stable Isotope Composition in the Precipitation of Islamabad,

Pakistan. *Advances in Meteorology*, *2015*. https://doi.org/10.1155/2015/817513.

Islam, S., Singh, R. K., & Khan, R. A. (2016). *Methods of Estimating Ground water Recharge Methods of Estimating Ground water Recharge*. (May).

Jacks, G., & Traoré, M. S. (2014). Mechanisms and rates of groundwater recharge at Timbuktu, Republic of mali. *Journal of Hydrologic Engineering*, *19*(2), 422–427. https://doi.org/10.1061/(ASCE)HE.1943-5584.0000801.

Jasechko, S., Sharp, Z. D., Gibson, J. J., Birks, S. J., Yi, Y., & Fawcett, P. J. (2013). Terrestrial water fluxes dominated by transpiration. *Nature*, *496*(7445), 347–350. https://doi.org/10.1038/nature11983.

Johnson, M.R., Anhauesser, C.R. & Thomas, R.J. (2006) *The geology of South Africa*. Geological Society of South Africa, Pretoria, 691.

Kattan, Z. (2001). Use of hydrochemistry and environmental isotopes for evaluation of groundwater in the Paleogene limestone aquifer of the Ras Al-Ain area (Syrian Jezireh). *Environmental Geology*, *41*(1–2), 128–144. https://doi.org/10.1007/s002540100354.

Kidston, J., C. Brümmer, T.A. Black, K. Morgenstern, Z. Nesic, J.H. McCaughey, and A.G. Barr. 2010. Energy balance closure using eddy covariance above two different land surfaces and implications for CO2 flux measurements. Boundary-Layer Meteorol. 136:193–218. doi:10.1007/s10546-010-9507-y.

Krabbenhoft, D. P., Bowser, C. J., Anderson, M. P., & Valley, J. W. (1990). Estimating groundwater exchange with lakes: 1. The stable isotope mass balance method. *Water Resources Research*, *26*(10), 2445–2453. https://doi.org/10.1029/WR026i010p02445.

Kumar, C. P. (2010). Microsoft Word - GWC_NIH_RDS_Paper.doc. *Change*, *247667*, 1–14.

Kumar, C. P. (2013). Hydrological Studies Using Isotopes. *International Journal of Innovative Research & Development*, *2*(13), 8–15. Retrieved from http://www.angelfire.com/nh/cpkbanner/publication/Isotope_Studies_IJIRD.pdf.

Kumar, N., & Arakeri, J. H. (2021). A fast method to measure the evaporation rate. *Journal of Hydrology*, *594*(October). https://doi.org/10.1016/j.jhydrol.2020.125642.

Kumar, V., Khan, S., Shaktibala, & Rahul, A. K. (2018). Review of Evapotranspiration Methodologies. *American Journal of Earth Science and Engineering*, *1*(2), 72–84. Retrieved from http://www.aascit.org/journal/archive2?journalId=933&paperId=6387.

Lai, C. T., & Ehleringer, J. R. (2011). Deuterium excess reveals diurnal sources of water vapor in forest air. *Oecologia*, *165*(1), 213–223. https://doi.org/10.1007/s00442-010-1721-2.

Landais, A., E. Barkan, and B. Luz (2008), Record of d18O and 17O ‐ excess in ice from Vostok Antarctica during the last 150,000 years, Geophys. Res. Lett., 35, L02709, doi:10.1029/2007GL032096.

Leketa, K., & Abiye, T. (2020). Investigating stable isotope effects and moisture trajectories for rainfall events in Johannesburg, South Africa. *Water SA*, *46*(3), 429–437. https://doi.org/10.17159/wsa/2020.v46.i3.8653.

Lerner D.N., A.S. Issar, and I. Simmers. 1990. Groundwater recharge, guide to understanding

and estimating natural recharge. International Association of Hydrogeologists, Kenilworth, Rep 8, 345 pp.

Liou, Y. A., & Kar, S. K. (2014). Evapotranspiration estimation with remote sensing and various surface energy balance algorithms-a review. *Energies*, *7*(5), 2821–2849. https://doi.org/10.3390/en7052821.

Liu, W., Zhang, B., & Han, S. (2020). Quantitative analysis of the impact of meteorological factors on reference evapotranspiration changes in Beijing, 1958-2017. *Water (Switzerland)*, *12*(8). https://doi.org/10.3390/w12082263.

Luz, B., & Barkan, E. (2010). Variations of 17O/16O and 18O/16O in meteoric waters. *Geochimica et Cosmochimica Acta*, *74*(22), 6276–6286. https://doi.org/10.1016/j.gca.2010.08.016.

Luz B. and Barkan E. (2000) Assessment of oceanic productivity with the triple-isotope composition of dissolved oxygen. Science 288, 2028–2031.

Lynch, S. (2004) *Development of a raster database of annual, monthly and daily rainfall, for Southern Africa*: Report No. 1156/1/04. Pretoria: Water Research Commission.

Majidi, M., Alizadeh, A., Farid, A., & Vazifedoust, M. (2015). Estimating evaporation from lakes and reservoirs under limited data condition in a semi-arid region. *Water Resources Management*, *29*(10), 3711–3733. https://doi.org/10.1007/s11269-015-1025-8.

Mance, D., Hunjak, T., Lenac, D., Rubini, J., & Roller-lutz, Z. (2014). *Stable isotope analysis of the karst hydrological systems in the Bay of Kvarner (Croatia)*. *90*, 23–34. https://doi.org/10.1016/j.apradiso.2014.03.001.

Maria, G., Linhares, G., Moreira, R. M., Colombo, R., Scarpelli, R. P., & Augusta, E. (2017). *STABLE ISOTOPE OXYGEN - 18 AND DEUTERIUM ANALYSIS IN SURFACE AND GROUNDWATER OF THE JEQUITIBÁ CREEK BASIN , SETE LAGOAS , MG*.

Mata, D. M. (2014). Evaluation of Evapotranspiration. *International Journal of Research in Engineering and Technology*, *03*(21), 43–47. https://doi.org/10.15623/ijret.2014.0321011.

McGUIRE, M. (2004). *Stable Isotopes in Ecology and Environmental Science, Second Edition Chapter 11. Stable Isotope Tracers in Watershed Hydrology*. 334–365.

Mendicino, G., & Senatore, A. (2012). The Role of Evapotranspiration in the Framework of Water Resource Management and Planning Under Shortage Conditions. *Evapotranspiration - Remote Sensing and Modeling*, (January). https://doi.org/10.5772/19171.

Miller, J. A., Watson, A. P., Fleischer, M., Eilers, A., Sigidi, N. T., van Gend, J., … de Clercq, W. P. (2018). Groundwater quality, quantity, and recharge estimation on the West Coast of South Africa. *Biodiversity & Ecology*, *6*(July), 86–95. https://doi.org/10.7809/b-e.00309.

Misstear, B. D. R. (2000). Groundwater Recharge Assessment: a Key Component of River Basin Management. *National Hydrology Seminar*, 51–58.

Mook, W. G. (2001). Environmental isotopes in the hydrological cycle: Principles and

applications, Volume I: Introduction: Theory, Methods, Review. *International Hydrological Programme IHP-V*, *1*, 1–165. Retrieved from http://www.hydrology.nl/ihppublications/149-environmental-isotopes-in-the-hydrological-cycle-principles-and-applications.html%5Cn.

Najmaddin, P. M., Whelan, M. J., & Balzter, H. (2017). Estimating daily reference evapotranspiration in a semi-arid region using remote sensing data. *Remote Sensing*, *9*(8). https://doi.org/10.3390/rs9080779.

Nemaxwi, P., Odiyo, J. O., & Makungo, R. (2019). Estimation of groundwater recharge response from rainfall events in a semi-arid fractured aquifer: Case study of quaternary catchment A91H, Limpopo Province, South Africa. *Cogent Engineering*, *6*(1). https://doi.org/10.1080/23311916.2019.1635815.

Novák, V., & Novák, V. (2012). Methods of Evapotranspiration Estimation. *Evapotranspiration in the Soil-Plant-Atmosphere System*, (March), 165–215. https://doi.org/10.1007/978-94-007-3840-9_9.

Obiefuna, G. I., & Orazulike, D. M. (2011). Application and comparison of groundwater recharge estimation methods for the semiarid Yola area, northeast, Nigeria. *Global Journal of Geological Sciences*, *9*(2), 177-204–204. https://doi.org/10.4314/GJGS.V9I2.

Oiro, S., Comte, J. C., Soulsby, C., & Walraevens, K. (2018). Using stable water isotopes to identify spatio-temporal controls on groundwater recharge in two contrasting East African aquifer systems. *Hydrological Sciences Journal*, *63*(6), 862–877. https://doi.org/10.1080/02626667.2018.1459625.

Oswald CJ, Rouse WR (2004) Thermal characteristics and energy balance of various-size Canadian shield lakes in the Mackenzie River basin. J Hydrometeorol 5(1):129–144. https://doi.org/10.1175/ 1525-7541(2004)0052.0.CO;2.

Otte, I., Detsch, F., Gütlein, A., Scholl, M., Kiese, R., Appelhans, T., & Nauss, T. (2017). Seasonality of stable isotope composition of atmospheric water input at the southern slopes of Mt. Kilimanjaro, Tanzania. *Hydrological Processes*, *31*(22), 3932–3947. https://doi.org/10.1002/hyp.11311.

Pfahl, S., & Wernli, H. (2008). Air parcel trajectory analysis of stable isotopes in water vapor in the eastern Mediterranean. *Journal of Geophysical Research Atmospheres*, *113*(20), 1–16. https://doi.org/10.1029/2008JD009839.

Pietersen, K., & Beekman, H. (2016). *Groundwater Management in the Southern African Development Community*. 94.

Pietersen, K., Beekman, H. E., & Holland, M. (2011). *South African Grounwater Governance Case Study*.

Risi, C., Landais, A., Winkler, R., & Vimeux, F. (2013). Can we determine what controls the spatio-temporal distribution of d-excess and 17O-excess in precipitation using the LMDZ general circulation model? *Climate of the Past*, *9*(5), 2173–2193. https://doi.org/10.5194/cp-9-2173-2013.

Rozendaal, A., Gresse, P. G., Scheepers, R. and de Beer, C. H. (1994) Structural setting of the

Riviera W-Mo deposit, Western Cape, South Africa, *South African Journal of Geology*, 97(2), pp. 184–195.

Rozendaal, A. & Gresse, P.G. (1994) Structural setting of the Riviera W-Mo deposit, Western Cape, South Africa. South African *Journal of Geology*, 97, 184.

Rukundo, E., & Doğan, A. (2019). Dominant influencing factors of groundwater recharge spatial patterns in Ergene river catchment, Turkey. Water (Switzerland), 11(4). https://doi.org/10.3390/w11040653.

Saadi, S., Boulet, G., Bahir, M., Brut, A., Delogu, É., Fanise, P., … Chabaane, Z. L. (2018). Assessment of actual evapotranspiration over a semiarid heterogeneous land surface by means of coupled low-resolution remote sensing data with an energy balance model: Comparison to extra-large aperture scintillometer measurements. *Hydrology and Earth System Sciences*, *22*(4), 2187–2209. https://doi.org/10.5194/hess-22-2187-2018.

SAHRA, Sustainability of semi-Arid Hydrology and Riparian Areas, Isotopes: Oxygen, Arizona, Ariz, USA, 2005.

Scanlon, B. R., Healy, R. W., & Cook, P. G. (2002). *Scanlon_et_al_2002_recharge_methods*. (February). https://doi.org/10.1007/s10040-0010176-2.

Scanlon, B. R., Jolly, I., Sophocleous, M., & Zhang, L. (2007). Global impacts of conversions from natural to agricultural ecosystems on water resources: Quantity versus quality. *Water Resources Research*, *43*(3). https://doi.org/10.1029/2006WR005486.

Schlaepfer, D. R., Ewers, B. E., Shuman, B. N., Williams, D. G., Frank, J. M., Massman, W. J., & Lauenroth, W. K. (2014). Terrestrial water fluxes dominated by transpiration: Comment. *Ecosphere*, *5*(5). https://doi.org/10.1890/ES13-00391.1.

Schulze, R.E., Maharaj, M., Warburton, M.L., Gers, C.J., Horan, M.J.C., Kunz, R.P., Clark, D.J., 2007. South African atlas of climatology and agrohydrology. Water Res. Comm. Pretoria, RSA, WRC Rep. 1489, 6.

Seddon, D., Kashaigili, J. J., Taylor, R. G., Cuthbert, M. O., Mwihumbo, C., & Macdonald, A. M. (2021). Journal of Hydrology : Regional Studies Focused groundwater recharge in a tropical dryland : Empirical evidence from central , semi-arid Tanzania. *Journal of Hydrology: Regional Studies*, *37*(August), 100919. https://doi.org/10.1016/j.ejrh.2021.100919.

Sharda, V. N., Kurothe, R. S., Sena, D. R., Pande, V. C., & Tiwari, S. P. (2006). Estimation of groundwater recharge from water storage structures in a semi-arid climate of India. *Journal of Hydrology*, *329*(1–2), 224–243. https://doi.org/10.1016/j.jhydrol.2006.02.015.

Sharma, B., Singh, R., Singh, P., Uniyal, D. P., & Dobhal, R. (2015). Water Resource Management through Isotope Technology in Changing Climate. *American Journal of Water Resources*, *3*(3), 86–91. https://doi.org/10.12691/ajwr-3-3-3.

Sigidi, N. T., Miller, J., Watson, A., Clarke, C. E., & Butler, M. (2017). Geochemical and Isotopic Tracing of Salt Loads into the Ramsar Listed Verlorenvlei Estuarine Lake, South Africa. *Procedia Earth and Planetary Science*, *17*(December), 909–912. https://doi.org/10.1016/j.proeps.2017.01.015.

Simpson, H. J., Herczeg, A. L., & Meyer, W. S. (1992). Stable isotope ratios in irrigation water can estimate rice crop evaporation. *Geophysical Research Letters*, *19*(4), 377–380. https://doi.org/10.1029/91GL02952.

Sophocleous, M. (2005). Groundwater recharge and sustainability in the High Plains aquifer in Kansas, USA. *Hydrogeology Journal*, *13*(2), 351–365. https://doi.org/10.1007/s10040-004-0385-6.

Souissi, D., Msaddek, M. H., Zouhri, L., Chenini, I., El May, M., & Dlala, M. (2018). Mapping groundwater recharge potential zones in arid region using GIS and Landsat approaches, southeast Tunisia. *Hydrological Sciences Journal*, *63*(2), 251–268. https://doi.org/10.1080/02626667.2017.1414383.

SRK (2009) *Preliminary assessment of impact of the proposed Riviera Tungsten Mine on groundwater resources*. SRK Consulting, Rondebosch, South Africa.

Terzer, S., Wassenaar, L. I., Araguás-Araguás, L. J., & Aggarwal, P. K. (2013). Global isoscapes for δ18O and δ2H in precipitation: Improved prediction using regionalized climatic regression models. *Hydrology and Earth System Sciences*, *17*(11), 4713–4728. https://doi.org/10.5194/hess-17-4713-2013.

Thamm, A. G. and Johnson, M. R. (2006) The Cape Supergroup, in Johnson, M. R., Anhaeusser, C. R., and Thomas, R. J. (eds) The Geology of South Africaeology of South Africa. Johannesburg: Geological Society of South Africa, pp. 443–460.

Thomas, J. M., & Rose, T. P. (2003). Environmental isotopes in hydrogeology. *Environmental Geology*, *43*(5), 532. https://doi.org/10.1029/99eo00169.

Tian, C., Wang, L., Kaseke, K. F., & Bird, B. W. (2018). Stable isotope compositions (δ2H, δ18O and δ17O) of rainfall and snowfall in the central United States. *Scientific Reports*, *8*(1), 1–15. https://doi.org/10.1038/s41598-018-25102-7.

Tian, C., Wang, L., Tian, F., Zhao, S., & Jiao, W. (2019). ScienceDirect O-excess in China. *Geochimica et Cosmochimica Acta*, *260*, 1–14. https://doi.org/10.1016/j.gca.2019.06.015.

Toth, J., 1970. A conceptual model of the groundwater regime and the hydrogeological environment. Journal of Hydrology 10, 164e176.

Toth, J. (1963). A Theoretical Analysis of Groundwater Flow in Small Drainage Basins'. *Journal of Geophysical Research*, *68*(15), 4795–4812.

Uemura, R., Barkan, E., Abe, O., and Luz, B., (2010), "Triple isotope composition of oxygen in atmospheric water vapor", Geophysical Research Letters, 37, L04402, doi:10.1029/2009GL041960.

van Rooyen, J. D., Watson, A. P., & Miller, J. A. (2020). Combining quantity and quality controls to determine groundwater vulnerability to depletion and deterioration throughout South Africa. *Environmental Earth Sciences*, *79*(11), 1–20. https://doi.org/10.1007/s12665-020-08998-1.

Vázquez-Suñé, E., Carrera, J., Tubau, I., Sánchez-Vila, X., & Soler, A. (2010). An approach to identify urban groundwater recharge. *Hydrology and Earth System Sciences Discussions*,

7(2), 2543–2576. https://doi.org/10.5194/hessd-7-2543-2010.

Walker, D., Parkin, G., Schmitter, P., Gowing, J., Tilahun, S. A., Haile, A. T., & Yimam, A. Y. (2019). Insights From a Multi-Method Recharge Estimation Comparison Study. *Groundwater*, *57*(2), 245–258. https://doi.org/10.1111/gwat.12801.

Wang, B., Ma, Y., Ma, W., Su, B., & Dong, X. (2019). Evaluation of ten methods for estimating evaporation in a small high-elevation lake on the Tibetan Plateau. *Theoretical and Applied Climatology*, *136*(3–4), 1033–1045. https://doi.org/10.1007/s00704-018-2539-9.

Wang, J., Sang, X., Zhai, Z., Liu, Y., & Zhou, Z. (2014). An Integrated Model for Simulating Regional Water Resources Based on Total Evapotranspiration Control Approach. *Advances in Meteorology*, *2014*. https://doi.org/10.1155/2014/345671.

Watson, A., Eilers, A., & Miller, J. A. (2020). Recharge estimation using cmb and environmental isotopes in the verlorenvlei estuarine system, south africa and implications for groundwater sustainability in a semi-arid agricultural region. *Water (Switzerland)*, *12*(5). https://doi.org/10.3390/w12051362.

Watson, A., Miller, J., Fink, M., Kralisch, S., Fleischer, M., & De Clercq, W. (2019). Distributive rainfall-runoff modelling to understand runoff-to-baseflow proportioning and its impact on the determination of reserve requirements of the Verlorenvlei estuarine lake, west coast, South Africa. *Hydrology and Earth System Sciences*, *23*(6), 2679–2697. https://doi.org/10.5194/hess-23-2679-2019.

Watson, A., Miller, J., Fleischer, M., & de Clercq, W. (2018). Estimation of groundwater recharge via percolation outputs from a rainfall/runoff model for the Verlorenvlei estuarine system, west coast, South Africa. *Journal of Hydrology*, *558*, 238–254. https://doi.org/10.1016/j.jhydrol.2018.01.028.

Weaver, J., Talma, A. & Cave, L. (1999) *Geochemistry and isotopes for resource evaluation in the fractured rock aquifers of the Table Mountain Group*. Water Research Commission Report 481/1/99, Pretoria, South Africa.

West, A. G., February, E. C., & Bowen, G. J. (2014). Spatial analysis of hydrogen and oxygen stable isotopes ("isoscapes") in ground water and tap water across South Africa. *Journal of Geochemical Exploration*, *145*, 213–222. https://doi.org/10.1016/j.gexplo.2014.06.009.

Weyhenmeyer, C. E., Burns, S. J., Waber, H. N., Macumber, P. G., & Matter, A. (2002). Isotope study of moisture sources, recharge areas, and groundwater flow paths within the eastern Batinah coastal plain, Sultanate of Oman. *Water Resources Research*, *38*(10), 2-1-2–22. https://doi.org/10.1029/2000wr000149.

Wirmvem, M. J., Mimba, M. E., Kamtchueng, B. T., Wotany, E. R., Bafon, T. G., Asaah, A. N. E., … Ohba, T. (2017). Shallow groundwater recharge mechanism and apparent age in the Ndop plain, northwest Cameroon. *Applied Water Science*, *7*(1), 489–502. https://doi.org/10.1007/s13201-015-0268-0.

Wu, H., Zhang, X., Xiaoyan, L., Li, G., & Huang, Y. (2015). *Seasonal variations of deuterium and oxygen-18 isotopes and their response to moisture source for precipitation events in the subtropical monsoon region*. (January). https://doi.org/10.1002/hyp.10132.

Wu, Q., Si, B., & He, H. (2019). *Determining Regional-Scale Groundwater Recharge with GRACE and GLDAS*.

Xu. Y., & H.E., Beekman. 2003. A box model for estimating recharge- the RIB method. Pages 81-88 in Xu. Y. and H.E. Beekman, editors. 2003. Groundwater recharge estimation in Southern Africa. UNESCO IHP No. 64, UNESCO Paris. ISBN 92-9220-000-3.

Xu, Y., & Van Tonder, G. J. (2001). Estimation of recharge using a revised CRD method. *Water SA*, *27*(3), 341–343. https://doi.org/10.4314/wsa.v27i3.4977.

Yagbasan, O. (2016). Impacts of climate change on groundwater recharge in Küçük Menderes River Basin in Western Turkey. *Geodinamica Acta*, *28*(3), 209–222. https://doi.org/10.1080/09853111.2015.1121802.

Yang, Z., Zhang, Q., & Hao, X. (2016). Evapotranspiration Trend and Its Relationship with Precipitation over the Loess Plateau during the Last Three Decades. *Advances in Meteorology*, *2016*. https://doi.org/10.1155/2016/6809749.

Yeh, H. F., Lee, C.-H., Hsu, K.-C., Chang, P.-H., & Wang, C.-H. (2009). Using Stable Isotopes for Assessing the Hydrologic Characteristics and Sources of Groundwater Recharge. *J. Environ. Eng. Manage*, *19*(4), 185–191.

Yeh, H. F., Lin, H. I., Lee, C. H., Hsu, K. C., & Wu, C. S. (2014). Identifying seasonal groundwater recharge using environmental stable isotopes. *Water (Switzerland)*, *6*(10), 2849–2861. https://doi.org/10.3390/w6102849.

Zhou, Y., & Li, W. (2011). A review of regional groundwater flow modeling. *Geoscience Frontiers*, *2*(2), 205–214. https://doi.org/10.1016/j.gsf.2011.03.003.

Appendix: Showing data of all the samples collected from the Verlorenvlei catchment.

Location	Sample Type	$d^{18}O$ VSMOW	$d^{17}O$ VSMOW	dD VSMOW	D-Excess	^{17}O-Excess	Distance from Coast (km)
Padstal	Groundwater	1,75	0,96	10,3	-3,8	32,23	64,9
Padstal	Groundwater	2,61	1,38	15,4	-5,5	7,82	
Padstal	Groundwater	4,66	2,46	24,0	-13,3	7,85	
Padstal	Groundwater	7,00	3,68	33,5	-22,5	-11,20	
Padstal	Groundwater	6,09	3,21	26,6	-22,1	-2,05	
Padstal	Groundwater	8,69	4,56	41,1	-28,4	-16,05	
Padstal	Groundwater	7,50	3,93	30,9	-29,1	-26,02	
Padstal	Precipitation	7,80	4,09	43,0	-19,4	-18,49	
Padstal	Precipitation	-0,24	-0,10	5,3	7,3	33,11	
Doornfontein	Groundwater	-2,75	-1,41	-11,8	10,2	47,14	22,6
Doornfontein	Groundwater	-2,92	-1,50	-13,2	10,2	43,25	
Doornfontein	Groundwater	-3,08	-1,58	-15,7	9,0	45,93	
Doornfontein	Groundwater	-2,98	-1,54	-14,0	9,8	30,59	
Doornfontein	Groundwater	-3,00	-1,55	-13,8	10,2	31,11	
Doornfontein	Groundwater	-2,97	-1,53	-13,5	10,3	36,75	
Doornfontein	Groundwater	-3,02	-1,56	-13,8	10,3	33,10	
Doornfontein	Groundwater	-2,99	-1,55	-13,6	10,4	30,56	
Doornfontein	Groundwater	-2,99	-1,54	-13,8	10,2	42,51	
Doornfontein	Groundwater	-2,96	-1,52	-13,6	10,0	37,21	

Doornfontein	Groundwater	-3,02	-1,55	-13,6	10,5	42,13
Doornfontein	Groundwater	-3,11	-1,63	-15,7	9,2	10,29
Doornfontein	Groundwater	-3,02	-1,56	-14,0	10,2	40,99
Doornfontein	Groundwater	-3,00	-1,54	-13,9	10,1	47,59
Doornfontein	Groundwater	-3,03	-1,57	-13,8	10,4	31,59
Doornfontein	Groundwater	-3,02	-1,54	-13,8	10,3	50,72
Doornfontein	Groundwater	-3,03	-1,58	-13,7	10,5	21,74
Doornfontein	Groundwater	-3,03	-1,57	-13,6	10,6	36,71
Doornfontein	Groundwater	-3,02	-1,55	-13,7	10,4	45,89
Doornfontein	Groundwater	-2,63	-1,35	-11,8	9,2	38,58
Doornfontein	Groundwater	-3,13	-1,62	-15,6	9,4	36,43
Doornfontein	Groundwater	-3,03	-1,54	-14,1	10,1	56,20
Doornfontein	Groundwater	-4,08	-2,11	-19,2	13,4	46,11
Doornfontein	Groundwater	-4,27	-2,21	-20,0	14,2	47,34
Doornfontein	Precipitation	-4,39	-2,27	-15,6	19,5	53,75
Doornfontein	Precipitation	0,78	0,44	11,2	4,9	28,83
Doornfontein	Precipitation	0,81	0,46	11,5	5,0	30,22
Doornfontein	Precipitation	-1,88	-0,95	0,2	15,3	40,44
Doornfontein	Precipitation	1,38	0,75	14,7	3,7	28,16
Doornfontein	Precipitation	-0,80	-0,38	0,0	6,4	42,24
Doornfontein	Precipitation	-1,12	-0,54	5,6	14,6	51,07
Doornfontein	Precipitation	-0,66	-0,32	0,6	5,9	28,82
Doornfontein	Precipitation	-0,10	-0,02	5,3	6,1	32,48

Kardoesie	Groundwater	-4,29	-2,23	-19,9	14,4	36,28	61,3
Kardoesie	Groundwater	-4,25	-2,19	-19,8	14,2	52,69	
Kardoesie	Groundwater	-4,30	-2,23	-19,9	14,5	49,38	
Kardoesie	Groundwater	-4,27	-2,22	-19,8	14,3	31,80	
Kardoesie	Groundwater	-4,27	-2,21	-19,7	14,4	46,33	
Kardoesie	Groundwater	-4,32	-2,23	-21,7	12,9	52,14	
Kardoesie	Groundwater	-4,29	-2,22	-20,3	14,1	53,30	
Kardoesie	Groundwater	-4,30	-2,22	-20,1	14,2	49,70	
Kardoesie	Groundwater	-4,28	-2,21	-20,0	14,3	51,00	
Kardoesie	Groundwater	-4,23	-2,17	-19,8	14,0	68,10	
Kardoesie	Groundwater	-4,26	-2,20	-20,0	14,1	54,13	
Kardoesie	Groundwater	-4,20	-2,18	-19,6	14,0	42,58	
Kardoesie	Precipitation	-3,30	-1,68	-6,6	19,8	65,17	
Kardoesie	Precipitation	-4,20	-2,15	-15,6	18,0	65,99	
Kardoesie	Precipitation	-4,27	-2,18	-11,4	22,8	75,69	
Kardoesie	Precipitation	-0,96	-0,47	8,9	16,5	32,42	
Kardoesie	Precipitation	-1,54	-0,77	1,4	13,7	39,45	
Kardoesie	Precipitation	-1,75	-0,88	3,1	17,1	43,17	
Kardoesie	Precipitation	-1,76	-0,89	-6,7	7,4	39,33	
Kardoesie	Precipitation	-5,08	-2,61	-19,7	20,9	73,16	
Kardoesie	Precipitation	-3,59	-1,84	-1,8	26,9	52,55	
Kardoesie	Precipitation	-1,11	-0,55	3,8	12,7	39,42	
Kardoesie	Precipitation	-3,07	-1,57	-4,6	20,0	52,73	

Kardoesie	Precipitation	-1,55	-0,78	1,7	14,1	41,46	
Kardoesie	Precipitation	-1,15	-0,54	12,0	21,2	65,17	
Kardoesie	Precipitation	-0,84	-0,38	10,1	16,8	59,28	
Kardoesie	Precipitation	-0,48	-0,23	-14,3	-10,5	20,87	
Kardoesie	Precipitation	-2,45	-1,25	-4,7	14,9	49,31	
Sebulon	Groundwater	-2,86	-1,46	-12,6	10,4	55,50	26,3
Sebulon	Groundwater	-2,80	-1,43	-12,1	10,3	51,92	
Sebulon	Groundwater	-2,91	-1,50	-14,4	8,9	43,00	
Sebulon	Groundwater	-2,78	-1,42	-12,2	10,0	50,95	
Sebulon	Groundwater	-2,78	-1,42	-12,3	10,0	49,76	
Sebulon	Groundwater	-2,77	-1,42	-12,1	10,1	48,44	
Sebulon	Groundwater	-2,84	-1,46	-11,9	10,7	41,22	
Sebulon	Groundwater	-2,78	-1,44	-11,9	10,4	36,05	
Sebulon	Precipitation	0,55	0,36	-0,3	-4,7	73,17	
Volgenvontein	Groundwater	-5,81	-3,02	-32,5	14,0	54,20	98,4
Volgenvontein	Groundwater	-5,88	-3,06	-33,5	13,5	48,74	
Volgenvontein	Groundwater	-5,92	-3,08	-33,9	13,5	57,29	
Volgenvontein	Groundwater	-6,03	-3,16	-35,3	12,9	31,95	
Volgenvontein	Groundwater	-5,92	-3,08	-34,3	13,1	53,06	
Volgenvontein	Groundwater	-5,93	-3,05	-34,2	13,2	85,66	
Volgenvontein	Groundwater	-5,96	-3,10	-34,1	13,5	50,69	
Volgenvontein	Groundwater	-5,96	-3,10	-34,1	13,5	49,64	
Volgenvontein	Groundwater	-5,96	-3,09	-34,2	13,5	67,72	

Volgenvontein	Precipitation	-3,86	-2,02	-21,7	9,2	17,24	
Volgenvontein	Precipitation	-1,36	-0,66	-4,1	6,8	61,95	
Volgenvontein	Precipitation	-2,78	-1,41	-10,5	11,8	61,62	
Beaverlac	Groundwater	-3,79	-1,96	-16,6	13,7	44,12	113,7
Beaverlac	Groundwater	-3,76	-1,94	-16,1	14,0	40,37	
Beaverlac	Groundwater	-3,81	-1,97	-16,2	14,2	39,21	
Beaverlac	Groundwater	-3,92	-2,03	-18,2	13,2	37,23	
Beaverlac	Groundwater	-3,82	-1,97	-16,5	14,0	53,81	
Beaverlac	Groundwater	-3,76	-1,95	-16,0	14,0	33,87	
Beaverlac	Groundwater	-3,82	-1,98	-16,1	14,5	38,20	
Beaverlac	Groundwater	-3,76	-1,92	-15,9	14,2	62,37	
Beaverlac	Groundwater	-3,73	-1,92	-16,0	13,8	49,81	
Beaverlac	Groundwater	-3,75	-1,94	-16,1	13,9	46,82	
Beaverlac	Groundwater	-3,75	-1,93	-15,8	14,2	50,13	
Beaverlac	Precipitation	-3,76	-1,93	-10,1	19,9	56,21	
Beaverlac	Precipitation	0,12	0,08	6,1	5,1	20,80	
Beaverlac	Precipitation	2,08	1,12	16,6	0,0	26,85	
Beaverlac	Precipitation	-3,02	-1,55	-11,0	13,1	43,94	
Beaverlac	Precipitation	-2,70	-1,39	-9,0	12,6	40,53	51,1
Farawayfields	Groundwater	-4,15	-2,13	-17,9	15,3	62,54	
Farawayfields	Groundwater	-4,34	-2,25	-21,1	13,7	43,81	
Farawayfields	Groundwater	-4,24	-2,19	-18,7	15,3	54,73	
Farawayfields	Groundwater	-4,14	-2,15	-18,1	15,0	40,24	

Farawayfields	Groundwater	-4,19	-2,17	-18,3	15,2	40,80
Farawayfields	Groundwater	-4,20	-2,17	-18,5	15,1	44,50
Farawayfields	Groundwater	-4,19	-2,16	-18,2	15,3	56,33
Farawayfields	Groundwater	-4,38	-2,24	-20,8	14,2	75,34
Farawayfields	Groundwater	-4,35	-2,22	-20,7	14,0	80,73
Farawayfields	Groundwater	-4,25	-2,17	-18,9	15,1	73,22
Farawayfields	Groundwater	-4,17	-2,13	-18,6	14,8	78,19
Farawayfields	Groundwater	-4,24	-2,15	-18,6	15,3	89,38
Farawayfields	Groundwater	-4,24	-2,15	-18,4	15,5	84,61
Farawayfields	Groundwater	-4,23	-2,16	-18,6	15,2	77,79
Farawayfields	Groundwater	-4,28	-2,19	-18,6	15,7	68,06
Farawayfields	Groundwater	-4,23	-2,16	-18,4	15,5	76,03
Farawayfields	Groundwater	-4,23	-2,17	-18,4	15,4	66,15
Farawayfields	Groundwater	-4,33	-2,22	-20,3	14,4	69,63
Farawayfields	Groundwater	-4,26	-2,18	-18,7	15,3	69,19
Farawayfields	Groundwater	-4,25	-2,15	-18,7	15,3	92,91
Farawayfields	Groundwater	-4,15	-2,12	-18,3	14,9	73,53
Farawayfields	Groundwater	-4,25	-2,17	-18,6	15,5	82,55
Farawayfields	Groundwater	-2,82	-1,44	-5,2	17,3	52,30
Farawayfields	Precipitation	-2,67	-1,35	-2,4	19,0	58,90
Farawayfields	Precipitation	-3,19	-1,62	2,9	28,4	63,78
Farawayfields	Precipitation	-3,31	-1,69	-6,7	19,7	59,12
Farawayfields	Precipitation	-3,93	-2,02	-15,8	15,6	57,25

Farawayfields	Precipitation	-5,52	-2,85	-22,1	22,0	64,95	
Farawayfields	Precipitation	-2,48	-1,26	-3,3	16,5	49,65	
Farawayfields	Precipitation	-2,71	-1,38	-5,9	15,7	46,31	
Farawayfields	Precipitation	-1,86	-0,95	2,3	17,1	34,70	
Farawayfields	Precipitation	-2,32	-1,19	-9,6	9,0	40,14	
Farawayfields	Precipitation	-1,86	-0,92	6,1	21,0	61,54	
Farawayfields	Precipitation	-4,60	-2,36	-12,5	24,4	76,71	
Farawayfields	Precipitation	-3,86	-2,00	-14,2	16,7	43,75	
Farawayfields	Precipitation	-1,29	-0,65	10,1	20,4	29,29	
Farawayfields	Precipitation	-0,25	-0,10	8,6	10,6	31,33	
Farawayfields	Precipitation	-2,59	-1,32	-1,2	19,5	44,76	
Farawayfields	Precipitation	-1,13	-0,56	5,1	14,1	37,84	
Farawayfields	Precipitation	-1,38	-0,69	6,8	17,9	35,92	
Farawayfields	Precipitation	-1,58	-0,80	-4,7	7,9	35,90	
Farawayfields	Precipitation	-2,94	-1,50	-2,7	20,8	56,33	
Farawayfields	Precipitation	-1,40	-0,70	1,8	13,0	39,45	
Farawayfields	Precipitation	-2,60	-1,32	-5,8	14,9	47,96	
Eagles Rest	Groundwater	-3,45	-1,76	-13,4	14,2	66,29	37,6
Eagles Rest	Groundwater	-3,55	-1,80	-15,2	13,2	75,50	
Eagles Rest	Groundwater	-3,50	-1,77	-13,7	14,3	75,60	
Eagles Rest	Groundwater	-2,08	-1,02	4,0	20,6	83,92	
Eagles Rest	Groundwater	-0,86	-0,39	0,4	7,3	64,94	
Eagles Rest	Groundwater	-2,22	-1,10	-2,6	15,1	72,15	

Eagles Rest	Precipitation	-8,02	-4,18	-47,1	17,0	63,02	
Eagles Rest	Precipitation	-4,83	-2,50	-21,3	17,4	53,83	
Eagles Rest	Precipitation	-2,58	-1,31	-1,3	19,3	51,33	
Eagles Rest	Precipitation	-2,39	-1,23	0,6	19,8	28,49	
Eagles Rest	Precipitation	-8,24	-4,30	-53,2	12,7	60,78	
Eagles Rest	Precipitation	-2,46	-1,27	-4,9	14,8	31,49	
Eagles Rest	Precipitation	-1,91	-0,96	-2,0	13,2	46,26	
Eagles Rest	Precipitation	-3,36	-1,73	-12,6	14,2	46,67	
Eagles Rest	Precipitation	-4,88	-2,54	-20,8	18,3	42,91	
Eagles Rest	Precipitation	-2,25	-1,16	-3,5	14,6	29,05	
Eagles Rest	Precipitation	-2,58	-1,30	-4,8	15,8	58,86	
Eagles Rest	Precipitation	-3,06	-1,58	-7,2	17,3	40,10	
Eagles Rest	Precipitation	-1,65	-0,83	0,7	13,9	44,68	
Eagles Rest	Precipitation	-3,87	-1,99	-11,1	19,9	56,79	
Eagles Rest	Precipitation	-4,24	-2,17	-14,4	19,6	70,74	
Kruispad	River Water	-2,38	-1,21	-8,1	10,9	43,24	13,3
Kruispad	River Water	-1,91	-0,96	-6,3	9,0	49,48	
Kruispad	River Water	-1,59	-0,80	-4,8	8,0	40,59	
Kruispad	River Water	-0,72	-0,37	-2,8	3,0	10,54	
Kruispad	River Water	-0,74	-0,33	-1,3	4,6	54,30	
Kruispad	River Water	-1,83	-0,92	-6,8	7,8	40,79	
Kruispad	River Water	-0,05	0,02	1,1	1,4	44,66	
Kruispad	River Water	0,85	0,46	5,3	-1,5	9,82	

Kruispad	River Water	1,19	0,68	6,7	-2,8	52,07	
Kruispad	Precipitation	-0,99	-0,46	1,6	9,5	61,41	
Kruispad	Precipitation	0,76	0,43	10,5	4,4	33,15	
Olifants_Doorn	Spring Water	-5,52	-2,83	-27,6	16,6	83,69	45,2
Olifants_Doorn	Spring Water	-5,58	-2,88	-28,2	16,5	76,16	
Olifants_Doorn	Precipitation	-5,11	-2,65	-21,5	19,4	52,01	